SACLANTCEN REPORT
serial no: SR-288

SACLANT UNDERSEA RESEARCH CENTRE REPORT

DEPLOYABLE UNDERWATER SURVEILLANCE SYSTEMS. ANALYSIS OF EXPERIMENTAL RESULTS. PART III.

L. Mozzone, S. Bongi

April, 1999

Report no. changed (Mar 2006): SR-288-UU

SACLANT Undersea Research Centre
Viale San Bartolomeo 400
19138 San Bartolomeo (SP), Italy

tel: +39-0187-5271
fax: +39-0187-527.420

e-mail: library@saclantc.nato.int

NORTH ATLANTIC TREATY ORGANIZATION

SACLANTCEN SR-288

Deployable Underwater Surveillance Systems - analysis of experimental results. Part III

L. Mozzone, S. Bongi

The content of this document pertains to work performed under Project 021-1 of the SACLANTCEN Programme of Work. The document has been approved for release by The Director, SACLANTCEN.

Jan L. Spoelstra
Director

intentionally blank page

Deployable Underwater Surveillance Systems – analysis of experimental results. Part III.

L. Mozzone, S. Bongi

Executive Summary:

Deployable Underwater Surveillance Systems (DUSS) a new active sonar concept are being developed at SACLANT Undersea Research Centre to address NATO operational requirements. The concept is based on distributed networks of small autonomous sonar nodes (transmitters and receivers) integrated into a multistatic system. The limited coverage of each node is extended by deploying multiple elements, forming a modular network tailored to operational requirements.

A measurement campaign was conducted from 29 June to 4 July, 1997, south of the island of Elba, with an experimental DUSS moored to the sea bed and a towed, calibrated echo repeater target. Ten runs were performed in 4 different target trajectories, acquiring 2610 echoes with three receivers, at two frequencies. Data analysis demonstrated that:

- Ranges of up to 10 km were typical of the tested node size with all target trajectories, although detection ranges of 22 km were achieved.
- Most target detections were in reverberation limited conditions. Long range target detection was limited by ambient and shipping noise.
- The two frequencies tested (1.9 and 3.5 kHz) gave approximately equivalent performance.
- Multistatic receivers performed as well as the monostatic receiver. Overall system performance and coverage were increased by additional multistatic receivers.
- Single node detection echoes fluctuated significantly from ping to ping due to independent signal fading. Combination of contacts from multiple receivers with geometric diversity improved overall signal to noise / reverberation ratio and contact confidence.

Further analyses are recommended with this valuable bistatic data set, in order to generalize performance estimation to a wider range of design hypotheses. Further experiments are necessary to assess the dependence of optimal working frequency on environment and node size. Modelling is also recommended as a system design aid.

intentionally blank page

Deployable Underwater Surveillance Systems – analysis of experimental results. Part III.

L. Mozzone, S. Bongi

Abstract: Deployable Underwater Surveillance Systems (DUSS) are a new active sonar concept based on a distributed network of small multistatic transmitter / receiver nodes. This study analyzes data acquired during the period 29 June to 4 July, 1997, south of the island of Elba, with an experimental DUSS set moored to the sea bed and a towed, calibrated echo repeater target. Maximum detection ranges of 22 km were noise limited, while ranges of operational interest around 10 km were achieved with all target trajectories in reverberation. Sonar equation terms are measured and discussed. The two tested frequencies of 1.9 and 3.5 kHz showed equivalent performance. Multistatic receivers performed as well as monostatic receivers and extended system coverage. Multistatic receivers improved overall Signal to Noise / Reverberation and detection accuracy in an environment with significant signal fluctuations and contact fading.

The characteristics of the test system and experimental criteria are summarized.

Keywords: Active – Deployable – Multistatic – Sonar – Performance – Experiment – Analysis – Shallow Water– FM – Echo Repeater – Calibrated – Measurements.

Contents

1 Introduction

Deployable Underwater Surveillance Systems (DUSS), a new active sonar concept under development at SACLANT Undersea Research Centre, consist of a distributed network of **small**, low cost or expendable **active** sonar systems optimized for **multistatic** operation against **small targets,** in **shallow** and coastal waters, with high levels of shipping **noise** and strong **reverberation**. The objective of this project is the investigation and assessment of performance of the DUSS concept by means of experimental campaigns conducted with a test system and technical demonstration of an optimized test system. This report is the third of a series describing the characteristics of the experimental system and the test results [1, 2].

This study reports the measurements collected in controlled conditions, with a calibrated echo repeater during the experiment "DUSS '97" conducted at sea on 29 June - 4 July, 1997, south of the island of Elba.

The objectives of this report are:

- To quantify detection performance of small sonar nodes with FM pulses in summer conditions, in shallow, reverberating waters by analyzing calibrated measurements, to assess the effect of resource constraints (receiver complexity, transmitted pulse energy) on system effectiveness.
- To investigate and compare different system configurations and operational geometries.
- To understand factors which determine system performance.
- To compare monostatic and bistatic receiver performance .
- To estimate increase in coverage resulting from extending a monostatic node with additional multistatic receivers.
- To present measured fluctuation in target echo level and to assess the independence of echo fluctuations under a variety of target/receiver geometries.
- To demonstrate and quantify the advantages of multiple bistatic receivers, in terms of diversity of propagation paths against echo fading, multiple coincident contacts for better localization and false alarm reduction.

The sections which follow describe the DUSS sonar concept (Section 2) and the test system (Section 3). The experiment "DUSS '97" is described in Section 4 with the results of the data analyses (Sections 5, 6). Conclusions are summarized in Section 7. Recommendations for further work are outlined in Section 8.

2

The concept of Deployable Underwater Surveillance Systems (DUSS)

A detailed discussion of the concept shown in Fig. 1 can be found in [1, 2]. The proposed design concept aims at achieving limited but reliable and robust surveillance ranges (volumes) in each sonar node with reduced resources. The limited individual coverage is enhanced by multiple sonar nodes (either receivers or transmitters) deployed at different locations and depths. This report demonstrates the advantages of DUSS in terms of receiver covertness, modularity, interoperability, reduced impact and risk, extended detection opportunities, contact localization accuracy.

3 The test system

Experiments were conducted with a test system, constructed from radically re-engineered commercial-off-the-shelf elements (Annex A). The receivers include 25 hydrophones in a planar, star shaped structure with 5 arms for all working frequency bands. The receivers are battery powered, moored to the sea bed and transmit base banded acoustic and compass data *via* radio link to the laboratory on *Alliance*. The transmitters are directive in the vertical plane to minimize interaction with sea boundaries. The 10 element 1.9 kHz transmitter is fixed. The 5 element 3.5 kHz transmitter may be either towed or deployed from the moored ship. The real time data acquisition, processing and display system is described in [1]. The echo repeater, towed by an auxiliary ship, stores digitally and transmits back impinging pulses with known, high target strength (TS). Radiation patterns were measured and given in [1]. Trajectories and frequency bands were planned to have nominal, aspect independent TS by taking into account the measured radiation patterns of the echo repeater. Depth of tow is electronically logged. A very important element of the multistatic test system is the precise localization of all assets (deployed transmitters, receivers, trajectories of target and source, when towed) for post-test analysis. This was accomplished by logging differential GPS and radar information which also provides the means to monitor shipping.

4

The experiment DUSS '97

The experiment was conducted from 29 June to 4 July 1997, south of the island of Elba (Fig. 2), an area representative of the harsh environments in which DUSS would be required to operate, with high levels of shipping noise, unfavourable sound velocity profile (SVP), shallow sloping bottom with continuous reverberation, bottom features and echoes from islands.

Three receivers were deployed on a sloping bottom, in a line parallel to the 160 m iso-depth line, with a 2 n.mi spacing. The transmitters were either towed by *Alliance* or suspended overboard while holding station. When the transmitter was fixed, the monostatic Receiver 1 was also deployed. During towed source runs, it was not in operation. LFM pulses were used throughout, usually of 1 s duration. The towed echo repeater was used as a target along selected trajectories, spanning the most significant aspect and distance configurations of a multistatic surveillance system (Fig. 3).

Acoustic data were stored, processed in real time and displayed on board *Alliance*, for quality monitoring and real time detection purposes. The three receivers acted as three independent sonars, with a skilled operator reporting contacts from each display station into a dedicated log book. Accurate geographical information is of paramount importance in multistatic sonar operations. Positions of all sonar assets were monitored and recorded using differential GPS and radar. The multistatic geometry of experiments was reconstructed in real time on a personal computer and during post-test analysis, including position data from submarine logs. Reconstructed data were cross-checked with acoustic contact localization. Radar tracks of shipping were stored and monitored to protect the deployed assets, to assess the effects of interfering shipping noise and to validate the acoustic contacts. Sound velocity profiles, sea state, currents and weather conditions were regularly sampled and recorded in log books and digital files. Several recording sessions were devoted to collecting specific transmission loss data for environmental characteristics assessment and propagation model tuning. The sources were either towed or deployed along the tested trajectories and a large number of pings collected for averaging. C-SNAP sound propagation predictions were run for optimal asset deployment geometries and experiment planning. Information on bottom characteristics was retrieved from SACLANTCEN databases [3,4]. Bathymetry measurements were collected with the ship's echo sounder during sound velocity profile surveys. Accurate charts were recorded of the experimental area. Acoustic source and target depths during tow were recorded in digital files.

4.1 Environmental conditions

Environmental data were collected and recorded during the experiment using the ship's meteorological system. Written log books were also maintained. During the experiment, the average sea state was 3-4, with winds of 8-12 kn. Some of the experiment was conducted under adverse weather conditions (sea state 7 and 38 kn winds), which forced *Alliance* to retrieve the monostatic receiver 1, abandon the mooring position and proceed to towed source operation. This did not interfere with regular operation of DUSS, which proved to be resistant to adverse conditions. Sunny and cloudy days alternated. As a consequence of the weather, the SVP maintained a surface mixed layer, about 20 m deep, followed by the strong gradient typical of the season (18 m/s variation in 20 m of depth). Velocity increase with depth in the isothermal column below 70 m was moderate or non-existent, which prevented the formation of a deep propagation channel. Propagation was therefore dominated by the strongly absorbing bottom, yielding high propagation losses, which was confirmed by subsequent acoustic modelling (Fig. 4). Continuous reverberation and discrete features from the bottom played a role in the results. Average recorded currents were about 0.3 kn. Shipping traffic was intense, with no respect for the limits of safe operation areas in spite of official messages. The survival and successful operation of the system in such conditions was a significant achievement.

Significant time and effort were devoted to propagation loss predictions and measurements. 76 sound velocity profiles, (SVP) were taken and 50 runs of the model C-SNAP [5] were performed in order to:

- Identify optimal input parameters for minimum bias between reality and model predictions.
- Assess the limits of fluctuation in Propagation Loss, (PL) as a function of SVP variations in space and time.
- Assess the limits of predictability and stability of optimal deployment depths and corresponding detection ranges.

Figure 5 shows an example of the range dependent propagation loss estimation. Figure of Merit was estimated and monitored in real time during the experiments by means of calibrated displays, which permit visual integration for detection while showing at the same time calibrated echo energy and noise spectral density values [1]. Noise levels were also monitored with a vertical line array, (VLA), during silent periods. Resulting performance matched model predictions reasonably well.

4.2 Runs Performed

The experiment was divided into "runs", each of which was characterized by a particular trajectory of source (if towed) and target, pulse type and environment (see tables below). Trajectory types "A", "C", "D", "F" for the target and "T" for the source are shown in Fig. 2. Run identification codes include day and run number (e.g. 2901 denotes June 29th, 1st run).

Speed of target: 5 kn.

Speed of towed sources: either 3 kn ("Towed") or moored ("Fixed").

Pulse: LFM, variable duration, 200 Hz bandwidth.

Pulse repetition interval: 60 s.

Source levels: 205.5 ± 2.5 dB at 3500 Hz and 204 dB at 1900 Hz.

Source vertical directivity: 10 element vertical string at 1900 Hz, 5 elements at 3500 Hz.

Depth of receivers: 110 m.

Target strength: 30 dB (echo repeater). Results are reduced to a 10 dB reference to better approximate realistic operational conditions.

Table 1 *Summary of runs.*

RUN	Frequency kHz	Pulse duration seconds	Duration minutes	Source depth metres	Target depth metres	Towed/Fixed source	Target trajectory
0102	1.9	1 s	90	80	90	Fixed	C
0103	3.5	1 s	90	110	90	Fixed	C
0201	1.9	1 s	120	80	90	Fixed	C
3002	1.9	1 s	120	84	90	Fixed	A
0203	3.5	1 s	120	110	90	Fixed	A
0104	3.5	1 s	60	110	90	Fixed	D
0200	1.9	1 s	60	80	90	Fixed	D
2901	3.5	1 s	120	93	60 - 90	Towed	F
0101	3.5	4 s	120	110	60 - 90	Fixed	F
0105	1.9	1 s	60	80	60 - 90	Fixed	F

5 Data analysis

This section describes the procedures and criteria adopted to process the data collected during the experiment, to extract, summarize and validate the results.

5.1 Real time detection

Three real time displays were used by three operators (one per receiver) to perform target detection during each run. The objective was to monitor data quality, to rapidly assess system performance and to aid the planning of subsequent runs to be tested. Detection was performed *a priori* knowledge of target trajectories, asset positions and radar tracks of traffic. The expected bearing and time of arrival of the target echo were computed in real time for each receiver. The presence of a "tag", a short pulse after the echo (180 dB, 0.25 s, CW), confirms the target location. Figure 6 shows an example of the display format used for detection which preserves information but does not permit easy understanding of run geometry (as time does not directly correspond to range). The echo is clearly visible, followed by the Tag. Figure 7 shows a display format which reconstructs the actual geometry, overlapping acoustic data on the geographical map. It permits sanity checks on data quality and the assessment of spatial reverberation characteristics on the different receivers.

5.2 Data analysis criteria

Post test analysis starts with the extraction of echoes from the recorded data. Each "run" consists of recordings of hydrophone data, arranged in "ping files", one for each of the three receivers and for each transmitted pulse (once a minute). A workstation performs beamforming, replica correlation and display in the format of Fig. 6. The operator confirms contact detection. Signal processing criteria are described in [1]. The geometry of the run is reconstructed and time series extracted (echo levels *versus* time) are compared with the recorded GPS positions of the target. Radar data contributed to validation of results. Noise and reverberation backgrounds just before and after the echo are extracted in a similar way. A correction for echo repeater delay was included. The background level acquired near the echo arrival was necessary to determine the signal to noise ratio (SNR) and data quality. The background measurement with delay compensation allows computation of SNR series resembling a real target (Annex B). Conclusions about performance, reverberation / noise limited detection and ranges of detection can now be drawn.

Figure 8 illustrates some useful definitions: *Bistatic angle* is the angle looking to the transmitter and the receiver from the target position. *Bistatic aspect angle* is the aspect of the target from its bow to the bisector of bistatic angle. *Monostatic equivalent range* is half the length of the whole transmitter - target - receiver path.

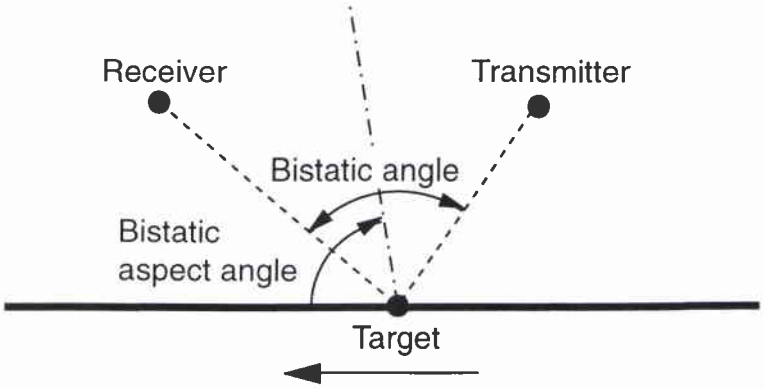

Figure 8 *Definition of terms.*

An example from Annex B is shown in Fig. 9. Plot 1 shows the geometry of source, receivers and target trajectory from GPS log files. Receivers 1 to 3 are plotted as green circles from NE to SW in the yellow box. The transmitter is co-located with Receiver 1. Target and (when towed) source trajectories are plotted with coloured dots. The colour scale from blue, green, yellow to red, shows elapsed time.

Plot 2 shows the distance of the target from the source (in cyan), the receiver (in red) *versus* ping number. The equivalent monostatic range (half the sum of the former distances) is shown in green). Note that for monostatic cases (Receiver 1) the three distances are coincident to the cyan line.

Plot 3 shows the processed data: Echo energy is plotted in dB ref. μPa*√s (in green). The background reverberation + noise levels averaged in a window just before (in cyan) and after (in blue) the echo arrival. Compensation has been made for echo repeater delay. The exact noise / reverberation series that would limit detection of a real target are shown here. The noise reference from a distant window of the same beam, averaged throughout the run, is shown in magenta, with a straight line. The relative position of noise and background around the echo show if detection is limited by reverberation.

Plot 4 shows computed SNR *versus* ping number from data above. Detection performance against a reference TS of 10 dB is reconstructed from the time series of Plot 3.

5.3 Sonar equation

The sonar equation for this sonar can be written as follows [6]:

SNR = EEL - NRL

where:

EEL is the echo energy level (energy of the received and processed pulse, as shown in plots) in dB ref. μPa*√s.

EEL = SL + 10 log(T) - PL1 + TS - PL2 - SysLoss

SL: Source Level in dB ref. μPa @ 1 m

T: pulse duration in seconds. The LFM pulses used here have uniform power across their duration. Tapered pulses would require a smaller "equivalent effective duration" term.

PL1: Propagation loss from source to target.

PL2: Propagation loss from target to receiver.

TS: Target strength in dB.

SysLoss: the sonar equation contains a 10 dB system loss term, where various effects are included: multipath, degradation of pulse coherence, distortion of the wavefront, unfavourable noise and reverberation statistics, scalloping loss due to beams, processing approximations. The last two terms are expected to be very low, due to the high quality of digital processing and the care taken analyzing data with tightly overlapped beams.

SysLoss = OD + CohLoss.

CohLoss: loss of coherence of the pulse due to propagation, which spreads and distorts the transmitted waveform. It is the ratio of pulse energy before and after the replica correlation processing. It can be measured only when the SNR before replica correlation is high enough (at least 6 dB). Coherence loss of the echo was estimated from available data to be slightly less than 4 dB.

OD: Operational Degradation, 6 dB, includes multipath loss and all other terms.

Multipath loss: it is generally assumed to be 6 dB in the two-way propagation path; it represents the difference between real wide band data and the ideal propagation loss that can also be computed by models, where a stationary single frequency case is assumed and modes

propagating through multiple paths are combined coherently. For simplicity these effects are grouped into two terms:

NRL: Noise and reverberation levels, against which target detection is performed. They are measured at the processor output and include the directivity of beams against the different spatial distributions of noise and reverberation and the reduction due to processor gain after replica correlation. Reverberation and noise levels sum incoherently and linearly, before conversion to the logarithmic dB scale. NRL is the background plotted on operator displays corresponding to power spectral density ("single sided", i.e. positive frequencies only), expressed in dB ref. μPa*√Hz. [1].

NRL = [NL - AG_N] linearly combined to [RL - AG_R - 10 $\log_{10}$(Bw)]

NL: noise power spectral density in the water, dB ref. μPa*√Hz.

RL: reverberation level (average power) in the water, dB ref. μPa.

Bw: bandwidth of the LFM sweep, Hz.

AG_N: array gain over ambient noise, dB, generally approximated with DI.

AG_R: array gain over reverberation, dB, generally approximated with AG_H , the array gain on the horizontal plane (3 dB beamwidth / 360°.

The sonar equation corresponds to the data shown on the real time displays and the plots of the post-test analyses: echo energy for the signal, noise or reverberation levels after beamforming and replica correlation for the background.

5.4 Measurements

The experimental data analyzed in this document show the measured time series of the terms EEL, PL1 + PL2, NRL. A separate estimation of system output noise (NL - AG_N) which includes fluctuating interference from shipping traffic (Annex B) was collected. The comparison of NRL and (NL - AG_N) permits determination of the transition from reverberation-limited to noise-limited detection.

Comparison between the noise background and NRL shows where the transition from reverberation limited to noise limited detection occurs, for different geometries (upslope, downslope target trajectories, monostatic and bistatic receivers) and system configurations (frequency, source vertical directivity, receiver beam pattern). Performance with lower source levels can also be inferred with simple measurement transforms.

SNR measurements provide a reliable measurement of system performance. The data shown refer to a TS of 10 dB, by subtracting 20 dB from echo level time series collected

with TS = 30 dB. The display of values below 10-12 dB (recognition differential needed for single-ping detection) allows analysis of performance for the hypothesis of weaker or stronger targets. Values below zero, shows what happens ***below*** detection thresholds. Hypotheses of larger targets or receivers can therefore be evaluated.

It is important to point out that measured SNR is computed from experimental data with the classical formula 10 log((eel - rnl) / standard deviation (rnl)), where rnl is RNL expressed in linear form (not in dB) and is the average background in two windows near the target, while standard deviation (rnl) is the corresponding standard deviation. This is equivalent to SNR in the sonar equation under the hypothesis of a stationary Gaussian background. Analyzed data show that rnl ≈ standard deviation (rnl) most of the time (in the present data set and [2]). It is therefore reasonable to apply the classical formulae to DUSS. Relevant deviations occurred only in the presence of strong individual reverberation features. These cases, however, pertain to the problem of false contact classification, rather than to the issue of detection in noise.

Comparison across frequency is straightforward as source levels are similar (204 - 205 dB). Vertical beam patterns are complementary (the receiver beam is narrower at 3500 Hz than at 1900 Hz, the transmitter beam is wider), while receiver indexes (DI, AG_H) are reasonably uniform. Note that the receiver hydrophone spacing allows grating lobes at both frequencies, but the results presented here are representative of a 25 channel system.

Table 2 *Source levels, source and receiver -3 dB beam widths in degrees, receiver DI and horizontal array gain (AG_H) in dB.*

Frequency	Source Level	Source Vertical Beamwidth	Receiver Vertical Beamwidth	Receiver DI	Receiver AG_H
1900 Hz	204 dB	10.5°	54.6°	13.3 dB	12.5 dB
3500 Hz	205 dB	20.8°	40.7°	12.9 dB	11.3 dB

6 Results

During DUSS '97 experiments the echo repeater performed 10 runs in 4 different target trajectories. 2610 echoes were collected with three receivers at two frequencies. LFM pulses of 1 s were transmitted. SNR series of the three receivers are overlaid on one plot for each run. The corresponding reconstructed target trajectories are also shown. Runs are grouped by target trajectory type. A catalogue of the results, with ping by ping analysis is given in Annex B. The SNR series refer to a TS of 10 dB, independent of target aspect angle. A conservative reference detection threshold of 10 dB is assumed for detection ranges. Lower values correspond to the pre-alerted conditions of an experiment. SNR values below the detection threshold have been plotted in order to permit larger target detection performance estimation .

6.1 Results with trajectory type "A"

This trajectory was designed to test long range performance down a sloping bottom. Figures 10 and 11 summarize the data collected at the two working frequencies. Maximum detection ranges of 22 km were obtained in noise-limited conditions, leaving margins for performance improvement if more powerful sources (e.g. tactical towed units) are employed. The transition from reverberation-limited to noise-limited detection occurs at 10 km for 1900 Hz and less than 15 km for 3500 Hz (Annex B). Performance is slightly better at 1.9 kHz. This long-range, reverberation-limited result is not influenced by different vertical directivity of transmitters. The overall performance of the three monostatic / multistatic receivers is equal.

Figures 12, 13 show the same SNR series *versus* ping number, with the corresponding target trajectory maps from target DGPS, (Figs. 14, 15). Fluctuations of SNR as the target slowly crosses variable propagation and background conditions can be observed. Background data series are very smooth (Annex B), particularly for the multistatic receivers (no ship noise). Variability therefore depends primarily on propagation loss, changing with time and target location. Cross checks with target depth information do not reveal any correlation. The propagation path from source to target is common and paths from the target to the three receivers (PL2) are only partially independent as shown by SNR fluctuations. A greater degree of independence is found in trajectory type "C", where PL2 for the three receivers is more varied. The fusion of all receivers as parts of a unit can be expected to improve overall system performance in the "C" type trajectory. Independent contact fading on one receiver can be compensated for. Simultaneous contacts on multiple receivers, however, offer the advantages of increasing contact confidence and localization precision, thus compensating for the limitations of reduced acoustic aperture of single units.

6.2 Results with trajectory type "F"

In the case of maximum detection ranges with *upslope* propagation, propagation is poorer, with shallower water and stronger reverberation. Target depths were not constant, but become shallower at the end of the trajectory. As with Trajectory "A", this case illustrates the positive effects of receiver diversity and allows comparison between monostatic and multistatic elements.

Maximum detection ranges of 11 - 14 km were obtained in noise limited conditions at 3.5 kHz (Fig. 16, 17). The transition from reverberation-limited to noise-limited detection occurs at around 8 - 11 km (Annex B). Performance at 1.9 kHz is inferior and reverberation limited out to 14 km (Fig. 18). Monostatic and multistatic receivers yield substantially equivalent performance. Benefits from multiple receiver fusion are expected also in this case (Figs. 19 - 24). As in the "A" case above, SNR series from the three receivers are correlated in the mean, but their fluctuations maintain a remarkable degree of independence.

6.3 Results with trajectory type "C"

This trajectory demonstrates the effectiveness of the multistatic system in extending coverage by means of additional receivers. The target sequentially offers equivalent detection opportunities, in terms of range and closest point of approach (CPA), to all receivers. Target strength of the echo repeater is aspect independent. Comparison between receivers and frequencies is therefore straightforward. Figures 25 - 27 show very good detection performance between 5 and 12 km. Both frequencies demonstrate equal performance. Detection is limited by reverberation and the transition from reverberation to noise-limited detection occurs at 10 km (1.9 kHz) or >10 km (3.5 kHz). The coverage offered by the bistatic receiver 2 n.mi from the source is equal to the contribution of the reference monostatic unit, with the advantage of being covert. Slightly inferior results are obtained with Receiver 3 (4 n.mi). Margins exist to test wider displacements between source and receiver with the present node size.

The best conditions for propagation path diversity are shown in Figs. 28 - 33. PL2 pertains to completely different and independent paths for the three receivers. A reduced degree of correlation between SNR series is evident. Each receiver yields the best SNR at different times. The independent SNR fluctuations and the open deployment geometry promise major improvements in contact localization after data fusion.

6.4 Results with trajectory type "D"

This configuration tests propagation paths with constant depth (across-the-slope), parallel to the iso-depth lines of the bottom slope, in very shallow water, with strong reverberation. It also offers data samples collected, ping by ping, at three different ranges from the target. Very good detection is achieved between 4 and 10 km, with equivalent overall performance at the two frequencies. Figures 34 - 35 clearly show that the

different distance does not affect SNR levels. Larger echo attenuation is compensated for by lower reverberation levels on the more distant multistatic receivers.

At 3.5 kHz, SNR series are more uniform (Figs. 36 - 39): Receivers 1 and 2 yield similar results, but with independent fading. Receiver 3 performs less well. A more pronounced degradation of SNR with distance on Receiver 3 is visible at 1.9 kHz. Propagation paths are closely correlated, because the PL2 components, from target to receiver are similar.

6.5 Coherence loss of the echo

By comparing echo energy before replica correlation to the calibrated sonar output, a share of the system loss (SL), to be included in the sonar equation can be measured. It corresponds to signal distortion (loss of correlation with the original replica waveform) due to propagation in the water. The estimation of this loss is possible when SNR at beam output is above 6 dB, which is large enough to eliminate interference. The measured loss was less than 4 dB.

6.6 Propagation Loss measurements

Propagation loss PL = (PL1 + PL2) / 2 is computed and plotted *versus* monostatic equivalent range in Figs. 40 - 49. Uncertainties depend on the estimation of SL, which could be measured only in the coherence loss component.

For each run, PL was computed from echo time series with a large SNR (better than 15 dB). This strict criterion avoids noise / reverberation background contamination of the results, which would produce optimistic estimations. The chosen threshold prevents noise peaks from being mistaken for weak echoes (with a probability close to 1).

PL values ranged from 75 to 80 dB for long distances (A and F trajectories, 10 - 20 km) and between 65 and 75 dB for short distances (C and D trajectories, 5 - 10 km). The latter cases do not account for asymmetrical PL1 and PL2 paths, but present just "equivalent monostatic" data. These plots show that propagation loss alone, rather than background variability, is responsible for most of the fluctuations observed in the SNR series.

7 Conclusions

Information has been acquired relevant to the design, handling, operation, performance and potential of a multistatic network of small deployed sonar units. 2610 echoes were collected by three receivers in various conditions and analyzed. Calibration of transducers, sensors and processing permitted the quantification of basic measurements such as detection range, contact SNR and propagation loss. The experience acquired during these field tests provided a better understanding of the main features of multistatic systems and an insight into their potential.

7.1 Performance of DUSS sonar nodes

This study demonstrates that small DUSS sonar nodes perform satisfactorily in unfavourable conditions. Low energy FM pulses were used in a difficult environment: sloping shallow waters with strong reverberation, a downward refracting sound velocity profile against a small (simulated) target. Reliable detection ranges of 5 - 22 km were confirmed in controlled experimental conditions and for a variety of system geometries and configurations (1900 Hz, 3500 Hz, upslope, downslope, across-bottom-slope propagation). The maximum ranges of the various runs varied between 10 and 22 km, on trajectories of type "A" and "F". Most of the measurements was collected at the intermediate ranges of 5 - 10 km, where excellent performance of the test system was demonstrated for all configurations. These ranges therefore can be considered the typical coverage to be expected from DUSS nodes of this size and complexity (SL = 205 dB, 25 hydrophones).

7.2 Reverberation and noise

Adverse detection background conditions are the expected environment for DUSS. In the ranges of interest (0 - 10 km) detection is limited by reverberation in both frequency bands. A limited reduction of transmitter resources (less SL) would thus maintain the levels of performance obtained over these ranges. The long range detections (10 - 22 km) are achieved against ambient and traffic noise. Margins for improvements therefore exist if more powerful (e.g. tactical) transmitters become available during operation. Note that the multistatic sonar nodes are generally less coupled to the noise radiated by the ship (from which the monostatic node was deployed).

7.3 Overall system performance versus frequency

As mentioned in Section 5.4, the direct comparison of results across frequency is justified by the equivalence of system characteristics. Previous reports [1, 2] show that the lowest frequency band for the test system, 900 Hz, requires greater system resources to be effective in the chosen ranges and deployment schemes. The two bands tested here (1.9, 3.5 kHz) are substantially equivalent at the ranges of interest (5 - 10 km), both were limited by reverberation. Tests at longer ranges (10 - 22 km) show that the lower band does better downslope, with an increasing depth of transmission channel. The higher band does better upslope, with water depths between 80 and 160 m, in spite of a wider vertical transmission beam.

These results confirm that the choice of the best working frequency is very sensitive to the diverse employment conditions. Results depend strongly on the environment. The test conditions were chosen to best represent the envisaged DUSS operational use. These results therefore provide valuable input to the design of an optimal DUSS prototype. Further research is recommended to explore different environmental conditions. More experimental samples of performance in the 2 - 4 kHz range would refine the conclusions. It should also be noted that the system frequency also depends on the size chosen for the sonar nodes and on the specifications of surveillance ranges.

7.4 Performance of monostatic versus multistatic receivers

Performance of monostatic and multistatic receivers was equal, with omnidirectional TS. Additional receivers substantially increase the area coverage of a single monostatic element. Further benefits were shown to derive from real-world aspect-dependent TS [2], where the SNR peaks typical of specular reflection were obtained sequentially, at different times by the three receivers. The overlapping coverage areas of the receivers also show potential for wider deployment patterns (with more than 4 n.mi from transmitter to receiver).

7.5 Advantages of multiple receivers

- The SNR of echoes on the three receivers presented pronounced fluctuations, which pertain to propagation only, as the radiation pattern of the echo repeater was uniform.

- When propagation paths were independent (e.g. trajectory C), the target was detected simultaneously by multiple receivers for most of the time. SNR fluctuations were only partially correlated and benefits are expected from contact fusion (redundancy yield increased confidence in target contacts and reduced confidence in false alarms)

- When propagation paths were similar for the three receivers (trajectories A, F, D), a residual degree of independence was still found in the data.

- The wide deployment geometry is promising for enhanced contact bearing localization.

- Deployment patterns more widely spaced than in the experiments are expected to allow contact tracks from one (covert) receiver to be passed to the next closest one, while the unalerted target crosses the surveillance field.

7.6 Propagation Loss

Measured PL values range from 75 to 80 dB for 10 - 20 km and between 65 and 75 dB for 5 - 10 km. These values are very good, considering the unfavourable test conditions: downward refracting SVP, absorbing bottom, sub-optimal depth of deployment of assets and target (due to mechanical constraints of the test system). The variability found in SNR series derives mostly from changing PL in time and space during target motion.

7.7 Towed source

A small portion of the experiment was conducted with a towed transmitter (3.5 kHz, target trajectory F), in rough sea conditions. The SL was the same (205 dB). The robustness of DUSS performance to degraded environmental conditions (ambient noise, reverberation, strumming noise from floating radio buoys) was demonstrated. This is also an excellent example of how DUSS could be integrated with tactical systems of opportunity. The advantages of a variable asset deployment pattern do not entail substantial degradation of performance (which might be due to ship noise and motion). Different operator displays, with motion compensation are of course necessary. On the other hand, the larger transmit power available on operational units permits the enhancement of detection ranges and SNR in the noise limited regions (10 - 20 km).

8 Recommendations

The data presented and analyzed here and in [2] should be generalized to a variety of environmental conditions by means of modelling, as for the previous test [1], to permit more widely applicable performance assessment, evaluation of sonar coverage and better definition of design requirements.

Wider bistatic displacements of the receiver from the source should be tested for the present node size of the test system. Improved radio links should therefore be considered for further research.

Further experiments are recommended in order to survey the most operationally significant environmental conditions. More general conclusions can then form the basis of system design proposals. In particular, an accurate definition of optimal working frequency changes as a function of sonar node size and operational conditions requires additional experiments in the band 1 - 4 kHz.

Acknowledgments

This work was made possible by the coordinated efforts and the enthusiasm of the technical support and ships' personnel of SACLANT Centre. In fact it relied on all the fields of expertise at the Centre for the collection and processing of a large set of experimental data.

9 References

[1] Mozzone, L., Bongi, S. Deployable Underwater Surveillance Systems - analysis of experimental results, SACLANTCEN SR-278. La Spezia, Italy, NATO SACLANT Undersea Research Centre, 1997.

[2] Mozzone, L., Bongi, S. Deployable Underwater Surveillance Systems - analysis of experimental results, Part II, SACLANTCEN SR-283. La Spezia, Italy, NATO SACLANT Undersea Research Centre, 1998.

[3] Spina, F. *et al.* SACLANTCEN bottom cores database on CD-ROM, in course of publication.

[4] Jensen, F.B. et al. Computational Ocean Acoustics, AIP Press, 1994.

[5] Ferla, M., Porter, M., Jensen, F.B. C-SNAP: Coupled SACLANTCEN normal mode propagation loss model, SACLANTCEN SM-274, La Spezia, Italy, NATO SACLANT Undersea Research Centre, 1993.

[6] Cox, H. Fundamentals of bistatic active sonar. In: Chan, Y.T., editor. Proceedings of the NATO Advanced Study Institute on underwater acoustic data processing, 18-29 July 1988. Dordrecht, Kluwer, 1989: pp. 3-24 [ISBN 88-36785].

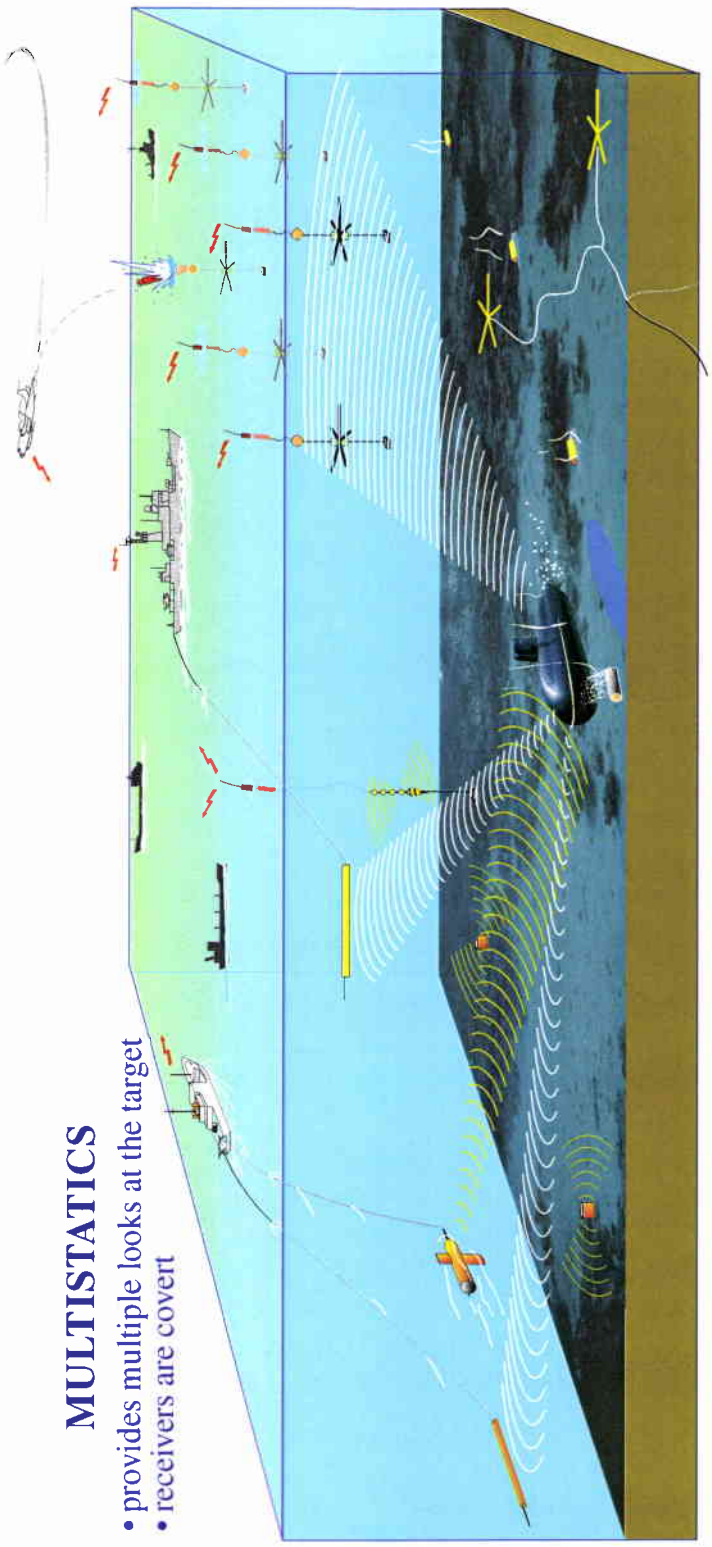

Figure 1 *Pictorial view of the DUSS concept.*

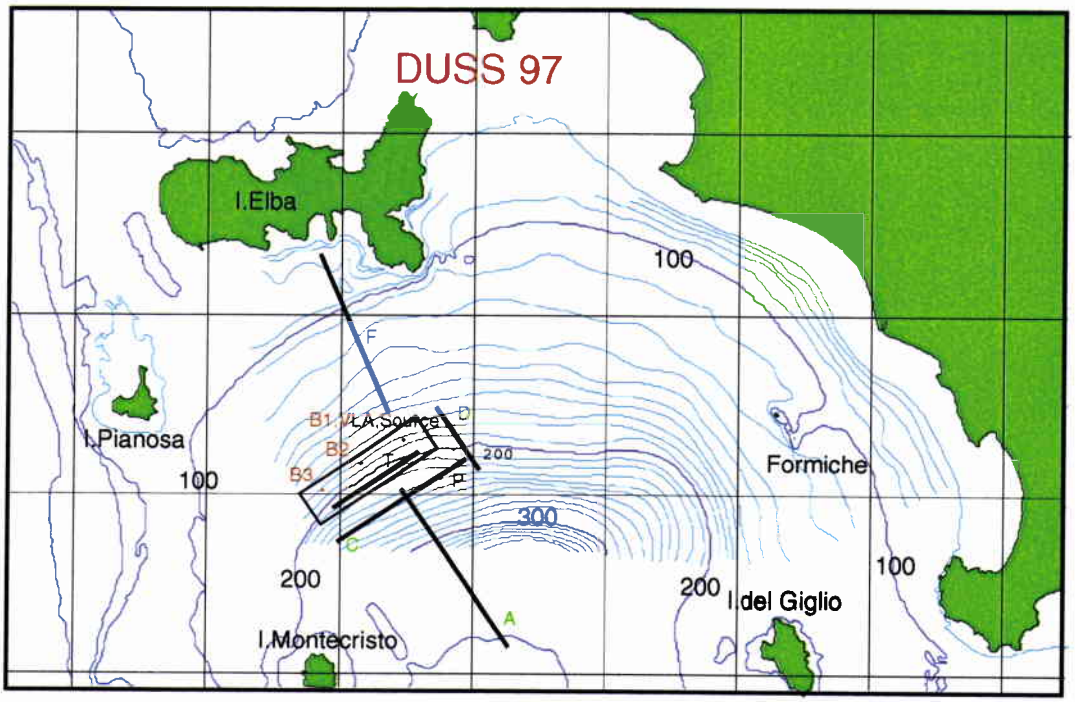

Figure 2 *Geographical map of the test area, showing bottom bathymetry and deployment positions of sonar elements. The box indicates the reserved area for system deployment. Target trajectories (A..F) and towing ship trajectories (T) are shown.*

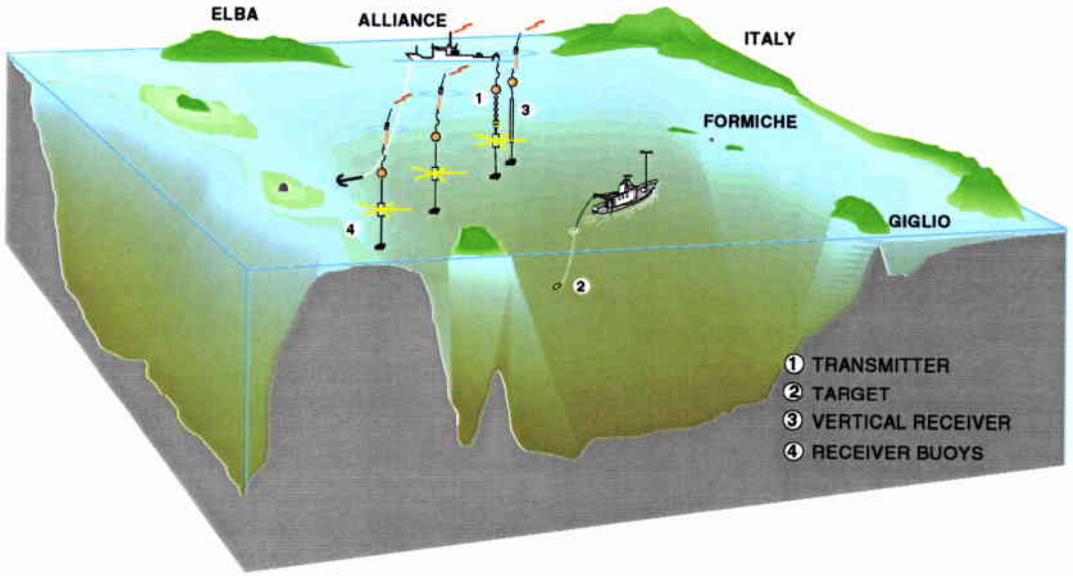

Figure 3 *Pictorial view of the experiment. The bottom and coast structure of the area are faithfully rendered.*

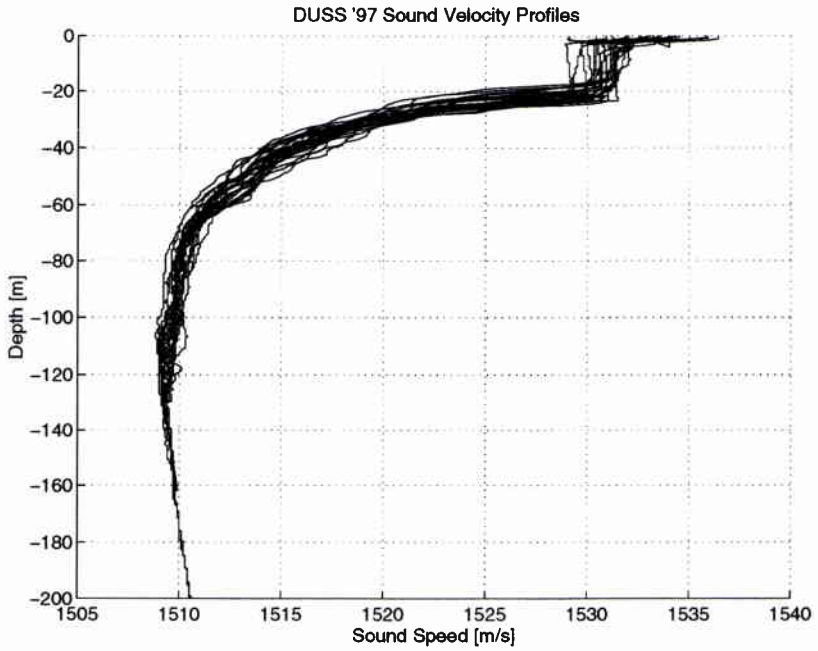

Figure 4. *Sound velocity profiles measured during the tests.*

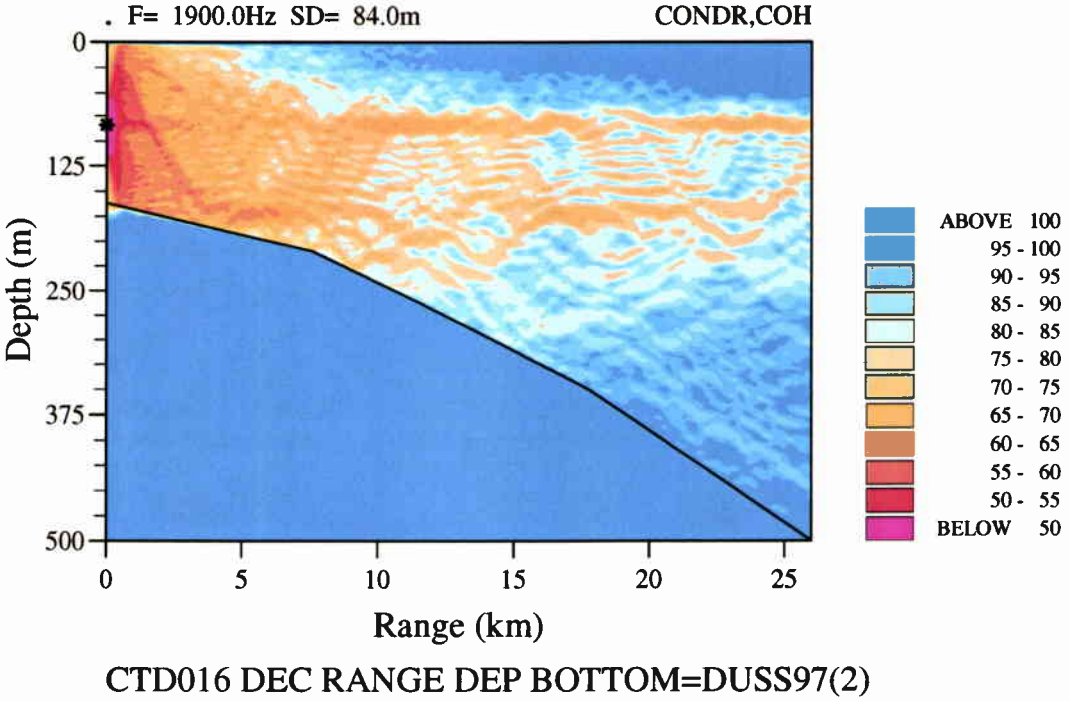

Figure 5 *Propagation Loss computed with C-SNAP.*

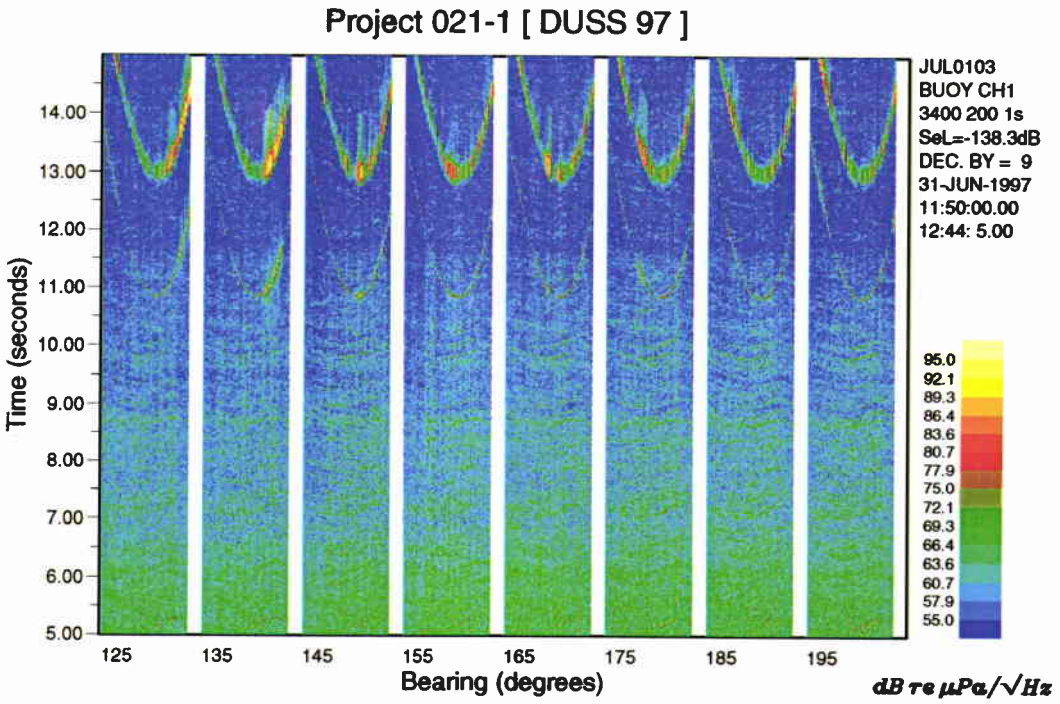

Figure 6 *A significant example of detection display, with evident target track. Each column corresponds to a beam aiming at a fixed direction. Color corresponds to calibrated echo energy (dB re. µPa*√s) and reverberation level (power spectral density, dB re uPa/√Hz). In each of these columns the X axis shows ping number and Y axis shows time after ping transmission.*

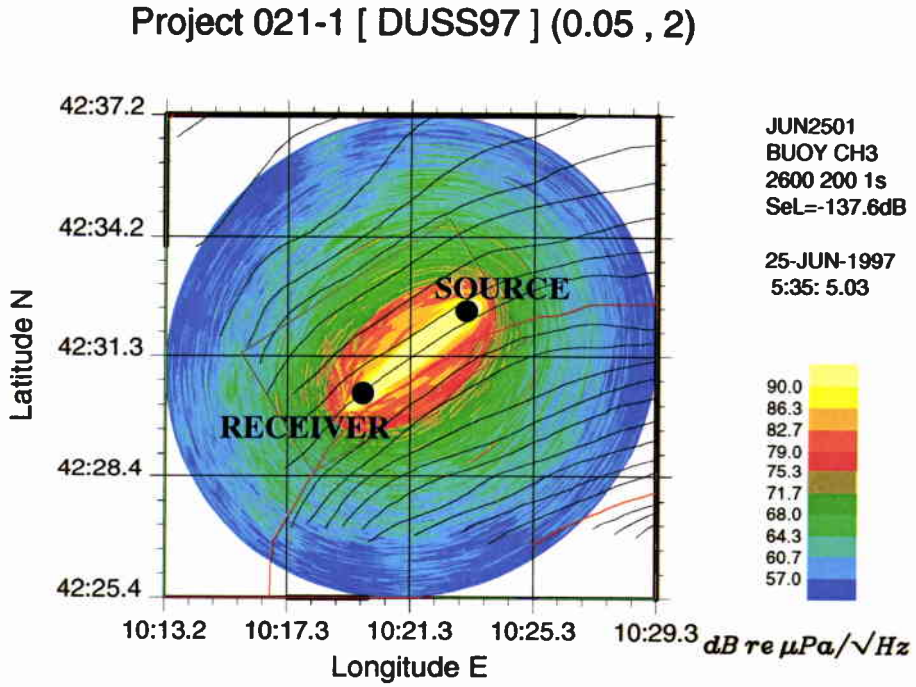

Figure 7 *Polar display of reverberation.*

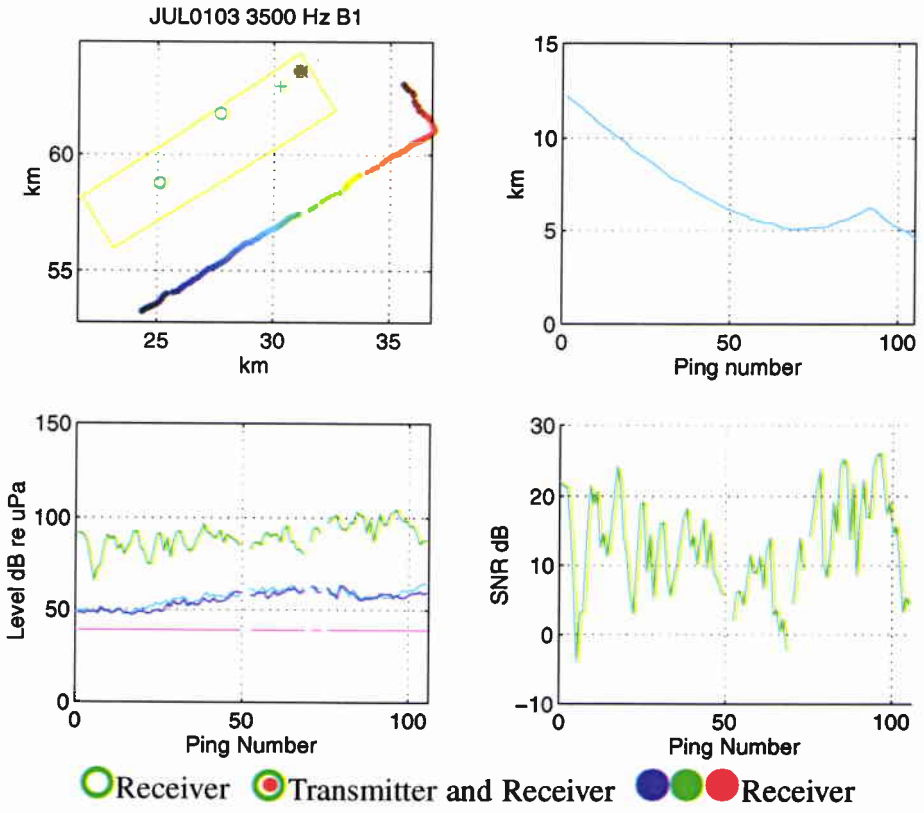

Figure 8 *Analysis of Run 0103, Receiver 2.*

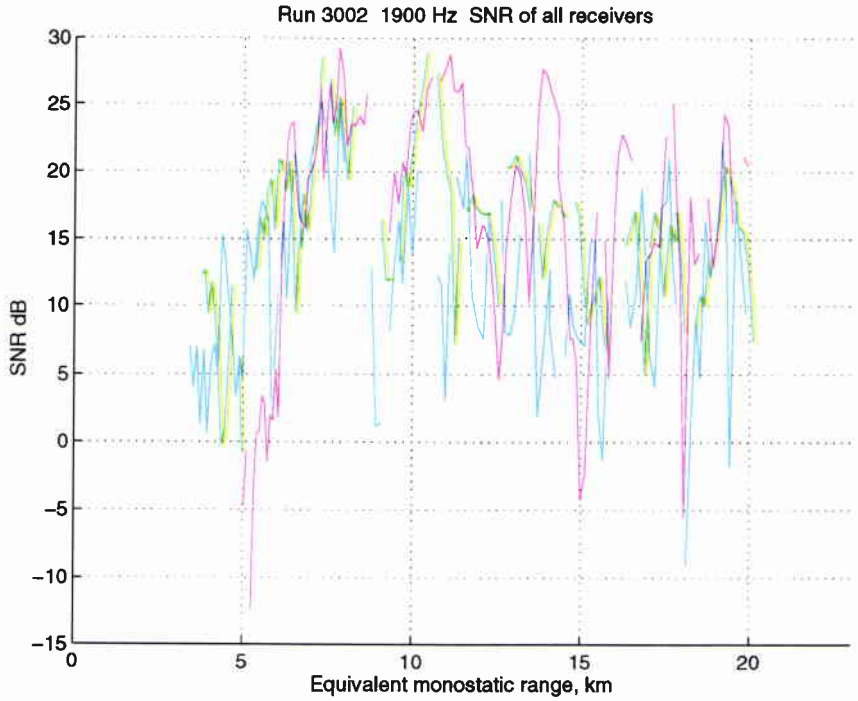

Figure 9 *Analysis of Run 3002, 1900 Hz. SNR of the three receivers (1: blue; 2: green; 3: red) versus equivalent monostatic range*

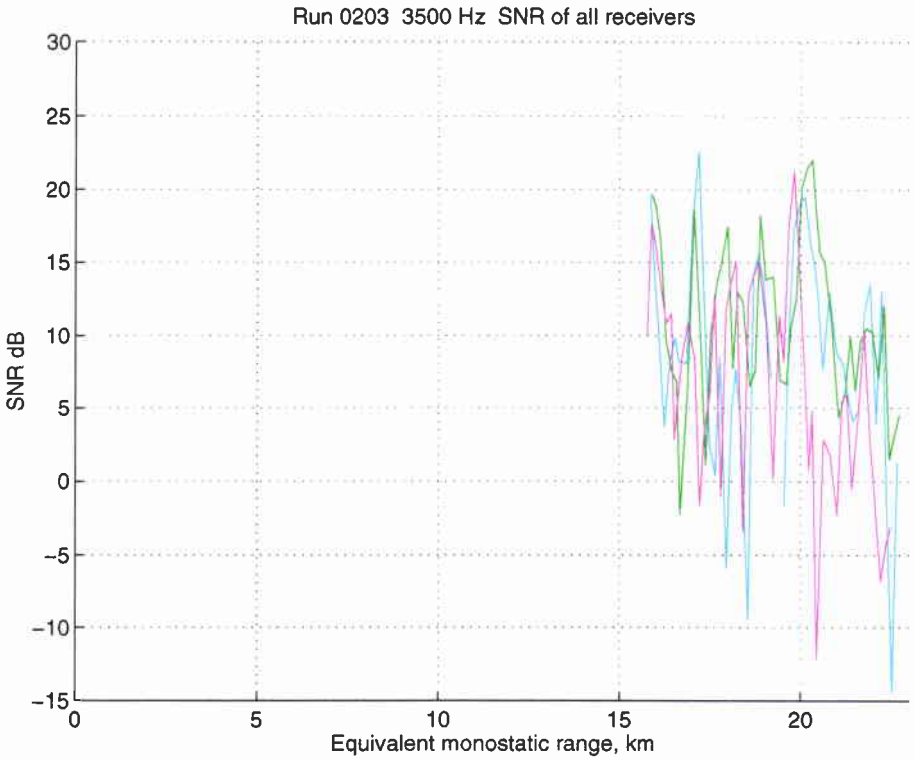

Figure 10 *Analysis of Run 0203, 3500 Hz. SNR of the three receivers (1: blue; 2: green; 3: red) versus equivalent monostatic range.*

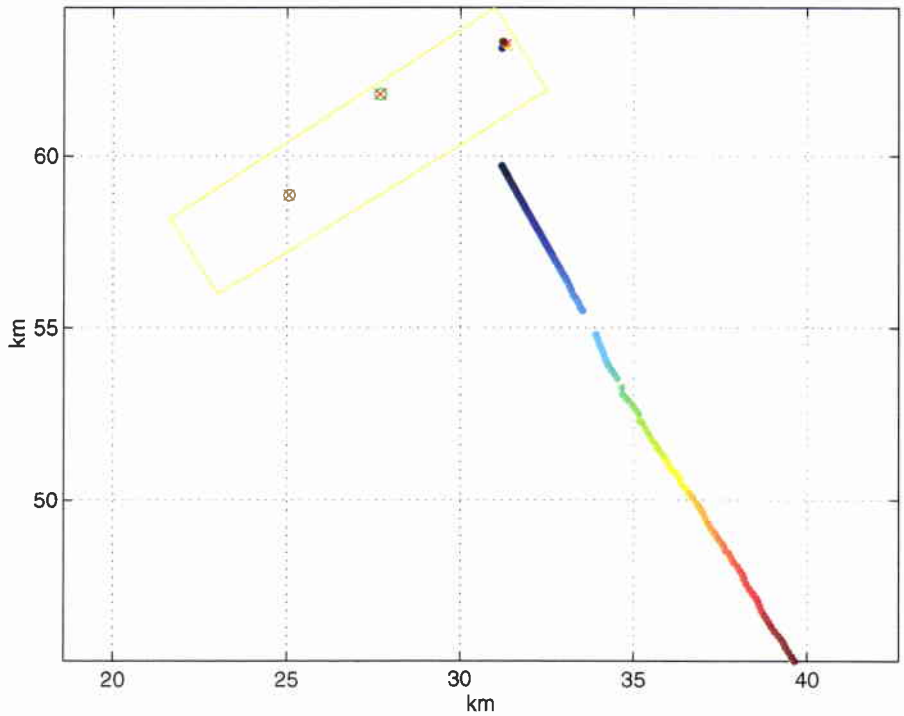

Figure 11 *Analysis of Run 3002, 1900 Hz. Target trajectory from GPS data.*

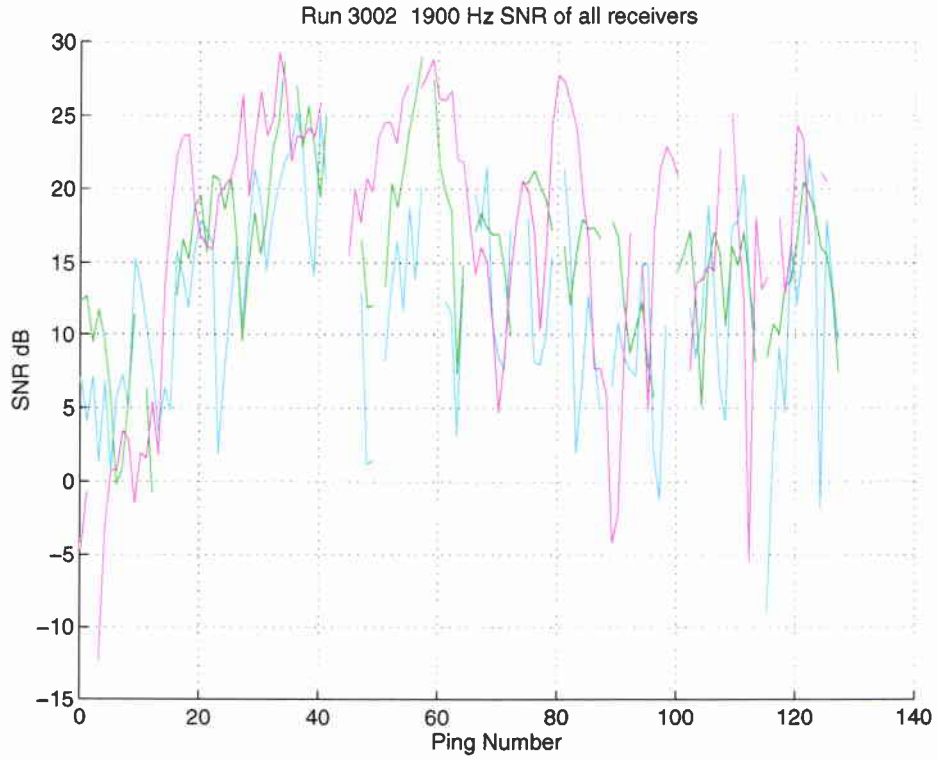

Figure 12 *Analysis of Run 3002, 1900 Hz. SNR of the three receivers (1: blue; 2: green; 3: red) versus ping number.*

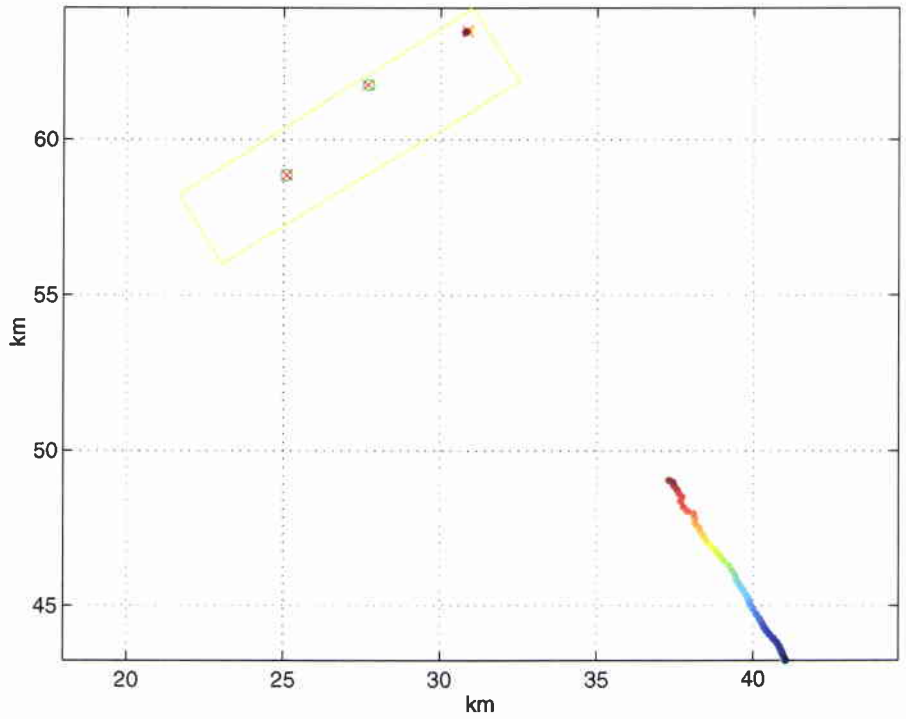

Figure 13 *Analysis of Run 0203, 3500 Hz. Target trajectory from GPS data*

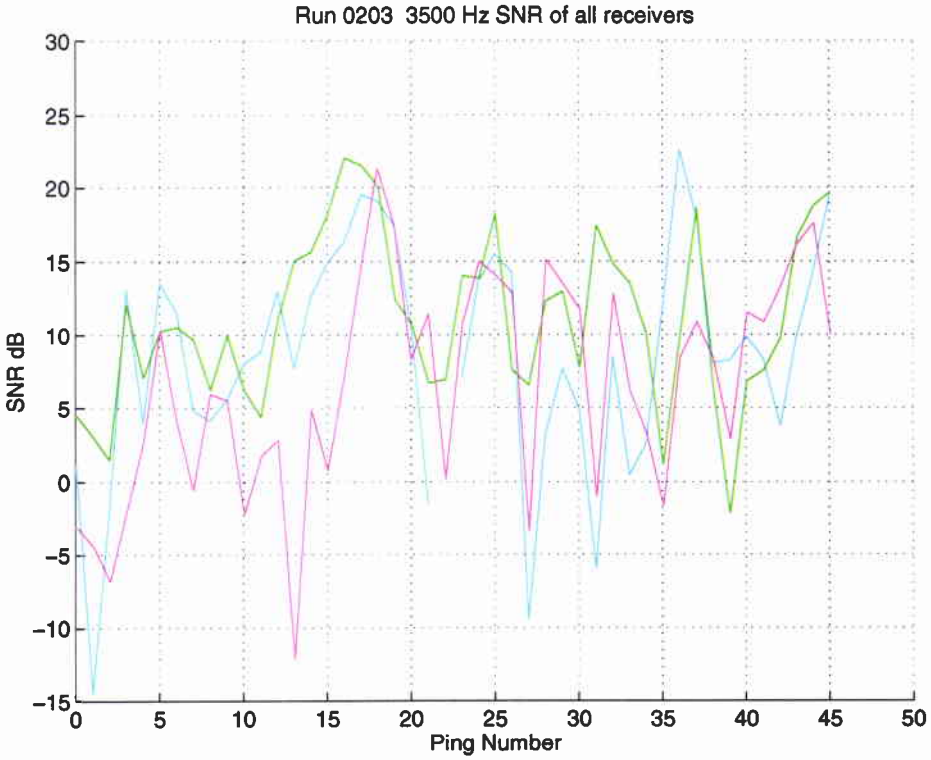

Figure 14 *Analysis of Run 0203, 3500 Hz. SNR of the three receivers (1: blue; 2: green; 3: red) versus ping number.*

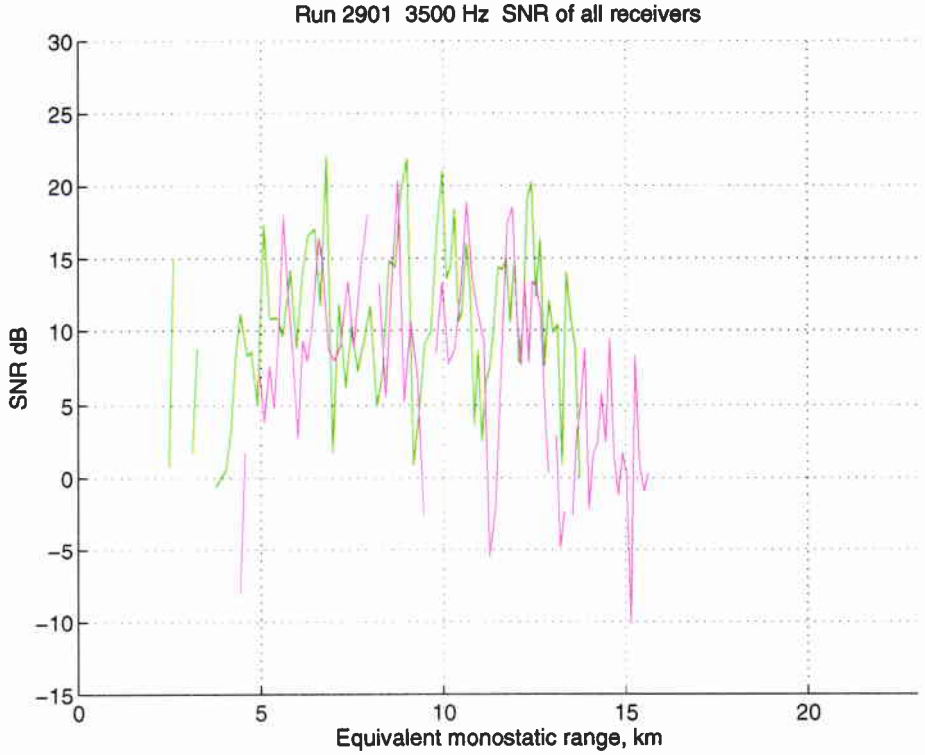

Figure 15 *Analysis of Run 2901, 3500 Hz. SNR of the three receivers (1: blue; 2: green; 3: red) versus equivalent monostatic range.*

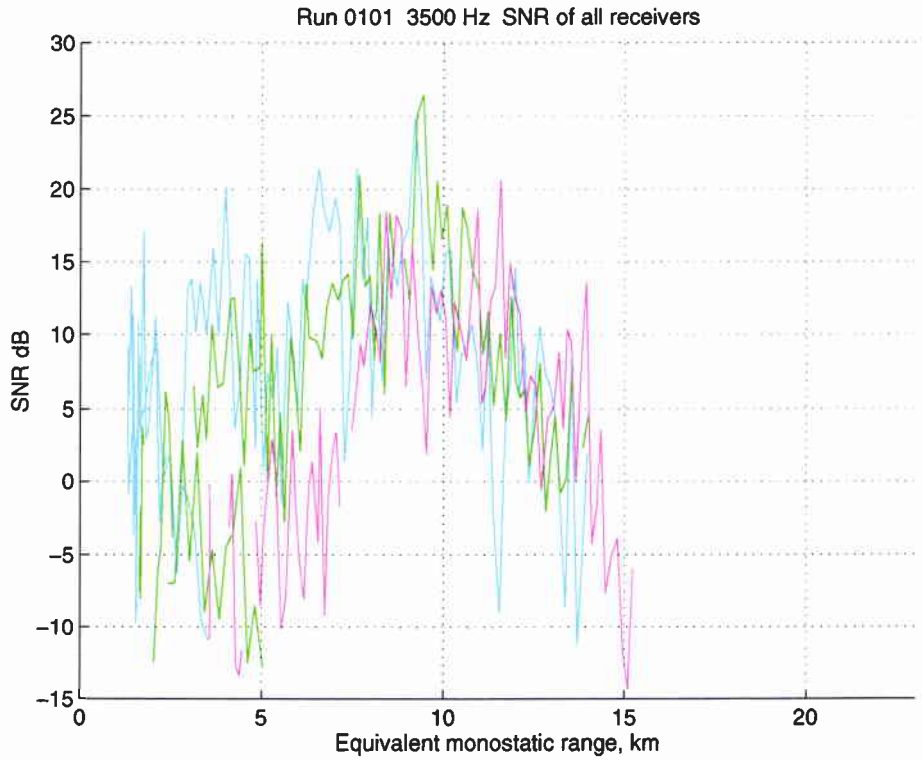

Figure 16 *Analysis of Run 0101, 3500 Hz. SNR of the three receivers (1: blue; 2: green; 3: red) versus equivalent monostatic range.*

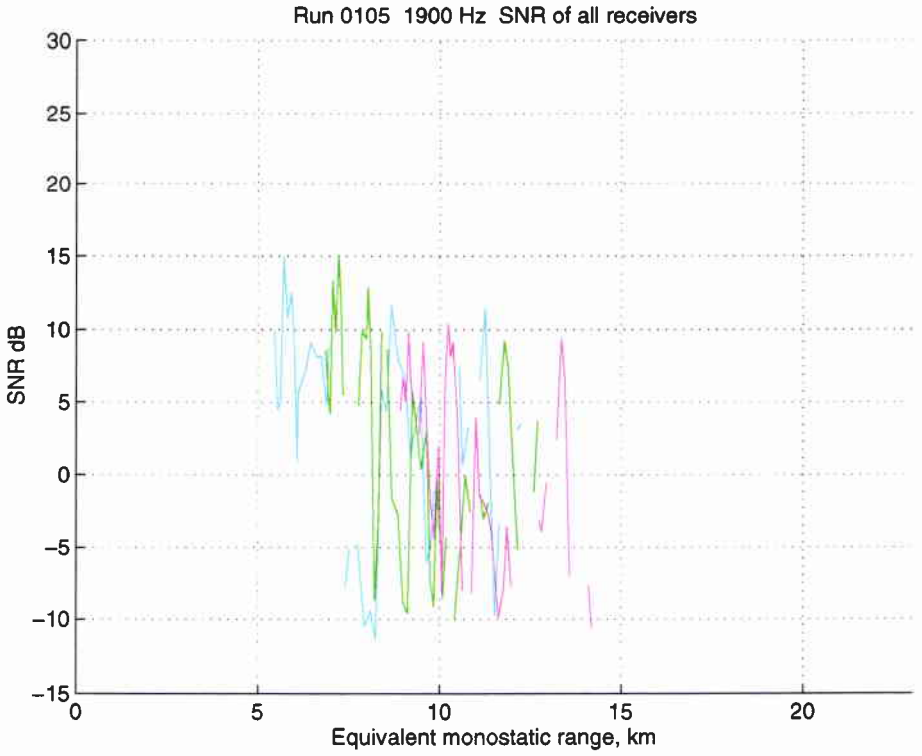

Figure 17 *Analysis of Run 0105, 1900 Hz. SNR of the three receivers (1: blue; 2: green; 3: red) versus equivalent monostatic range.*

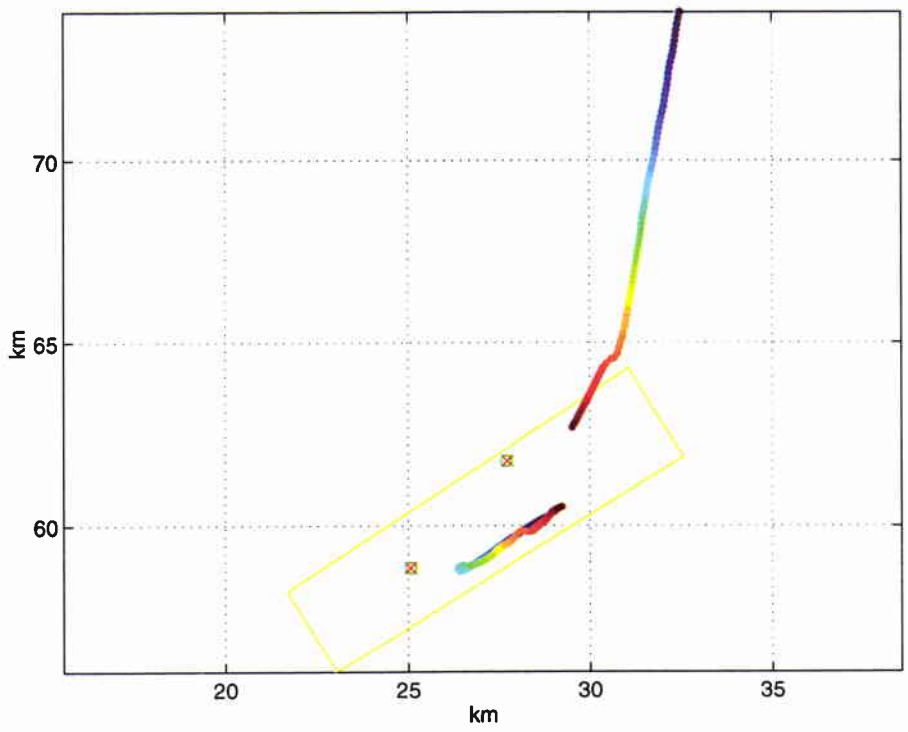

Figure 18 *Analysis of Run 2901, 3500 Hz. Target trajectory from GPS data.*

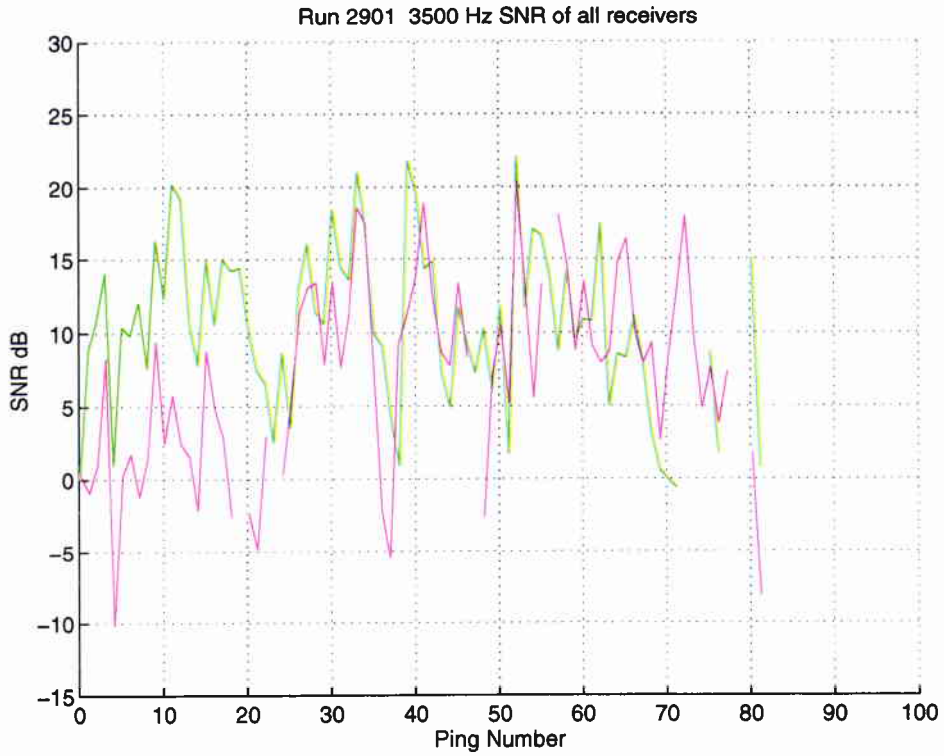

Figure 19 *Analysis of Run 2901, 3500 Hz. SNR of the three receivers (1: blue; 2: green; 3: red) versus ping number.*

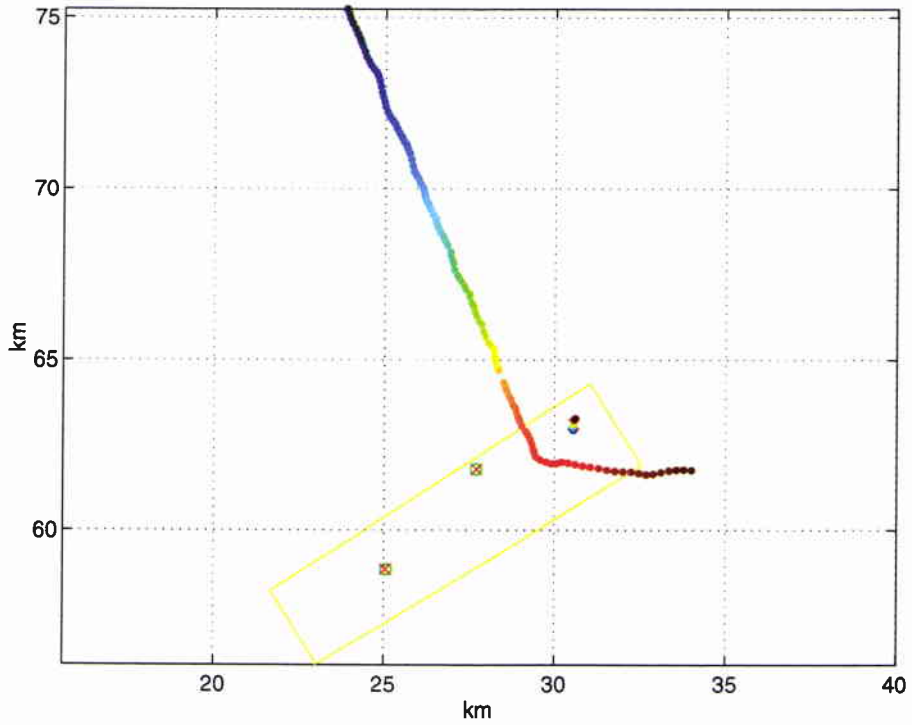

Figure 20 *Analysis of Run 0101, 3500 Hz. Target trajectory from GPS data.*

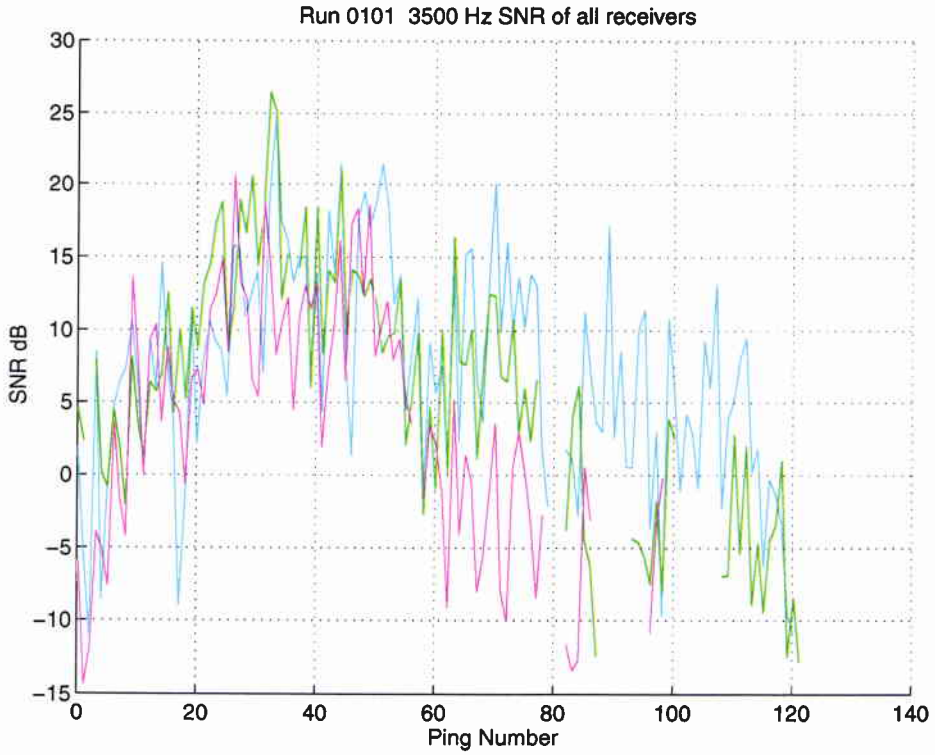

Figure 21 *Analysis of Run 0101, 3500 Hz. SNR of the three receivers (1: blue; 2: green; 3: red) versus ping number.*

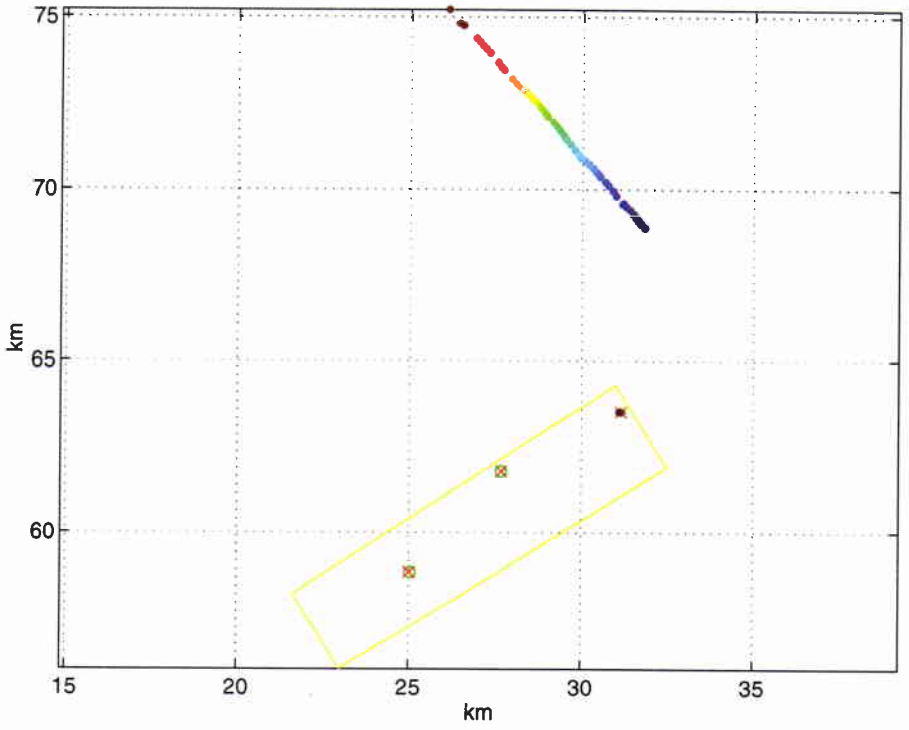

Figure 22 *Analysis of Run 0105, 1900 Hz. Target trajectory from GPS data.*

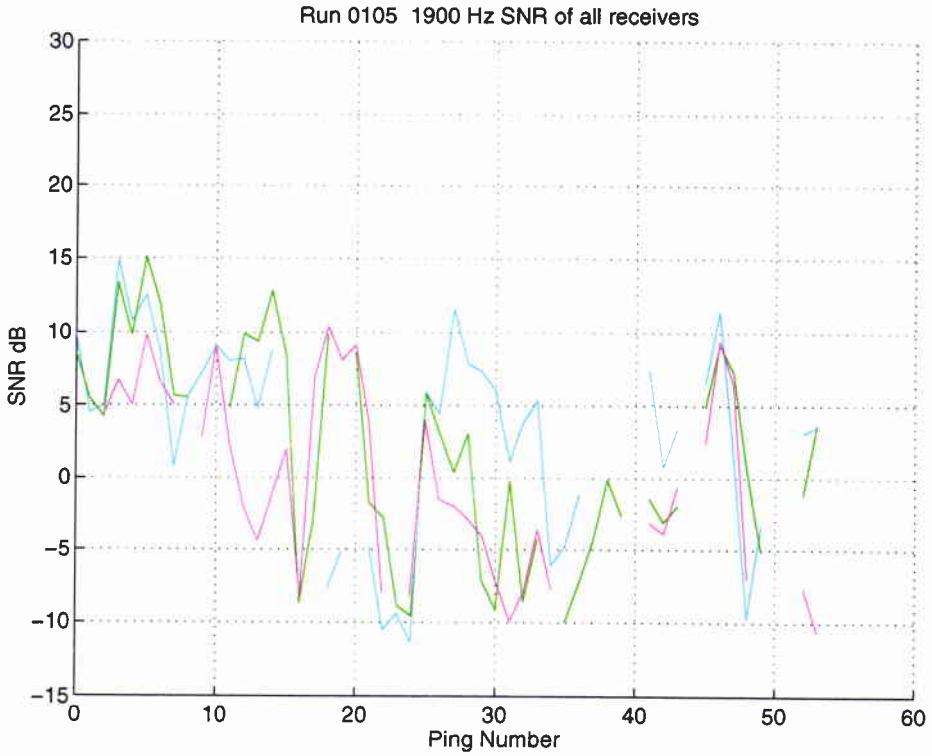

Figure 23 *Analysis of Run 0105, 1900 Hz. SNR of the three receivers (1: blue; 2: green; 3: red) versus ping number.*

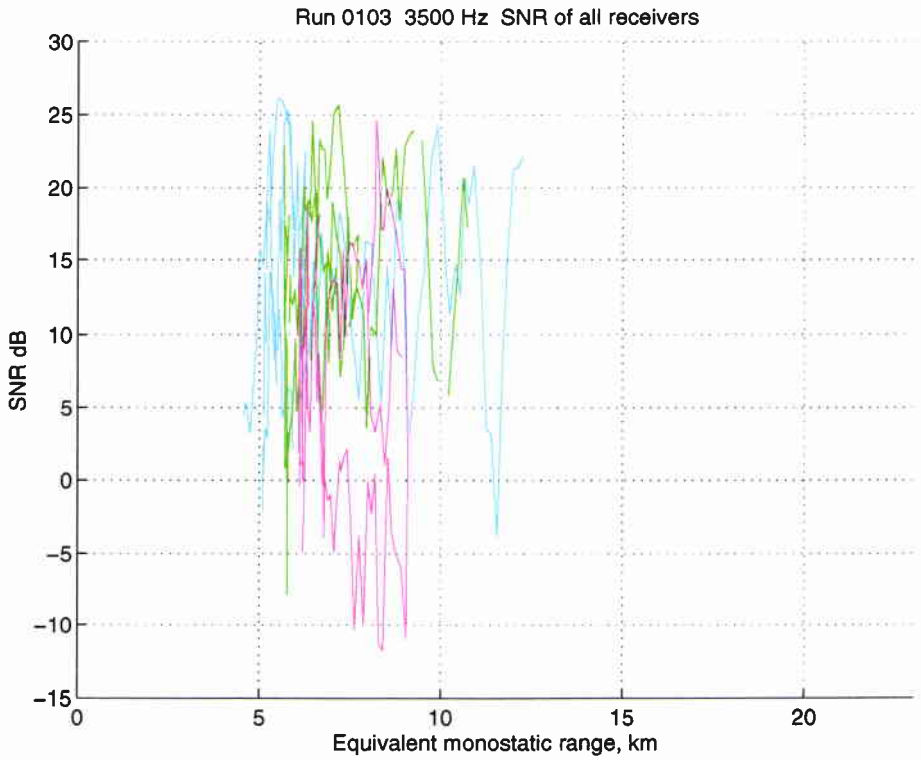

Figure 24 *Analysis of Run 0103, 3500 Hz. SNR of the three receivers (1: blue; 2: green; 3: red) versus equivalent monostatic range.*

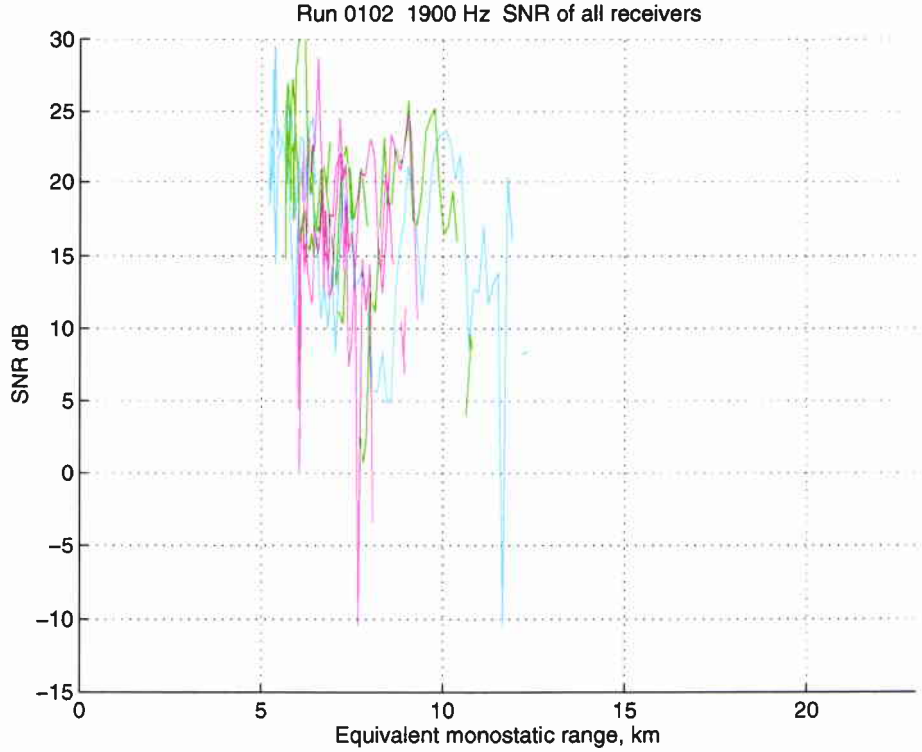

Figure 25 *Analysis of Run 0102, 1900 Hz. SNR of the three receivers (1: blue; 2: green; 3: red) versus equivalent monostatic range.*

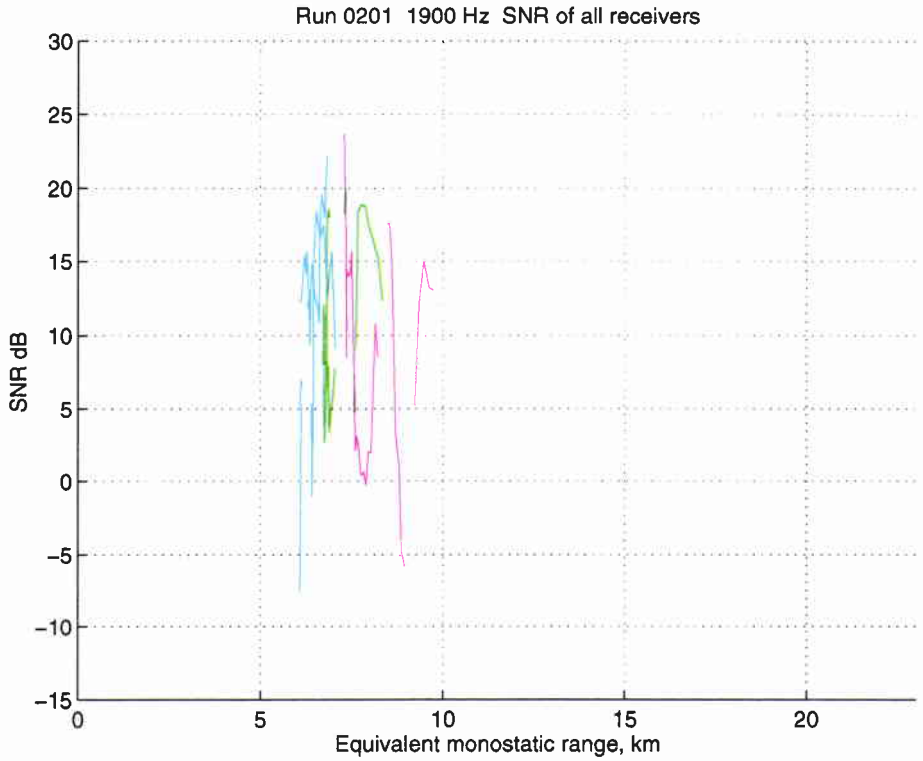

Figure 26 *Analysis of Run 0201, 1900 Hz. SNR of the three receivers (1: blue; 2: green; 3: red) versus equivalent monostatic range.*

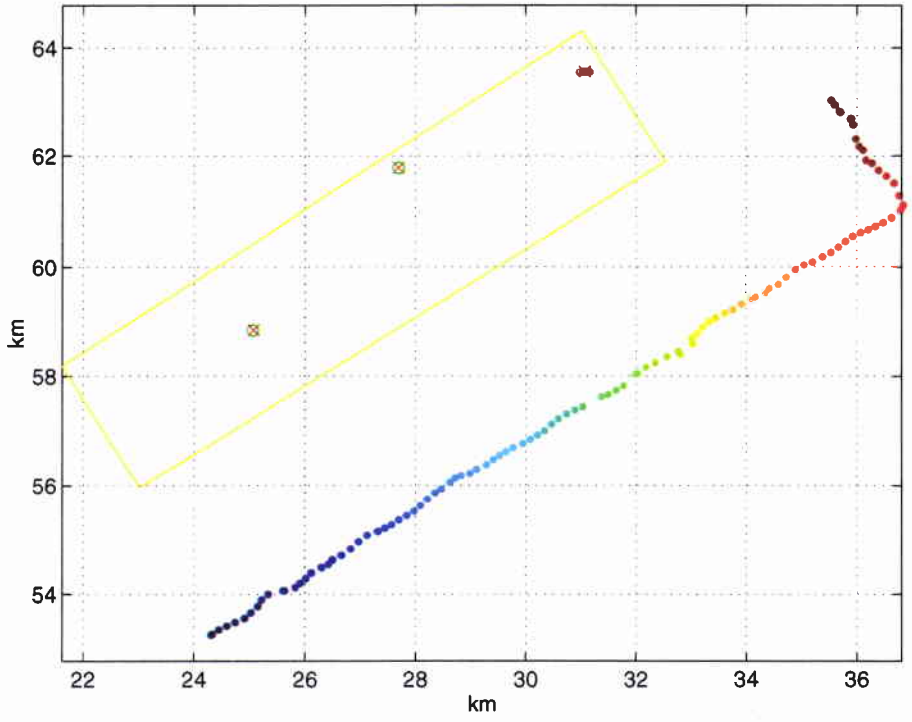

Figure 27 *Analysis of Run 0103, 3500 Hz. Target trajectory from GPS data.*

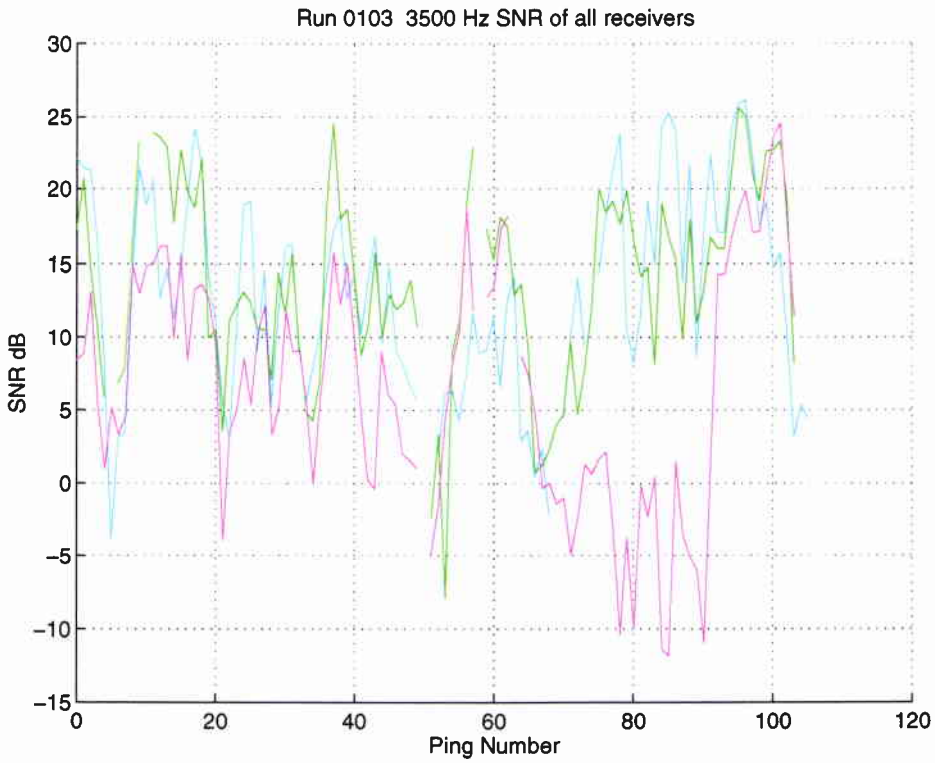

Figure 28 *Analysis of Run 0103, 3500 Hz. SNR of the three receivers (1: blue; 2: green; 3: red) versus ping number.*

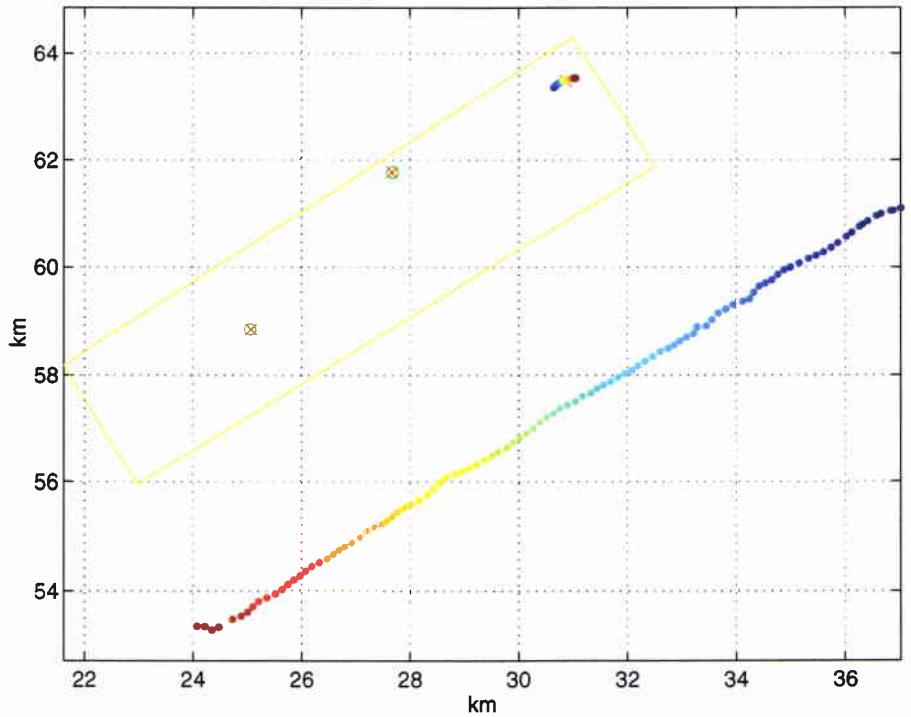

Figure 29 *Analysis of Run 0102, 1900 Hz. Target trajectory from GPS data.*

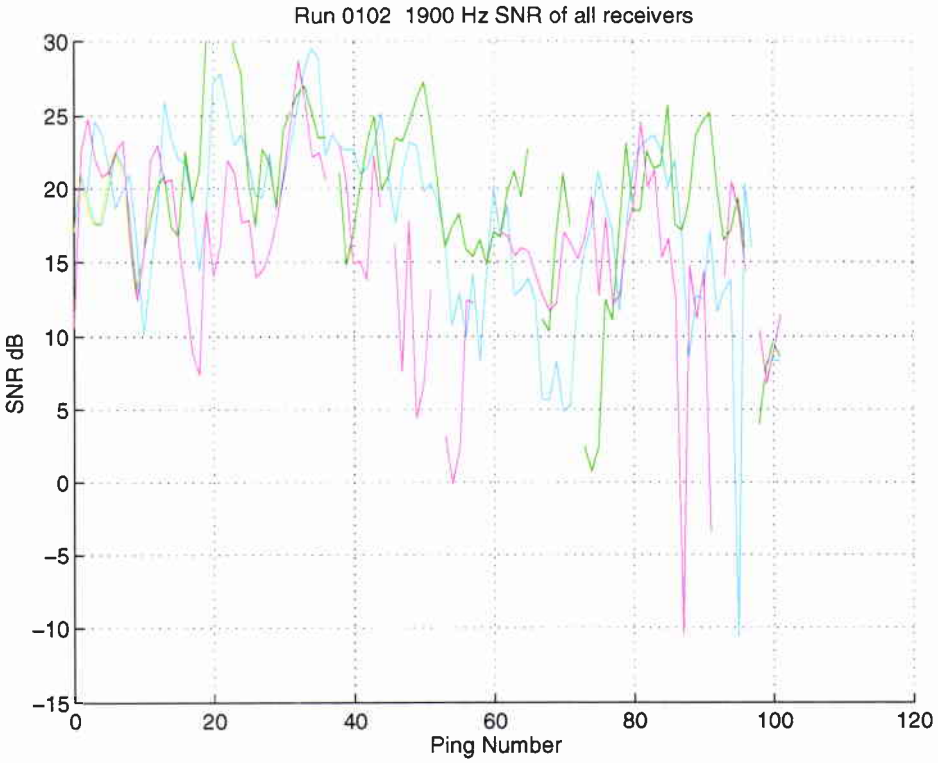

Figure 30 *Analysis of Run 0102, 1900 Hz. SNR of the three receivers (1: blue; 2: green; 3: red) versus ping number.*

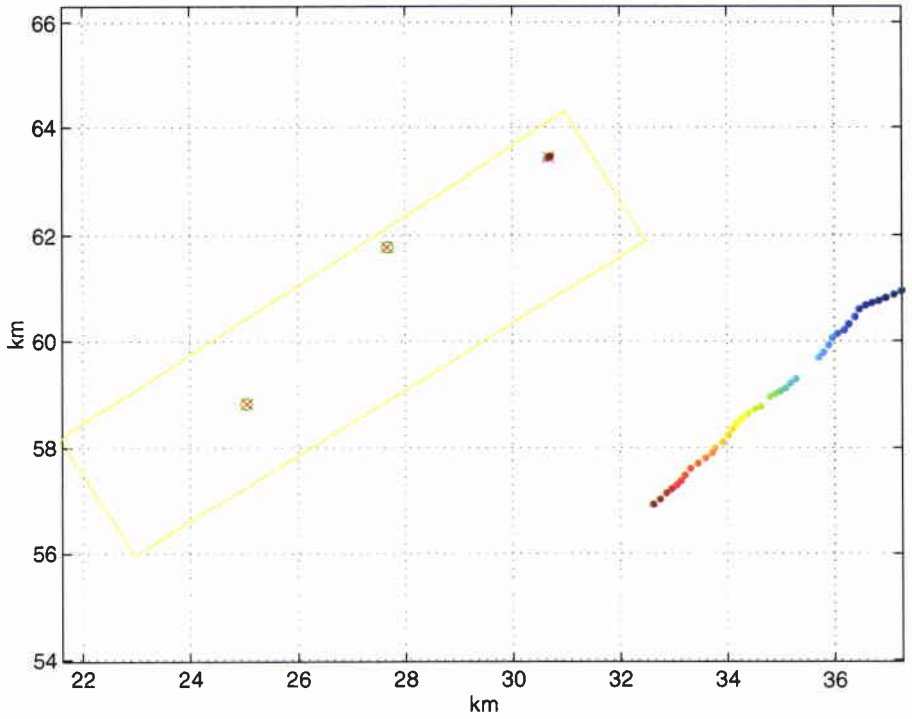

Figure 31 *Analysis of Run 0201, 1900 Hz. Target trajectory from GPS data.*

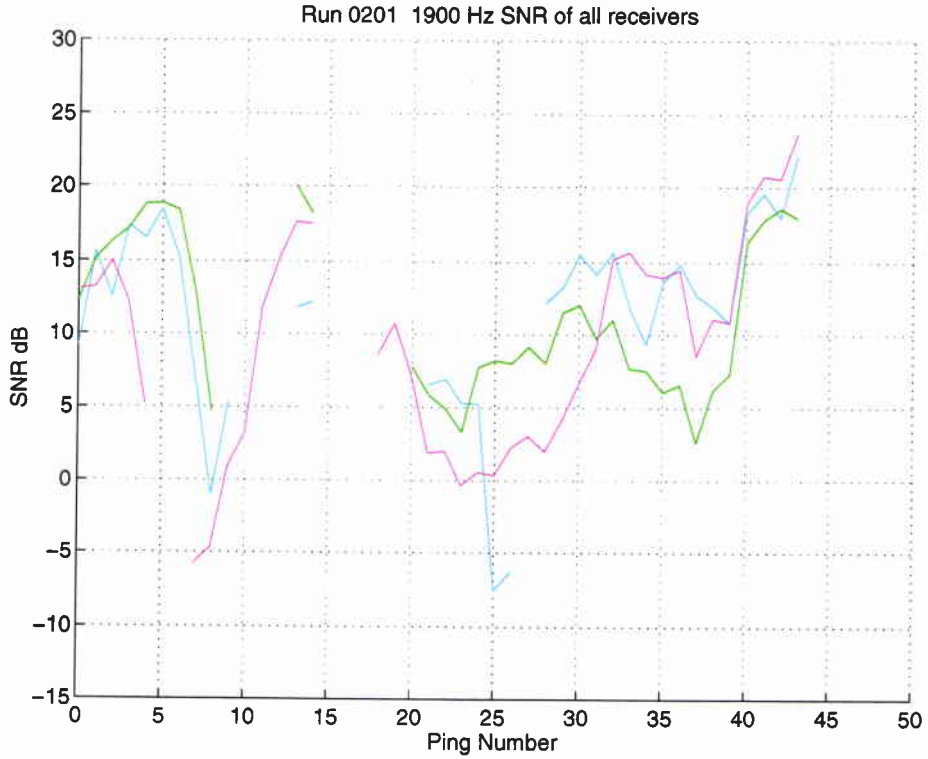

Figure 32 *Analysis of Run 0201, 1900 Hz. SNR of the three receivers (1: blue; 2: green; 3: red) versus ping number.*

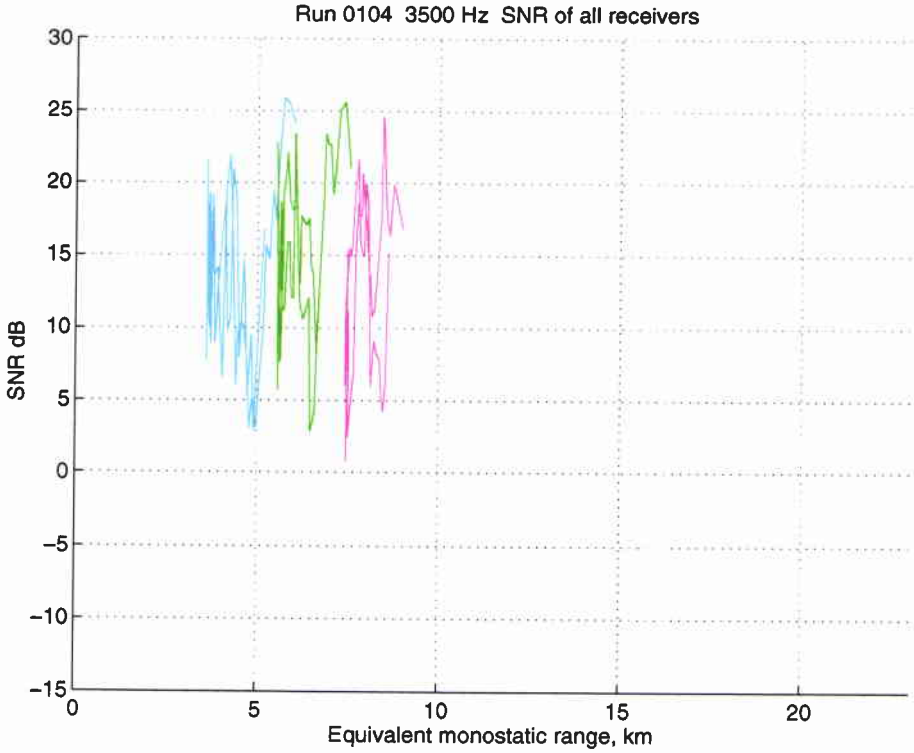

Figure 33 *Analysis of Run 0104, 3500 Hz. SNR of the three receivers (1: blue; 2: green; 3: red) versus equivalent monostatic range.*

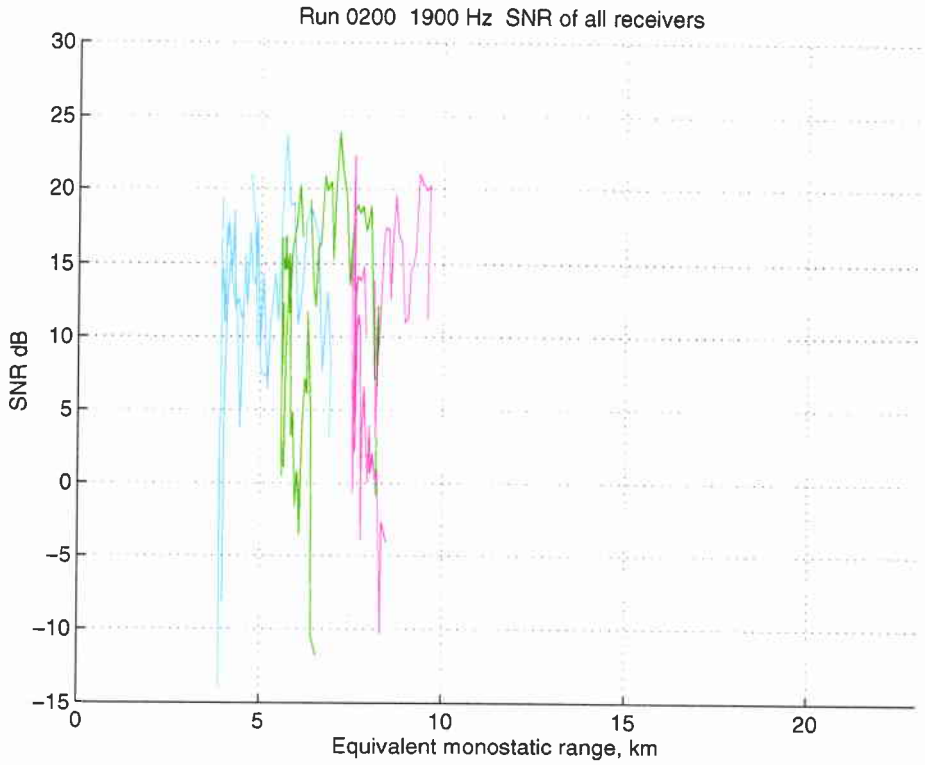

Figure 34 *Analysis of Run 0200, 1900 Hz. SNR of the three receivers (1: blue; 2: green; 3: red) versus equivalent monostatic range.*

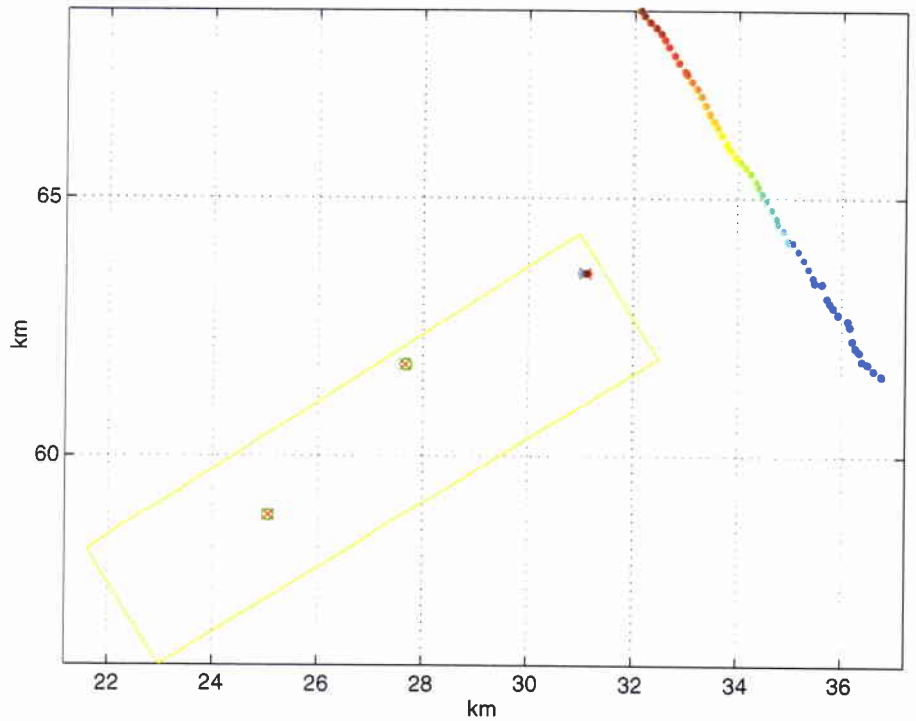

Figure 35 *Analysis of Run 0104, 3500 Hz. Target trajectory from GPS data.*

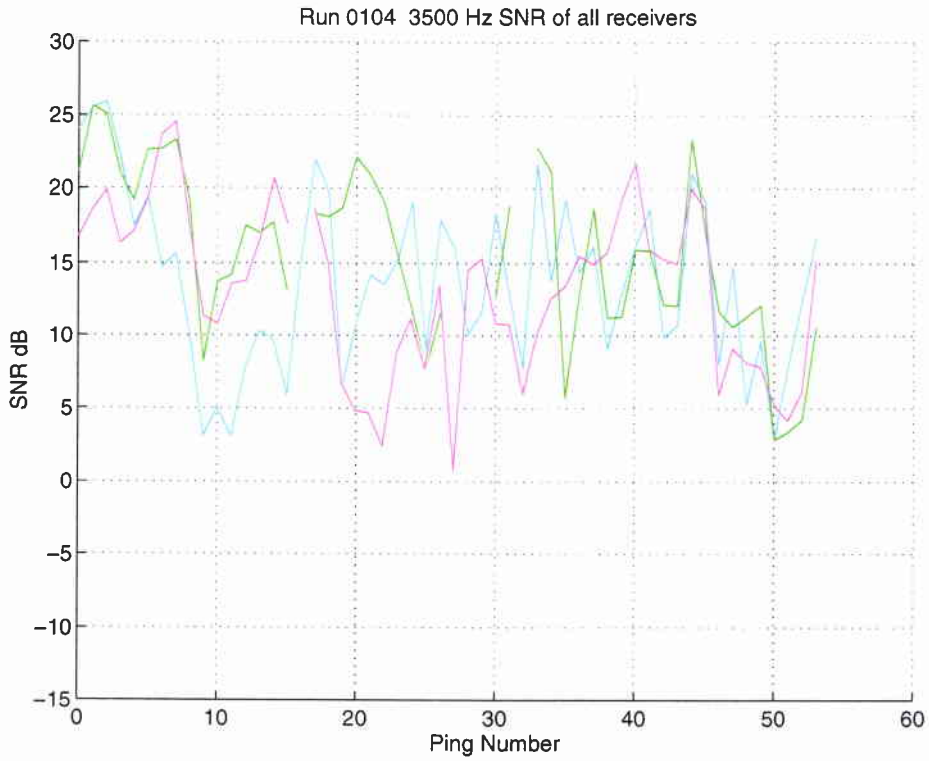

Figure 36 *Analysis of Run 0104, 3500 Hz. SNR of the three receivers (1: blue; 2: green; 3: red) versus ping number.*

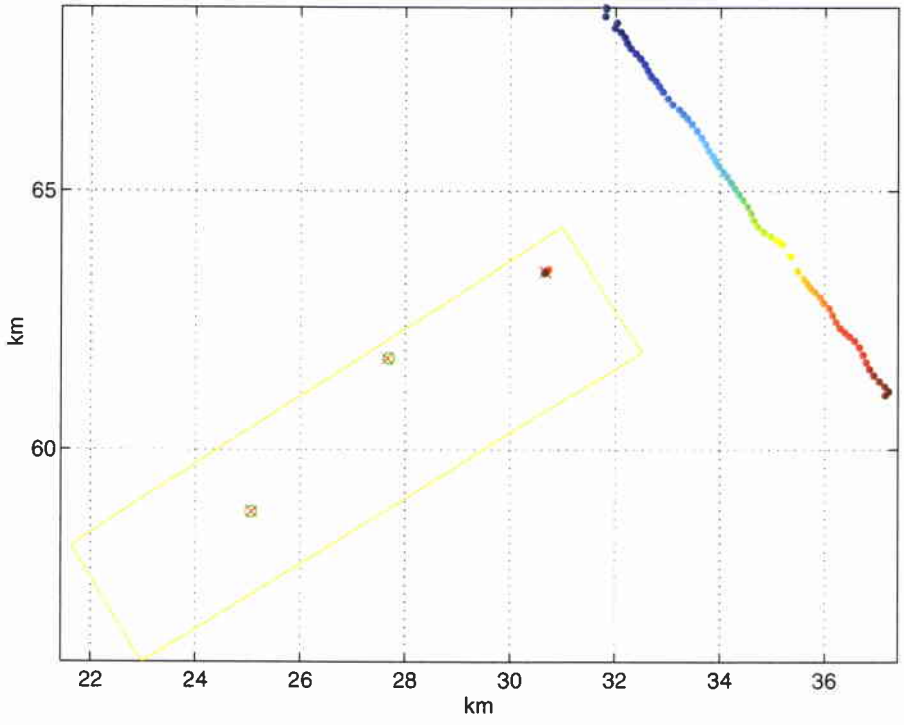

Figure 37 *Analysis of Run 0200, 1900 Hz. Target trajectory from GPS data.*

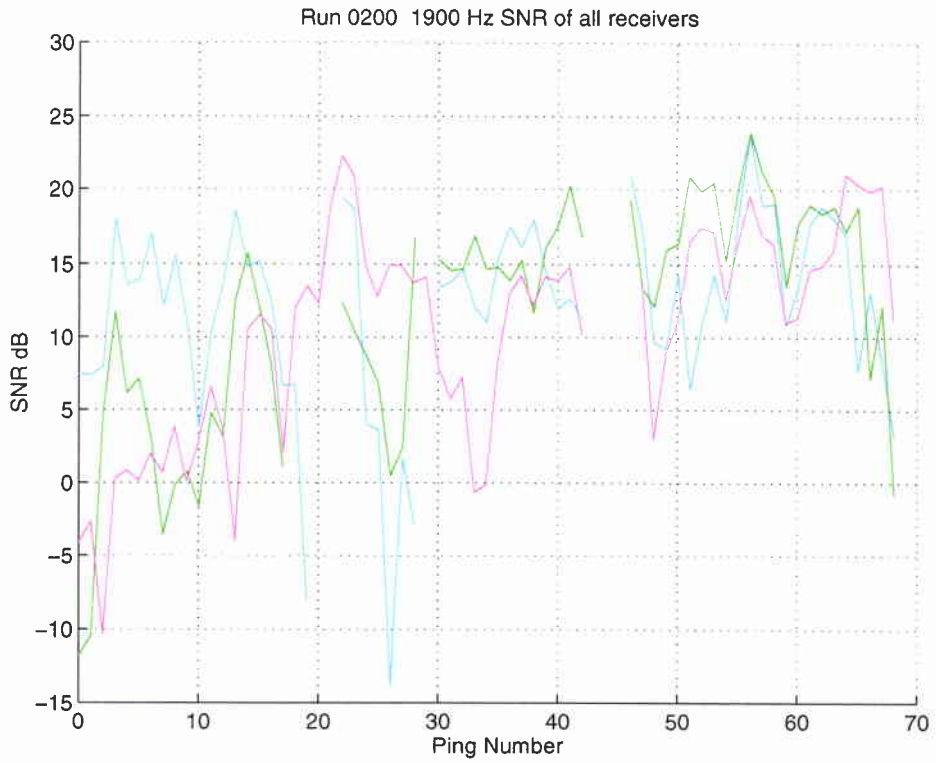

Figure 38 *Analysis of Run 0200, 1900 Hz. SNR of the three receivers (1: blue; 2: green; 3: red) versus ping number.*

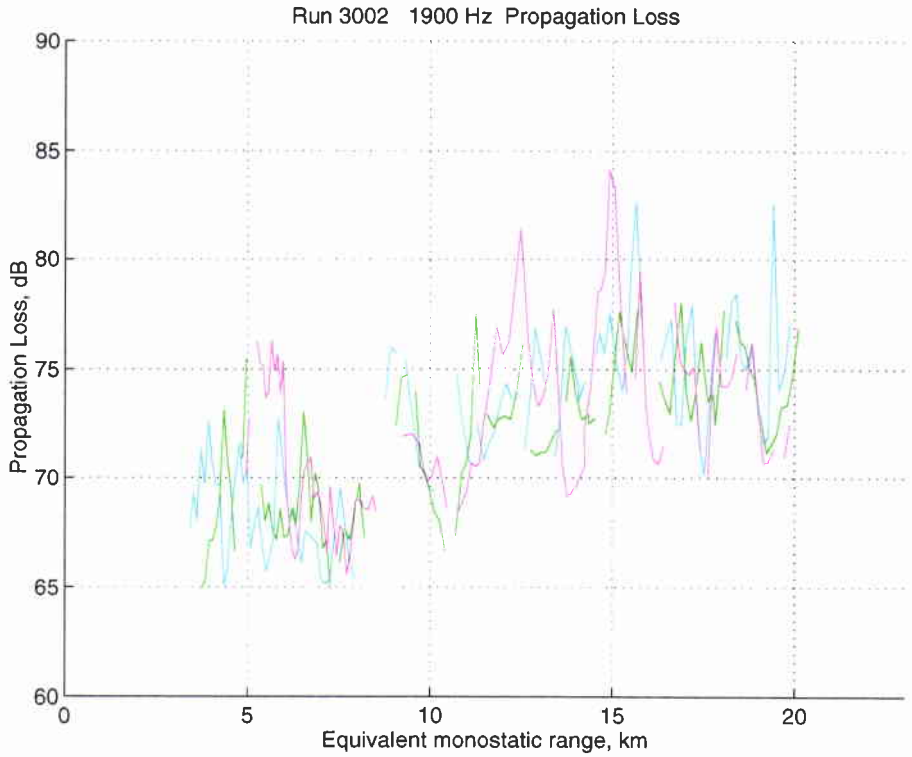

Figure 39 *Run 3002, 1900 Hz. Propagation Loss for the three receivers (1: blue; 2: green; 3: red) versus equivalent monostatic range. Trajectory A.*

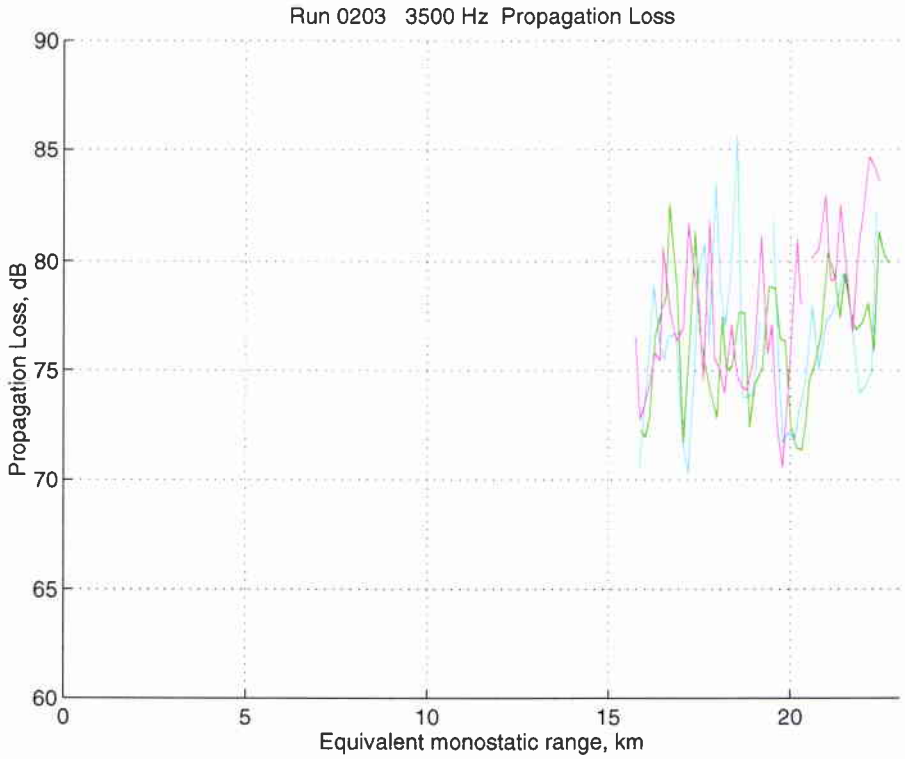

Figure 40 *Run 0203, 3500 Hz. Propagation Loss for the three receivers (1: blue; 2: green; 3: red) versus equivalent monostatic range. Trajectory A.*

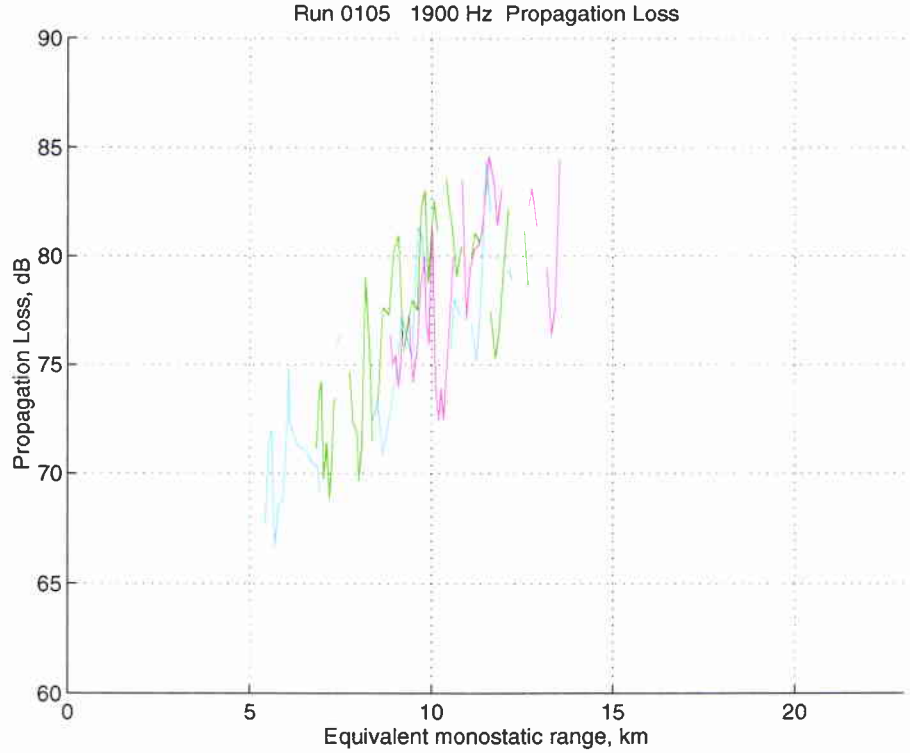

Figure 41 *Run 0105, 1900 Hz. Propagation Loss for the three receivers (1: blue; 2: green; 3: red) versus equivalent monostatic range. Trajectory F.*

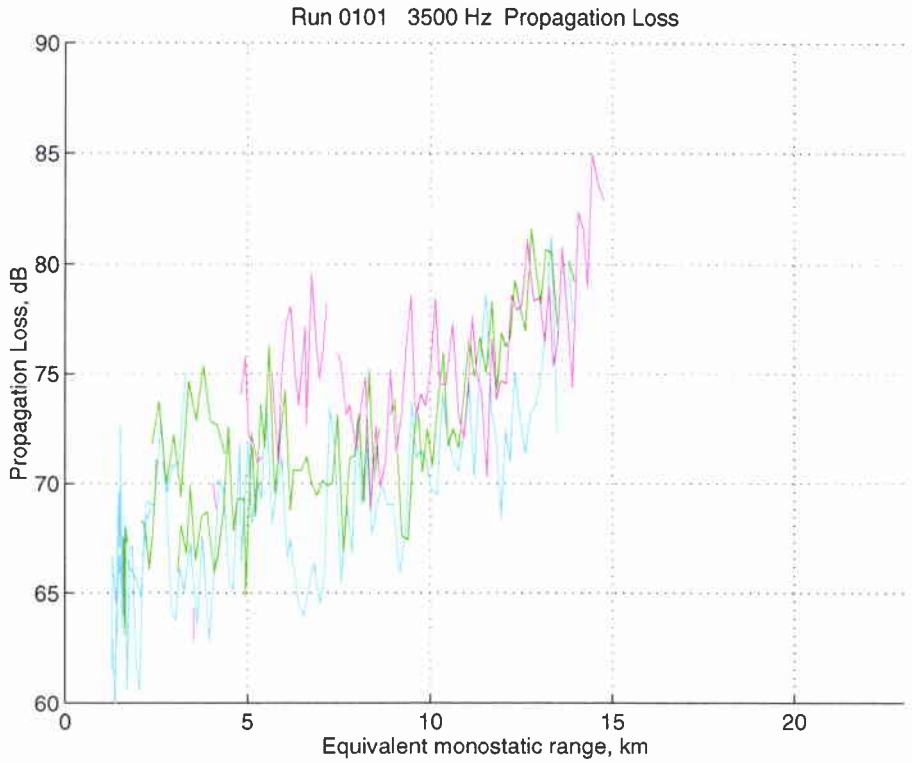

Figure 42 *Run 0101, 3500 Hz. Propagation Loss for the three receivers (1: blue; 2: green; 3: red) versus equivalent monostatic range. Trajectory F.*

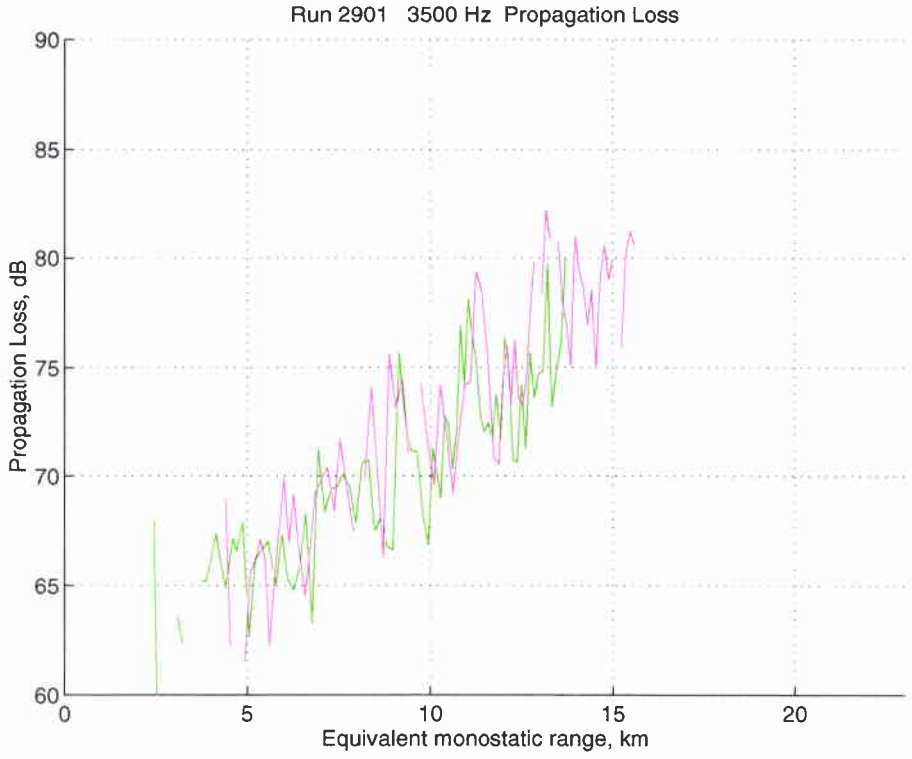

Figure 43 *Run 02901, 3500 Hz. Propagation Loss for the three receivers (1: blue; 2: green; 3: red) versus equivalent monostatic range. Trajectory F.*

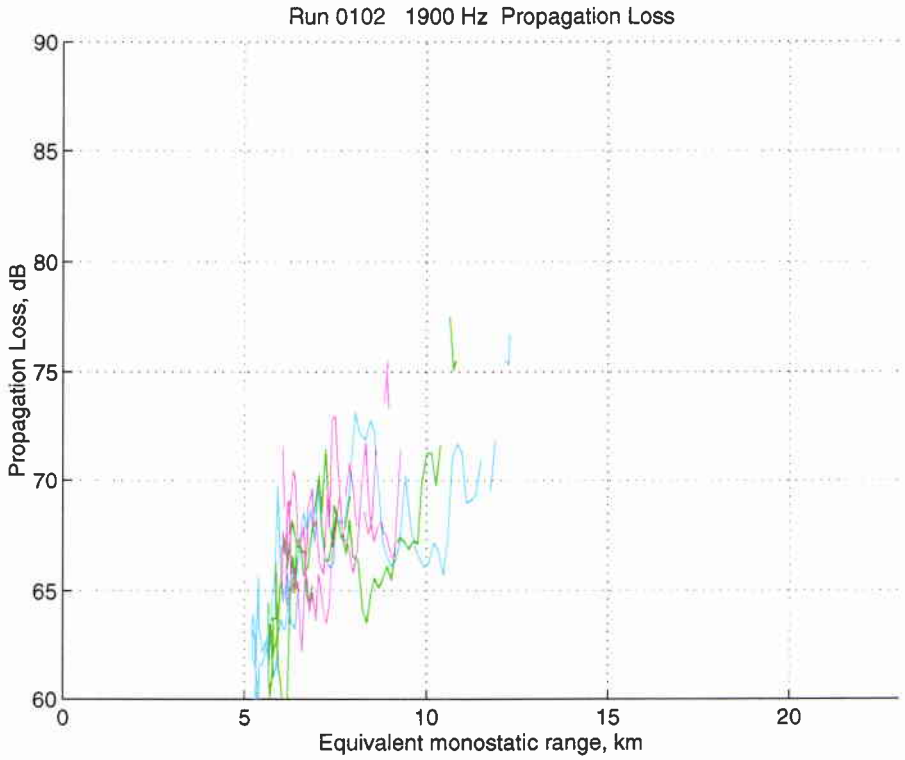

Figure 44 *Run 0102, 1900 Hz. Propagation Loss for the three receivers (1: blue; 2: green; 3: red) versus equivalent monostatic range. Trajectory C.*

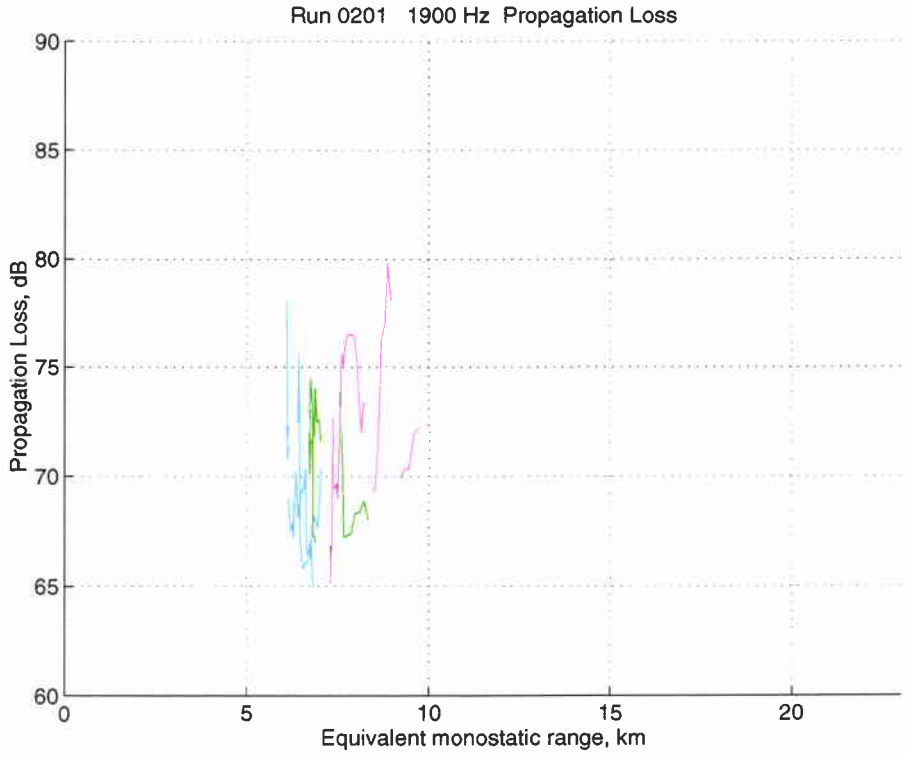

Figure 45 *Run 0201, 1900 Hz. Propagation Loss for the three receivers (1: blue; 2: green; 3: red) versus equivalent monostatic range. Trajectory C.*

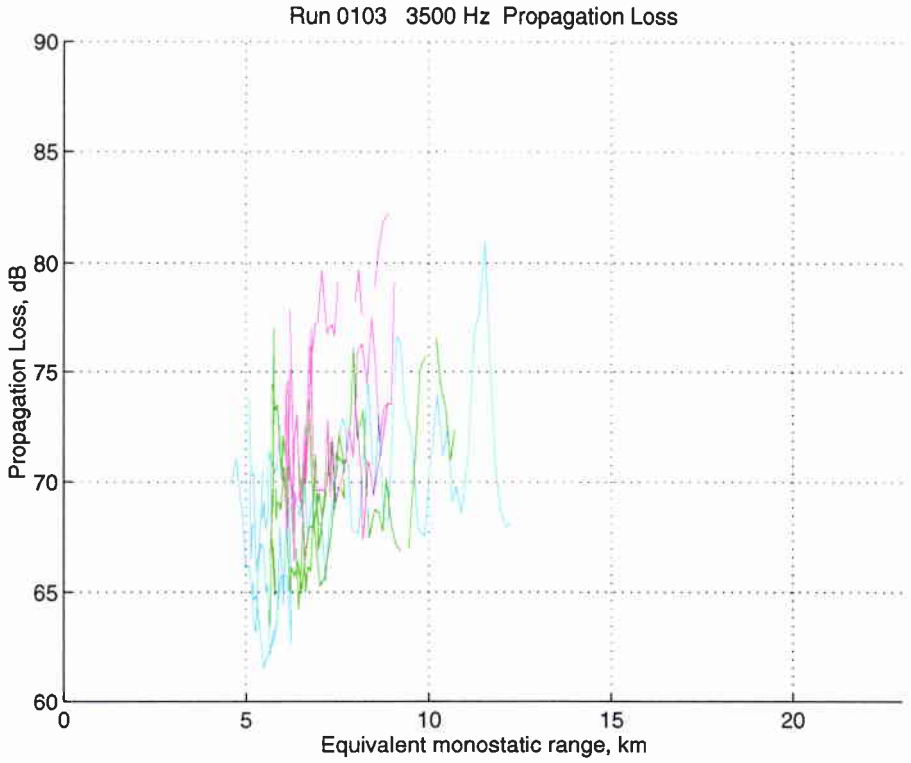

Figure 46 *Run 0103, 3500 Hz. Propagation Loss for the three receivers (1: blue; 2: green; 3: red) versus equivalent monostatic range. Trajectory C.*

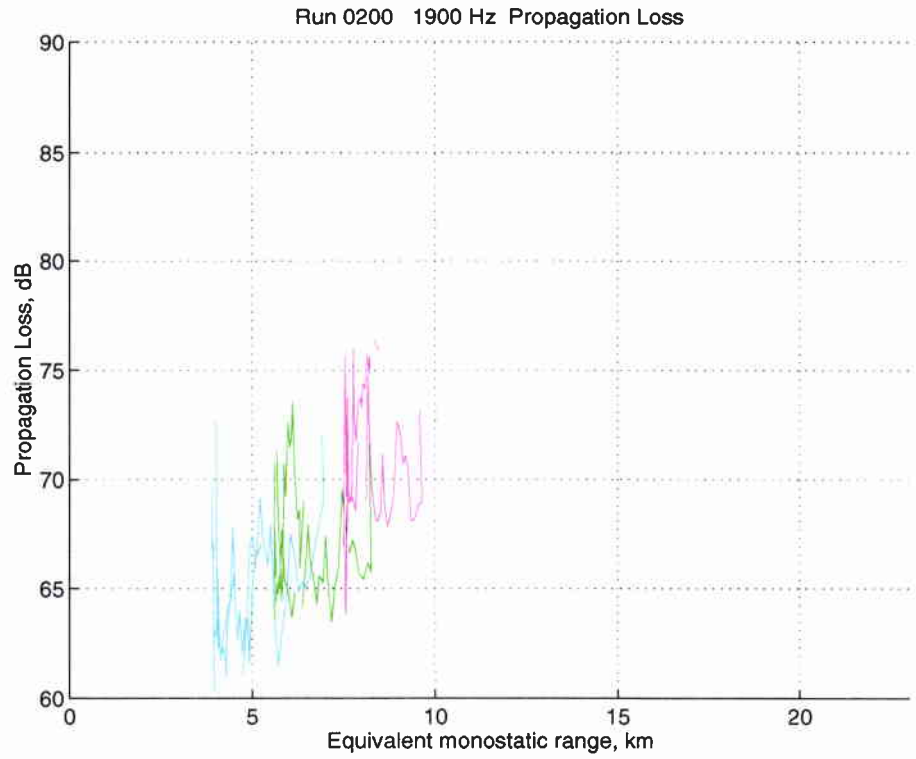

Figure 47 *Run 0200, 1900 Hz. Propagation Loss for the three receivers (1: blue; 2: green; 3: red) versus equivalent monostatic range. Trajectory D.*

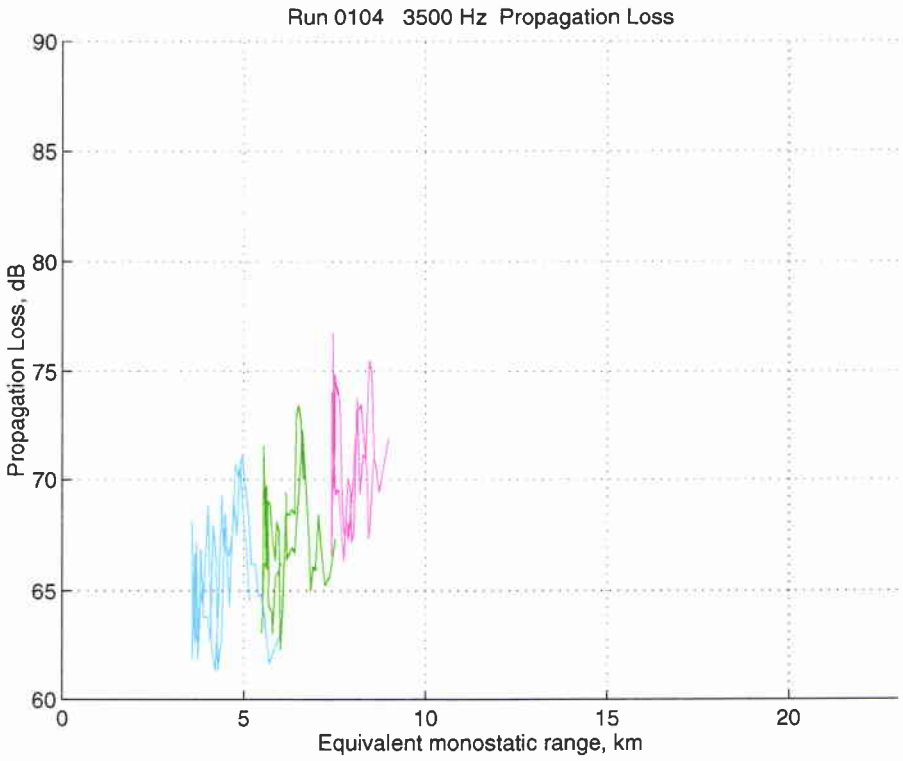

Figure 48 *Run 0104, 3500 Hz. Propagation Loss for the three receivers (1: blue; 2: green; 3: red) versus equivalent monostatic range. Trajectory D.*

Annex A - The experimental sonar system

1900 Hz Transmitter: SL = 204 dB, 200 Hz bandwidth, 10 elements at 0.5 lambda, no shading is used. Maximum depth: 90 m, battery powered and activated via radio. During the tests it was hanging overboard while the ship was kept on station.

0.9 kHz Transmitter: SL = 210 dB, 150 Hz bandwidth, 2 elements at 0.5 lambda. It was either hanging overboard or towed. It included a depth sensor, the readings of which are recorded.

3.5 kHz Transmitter: SL = 205.5 ±2.5 dB, 200 Hz bandwidth, 5 elements at 0.5 lambda. It was coupled to the transmitter above.

Table A1 *Source Levels and -3 dB Beam widths in degrees*

Frequency	Source Level	Vertical Beamwidth
900 Hz	210 ± 0 dB	100°
1900 Hz	204 ± 0 dB	10.5°
2500 Hz	215.5 ± 2.5 dB	16.2°
3500 Hz	205.5 ± 2.5 dB	20.8°

Receivers:
25 star shaped, calibrated hydrophones. The length of the arms was tuned for best performance in the three bands above. The receivers were moored to the bottom (80 m depth), battery powered and transmitted base banded data *via* radio link to *Alliance*. They were triggered by transmitter pulse to work on a band of +/- 120 Hz for 50 s, after which they return to stand-by mode. They included a compass to allow beamforming relative to the North.

Frequency	Horizontal	Vertical	DI	AG_H
900 Hz	28.1°	81.6°	10.5 dB	9.8 dB
1900 Hz	13.2°	54.6°	13.3 dB	12.5 dB
2700 Hz	9.3°	46.4°	13 dB	11.4 dB
3500 Hz	7.1°	40.7°	12.9 dB	11.3 dB

Table A2 *Shows -3 dB Beam widths in degrees, DI and horizontal Array Gain (AG_H) in dB:*

Positioning: Positions and trajectories of all elements, including shipping traffic and sonar moored assets, were measured with GPS or radar and stored. They are vital for reconstruction of the multistatic geometry of the experiments. A system named RELAPS allows real time transmission of the position of a remote ship or sonar *via* radio to *Alliance*.

Processing: Data from receivers are stored on Exabyte tape, signals are processed in real time by general purpose Alpha workstations, (beam forming, replica correlation and display processes).

Annex B - Analysis of runs

This section documents the data processed and analyzed in this study with a common set of plots. Noise levels, reverberation and ranges are shown in the sequence of figures indicated by Table B1.

RUN	Frequency kHz	Pulse duration seconds	Duration minutes	Source depth metres	Target depth metres	Towed/Fixed source	Target trajectory
0102	1.9	1 s	90	80	90	Fixed	C
0103	3.5	1 s	90	110	90	Fixed	C
0201	1.9	1 s	120	80	90	Fixed	C
3002	1.9	1 s	120	84	90	Fixed	A
0203	3.5	1 s	120	110	90	Fixed	A
0104	3.5	1 s	60	110	90	Fixed	D
0200	1.9	1 s	60	80	90	Fixed	D
2901	3.5	1 s	120	93	60 - 90	Towed	F
0101	3.5	4 s	120	110	60 - 90	Fixed	F
0105	1.9	1 s	60	80	60 - 90	Fixed	F

Table B1 *Summary of runs.*

Plot 1 shows the geometry of source, receivers and target trajectory from GPS log files. Receivers 1 to 3 are plotted as green circles from NE to SW in the yellow box. The transmitter is co-located with Receiver 1. Target and (when towed) source trajectories are plotted with coloured dots. The colour scale shows elapsed time.

Plot 2 shows the distance of the target from the source (in cyan), the receiver (in red) *versus* ping number. The equivalent monostatic range (half the sum of the former distances) is shown in green). Note that for monostatic cases (Receiver 1) the three distances are coincident to the cyan line.

Plot 3 shows the processed data: Echo energy is plotted in dB ref. $\mu Pa*\sqrt{s}$ (in green). The background reverberation + noise levels averaged in a window just before (in cyan) and after (in blue) the echo arrival. Echo repeater delay was compensated for. The exact noise / reverberation series that would limit detection of a real target are shown. The noise reference from a distant window of the same beam, averaged throughout the run, is shown in magenta, with a straight line. The relative position of noise and background around the echo show if detection is limited by reverberation.

Plot 4 shows computed SNR *versus* ping number. Detection performance against a reference TS of 10 dB is reconstructed from the time series in Plot 3.

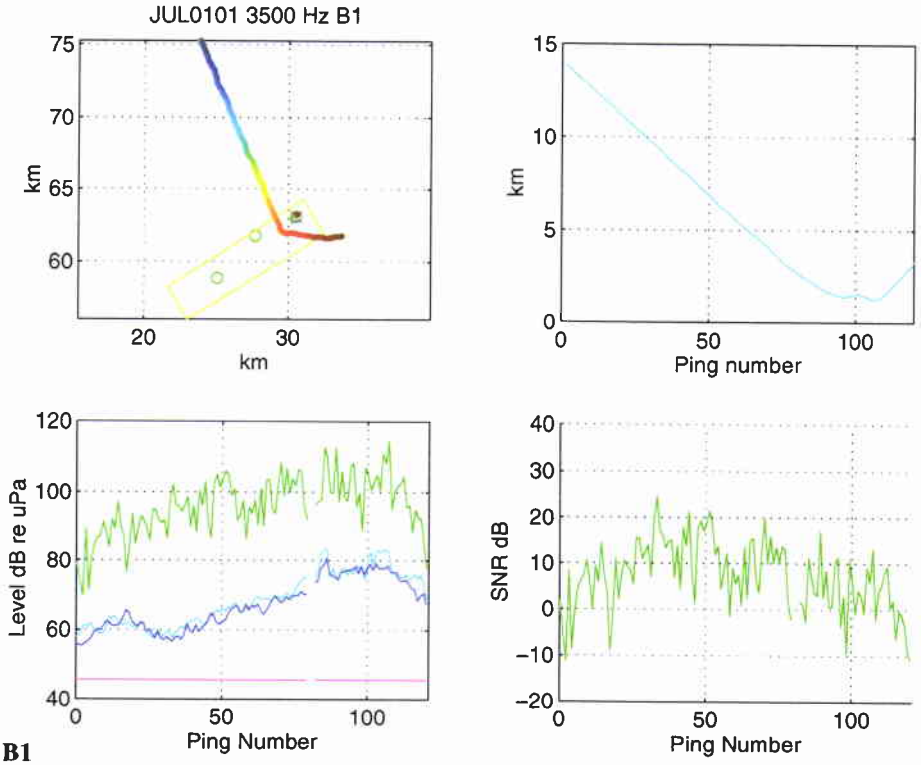

Figure B1

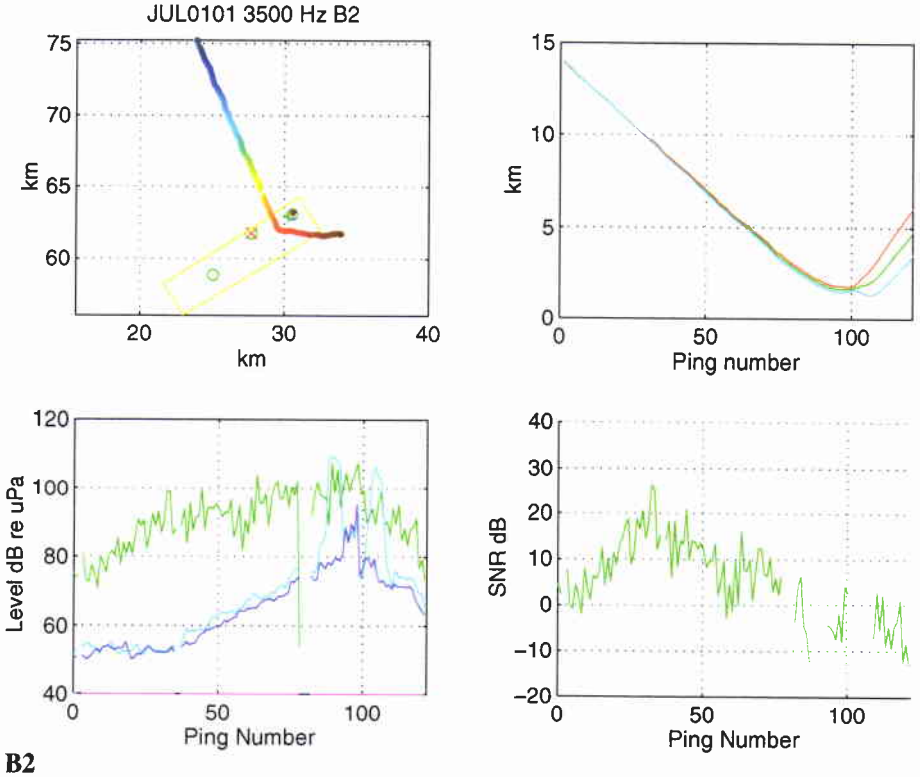

Figure B2

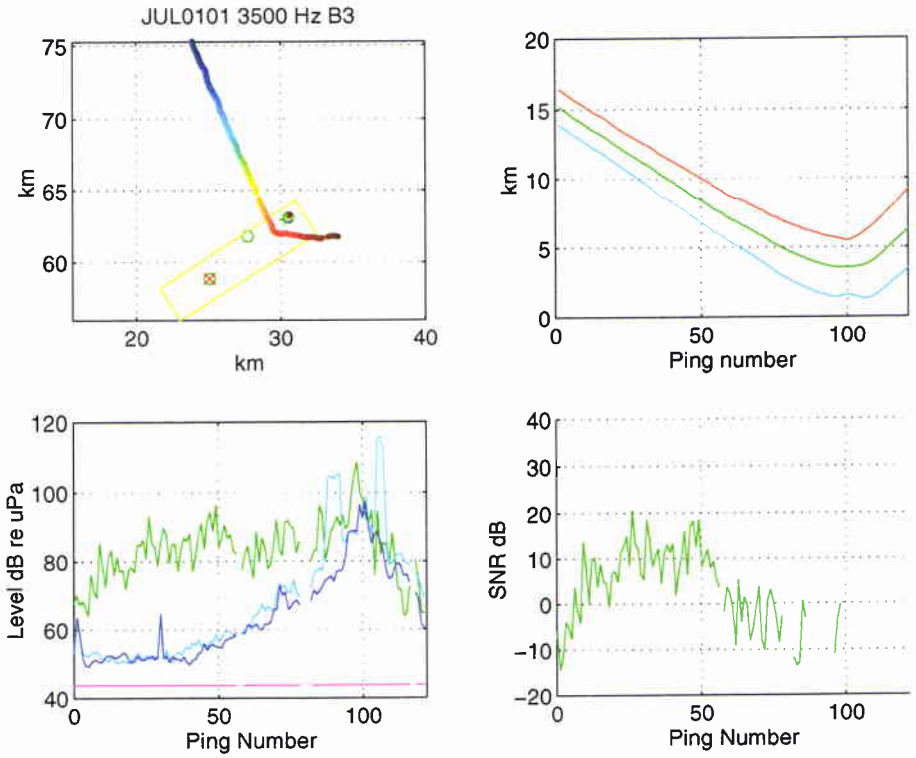

Figure B3

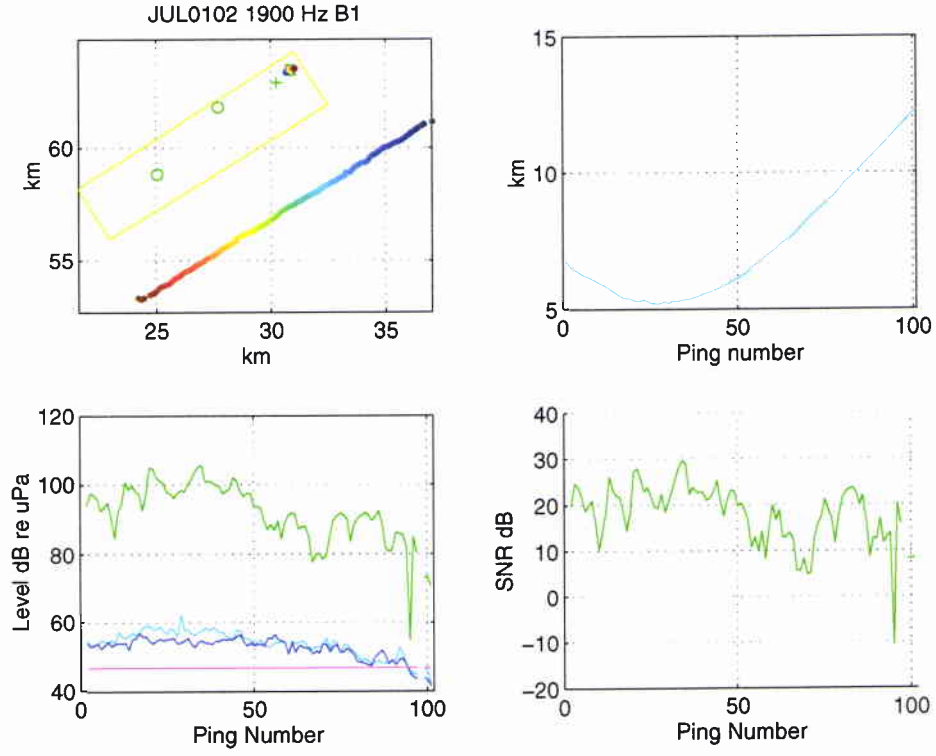

Figure B4

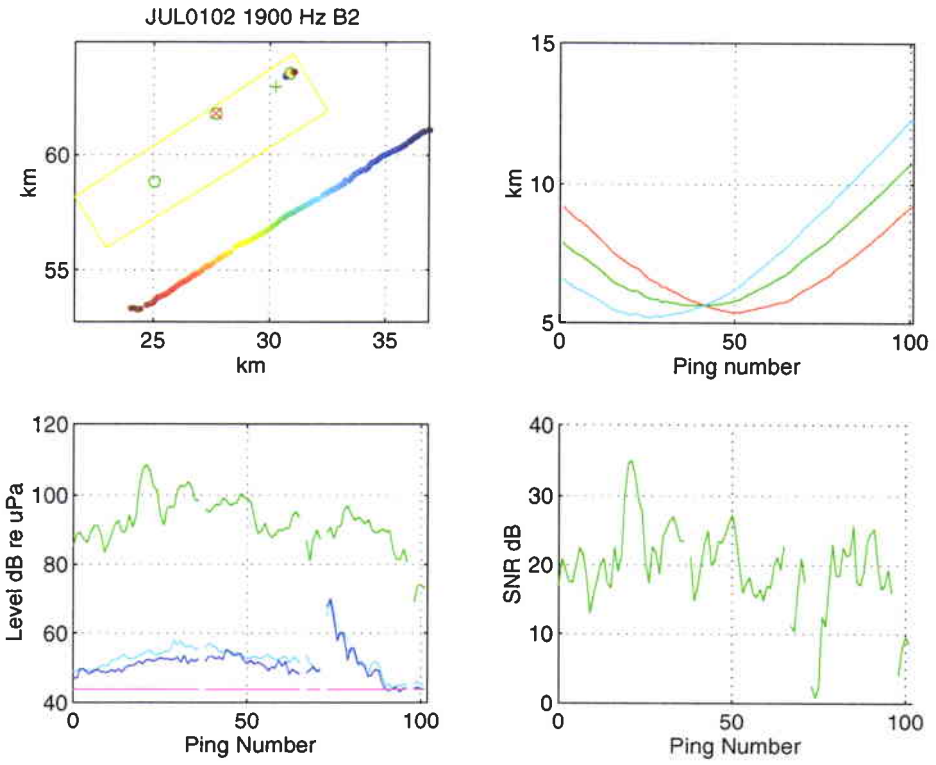

Figure B5

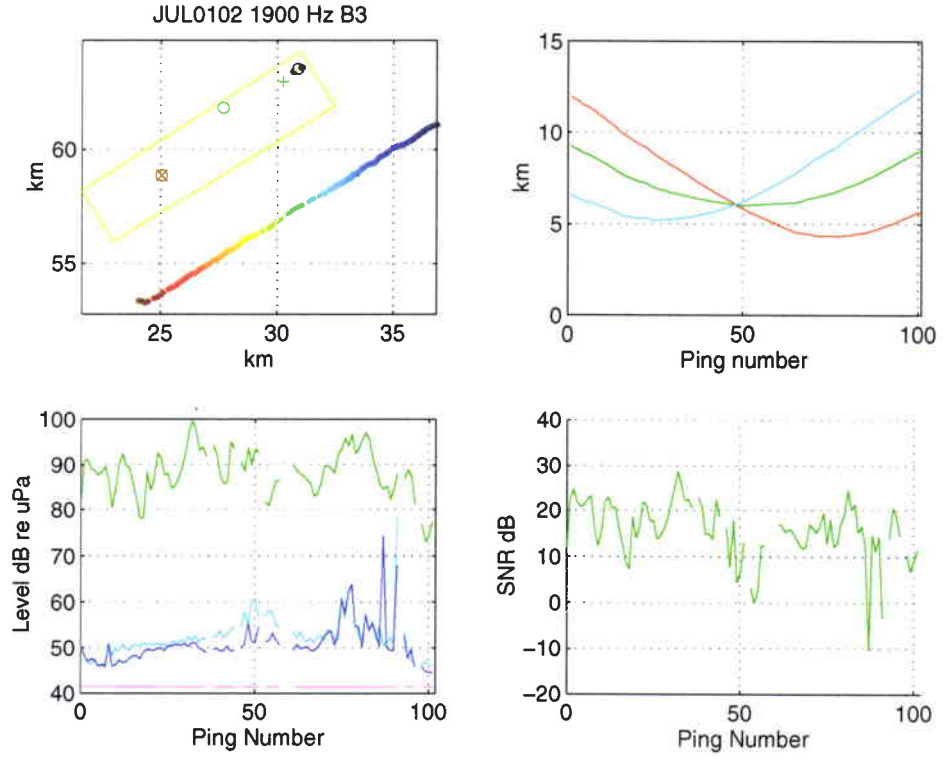

Figure B6

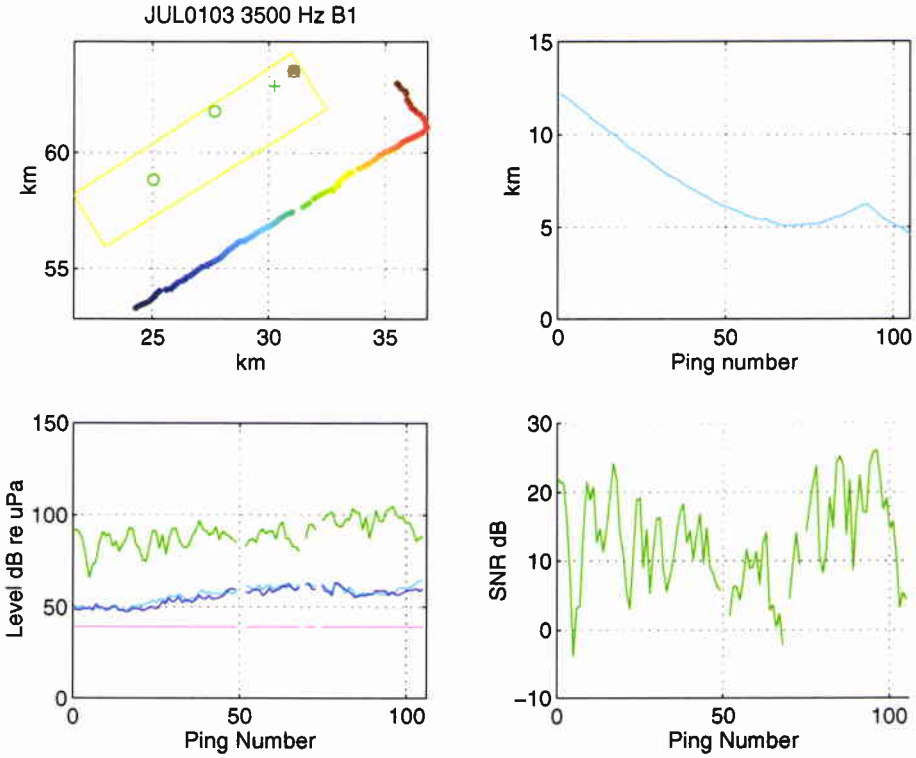

Figure B7

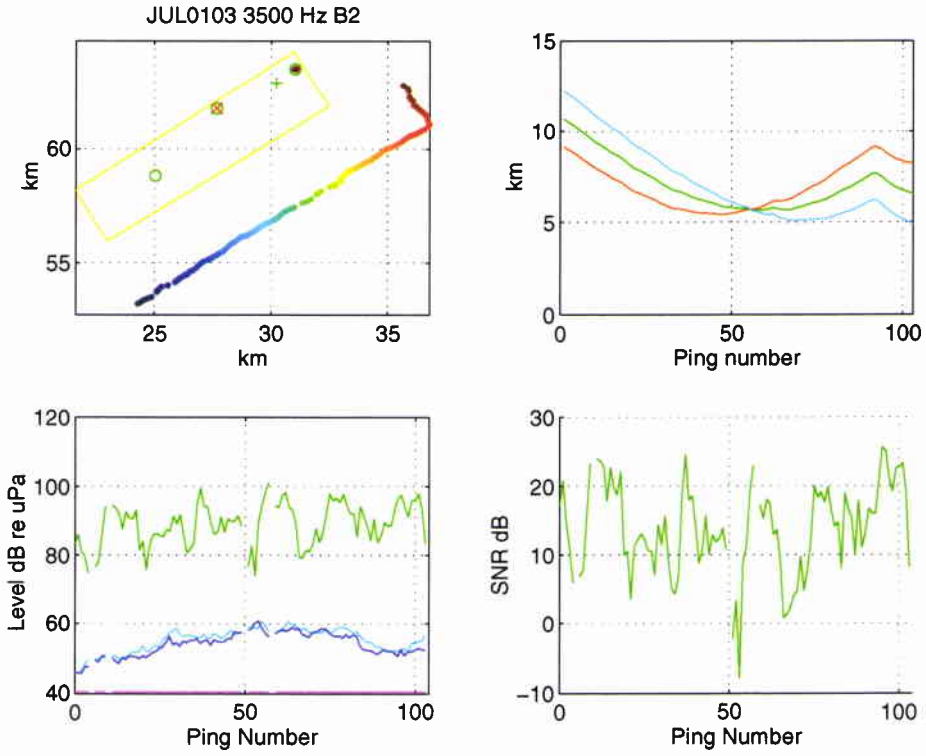

Figure B8

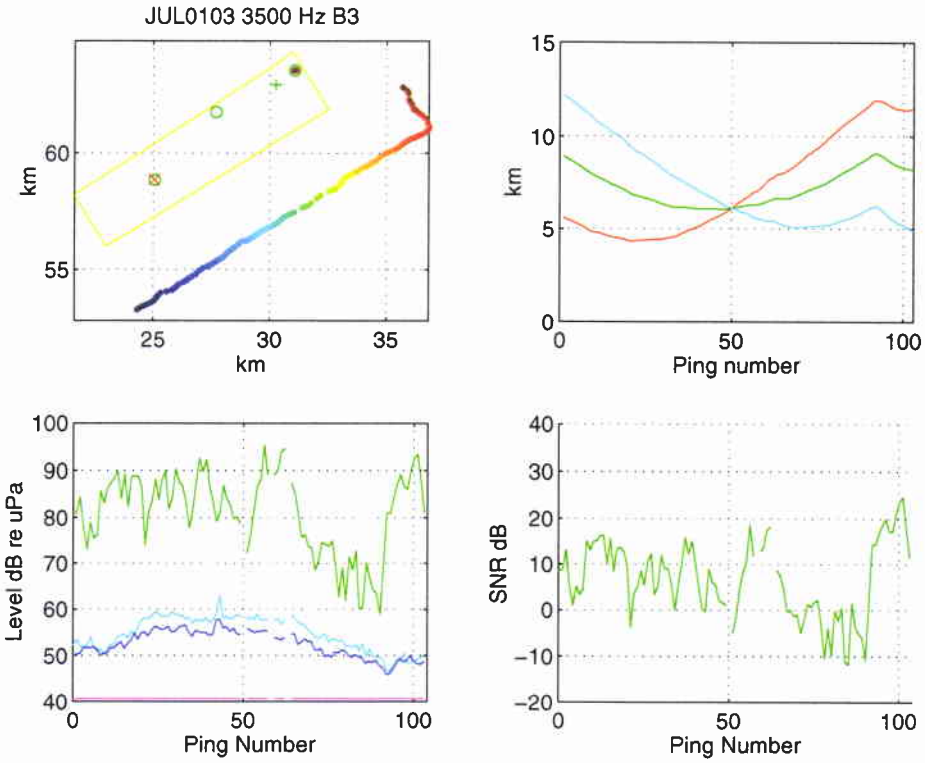

Figure B9

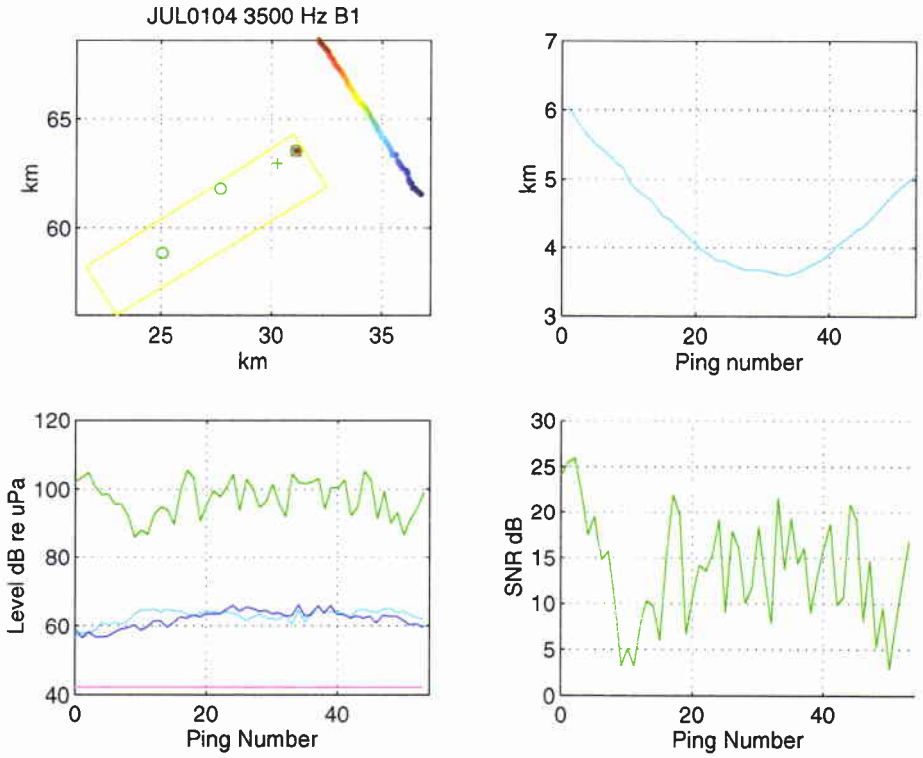

Figure B10

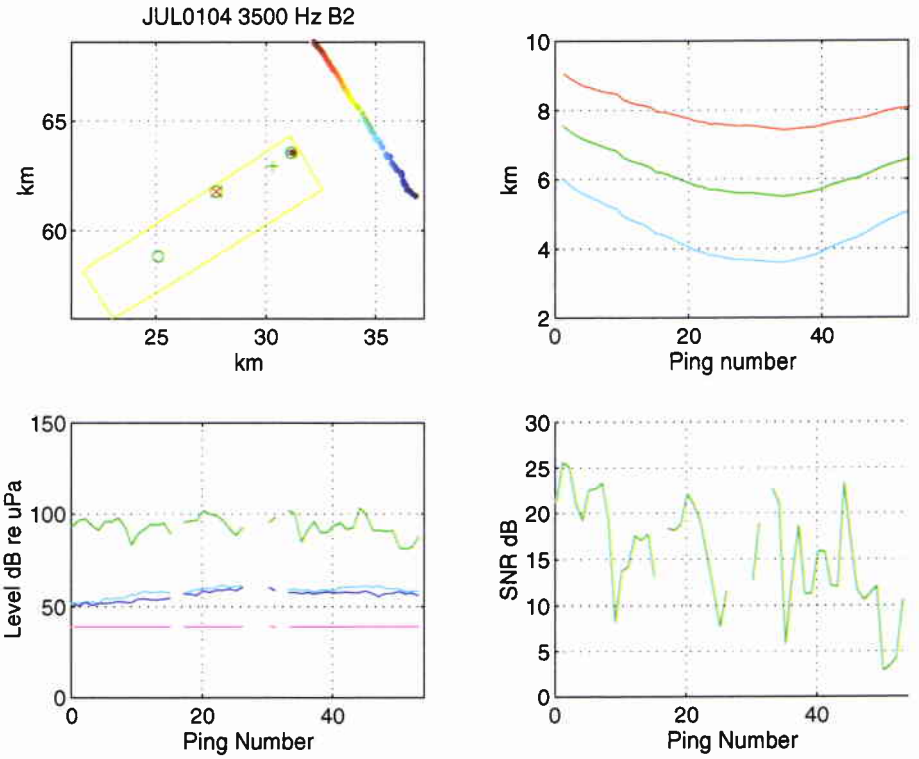

Figure B11

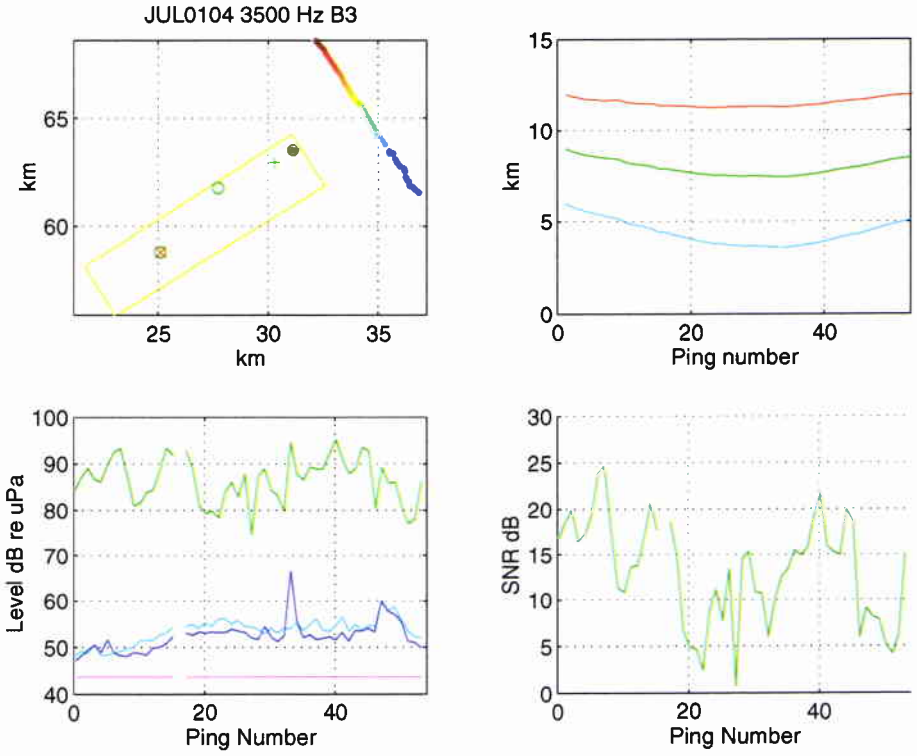

Figure B12

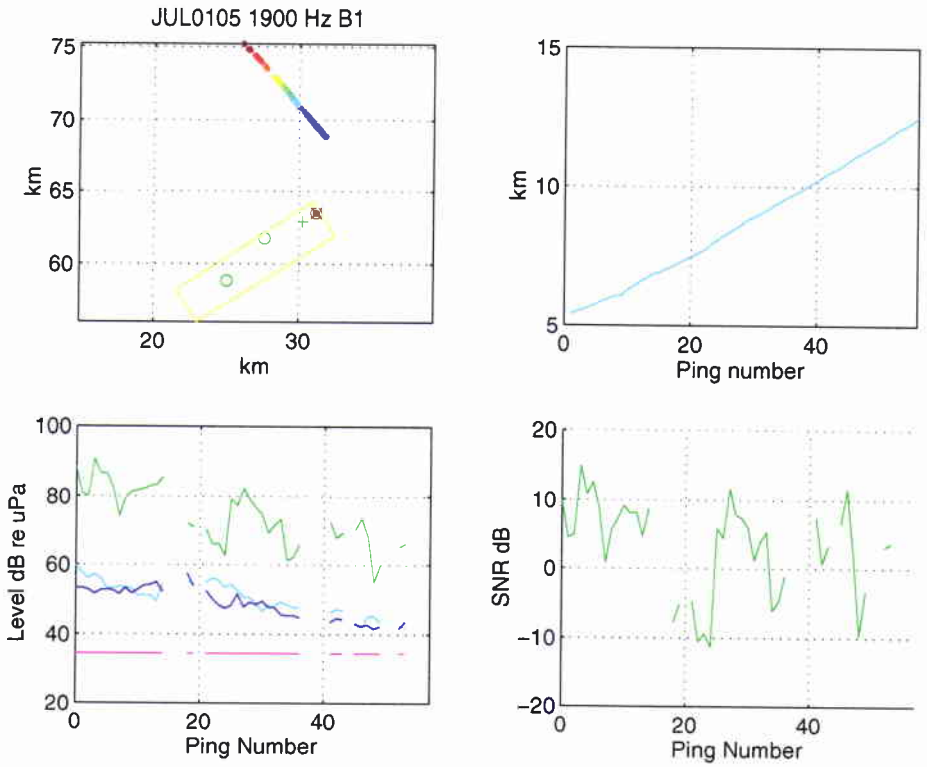

Figure B13

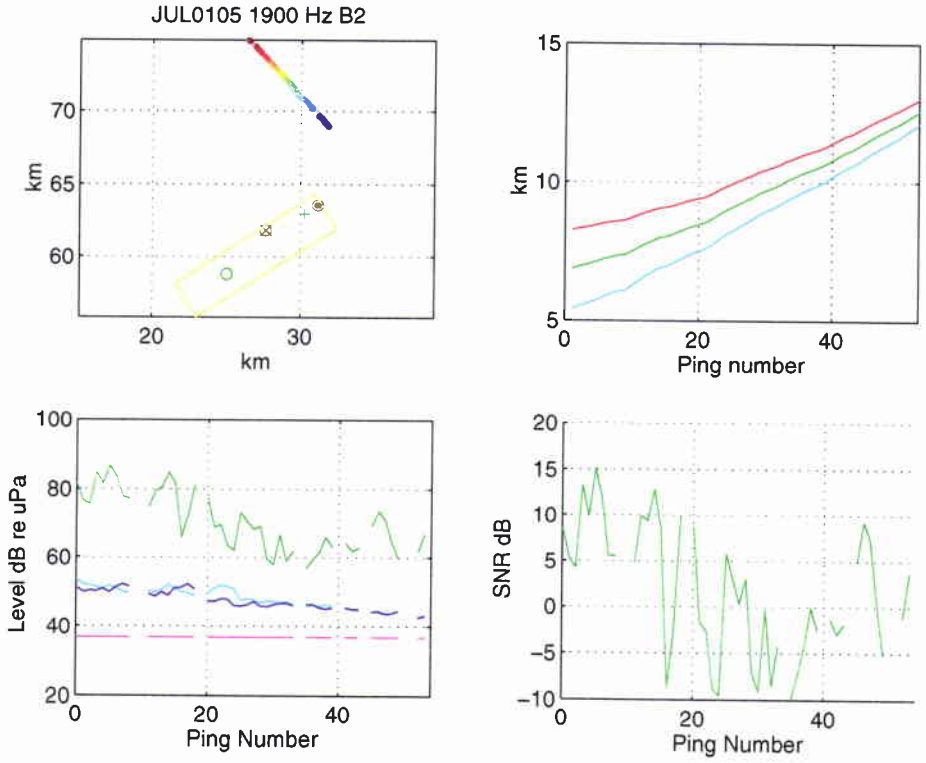

Figure B14

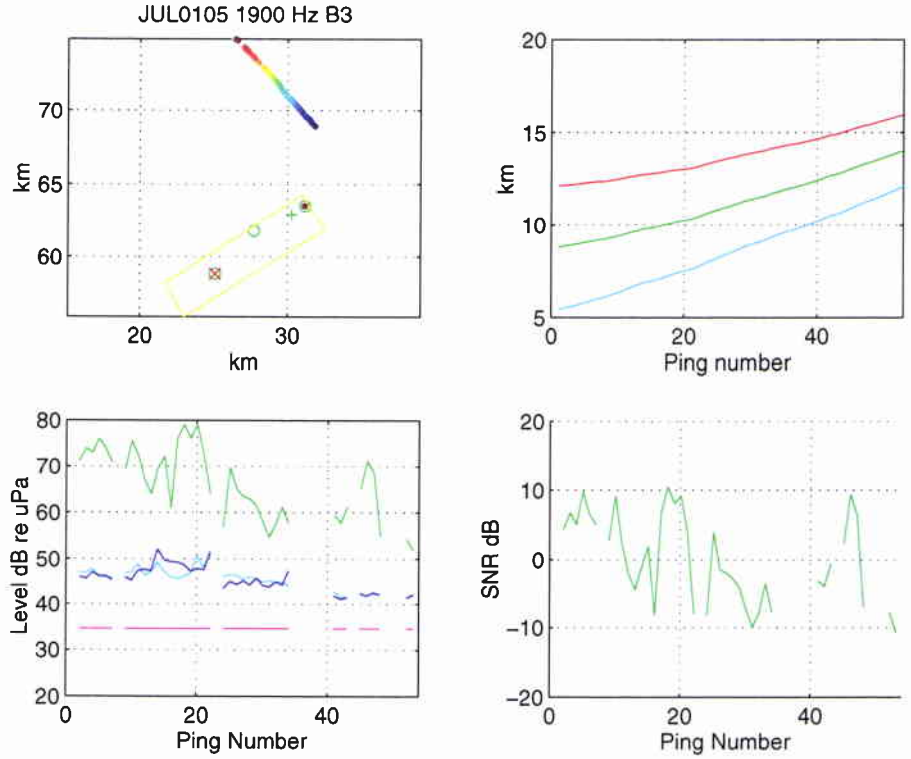

Figure B15

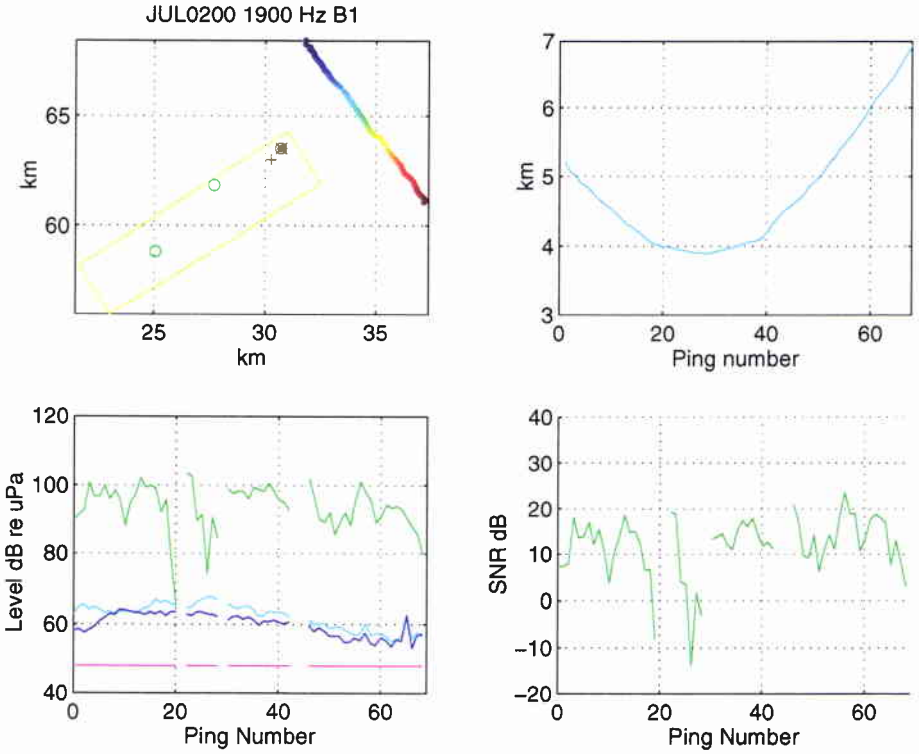

Figure B16

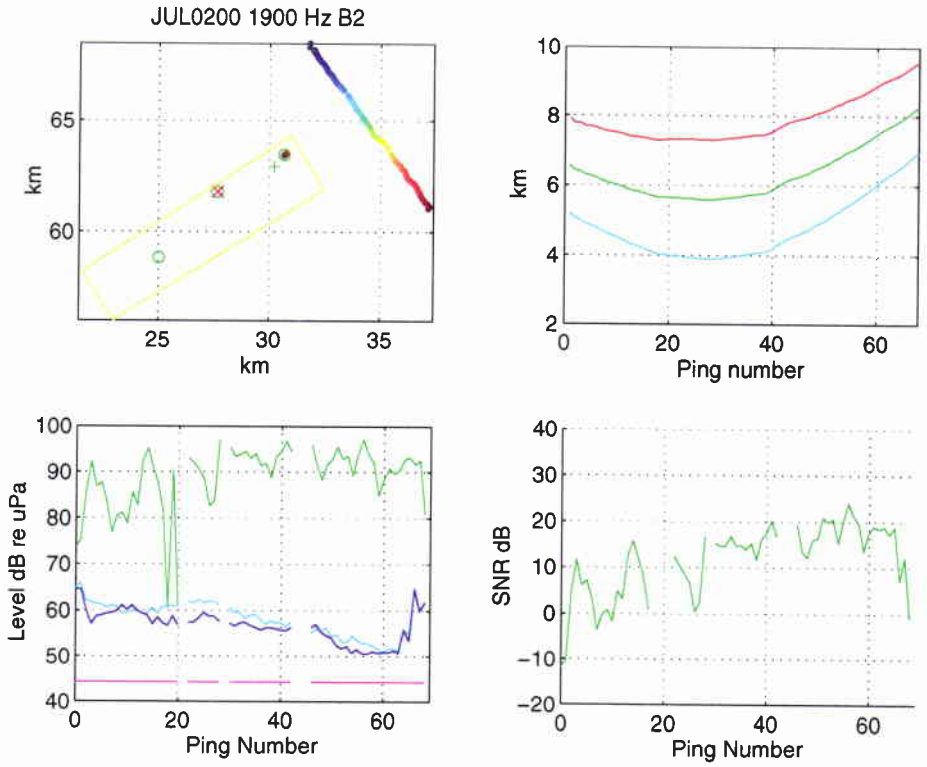

Figure B17

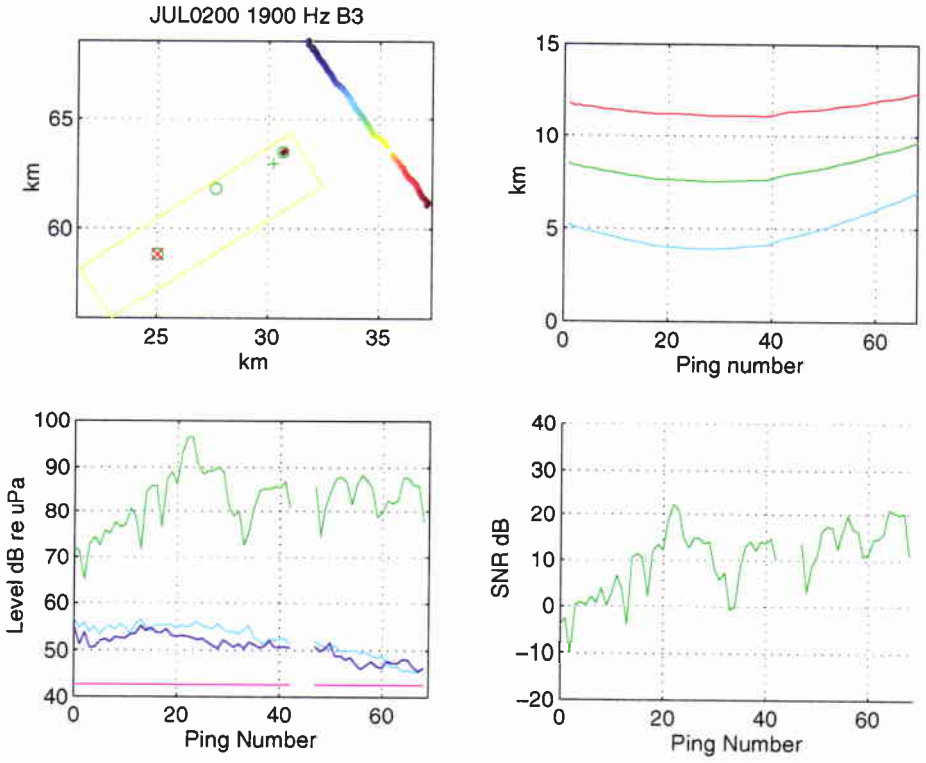

Figure B18

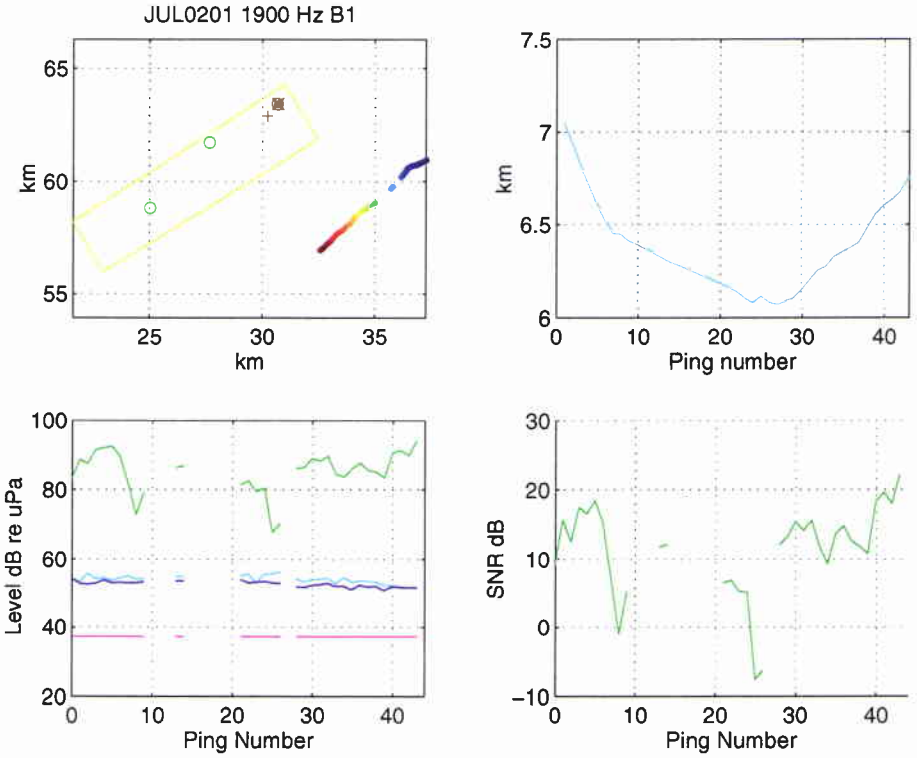

Figure B19

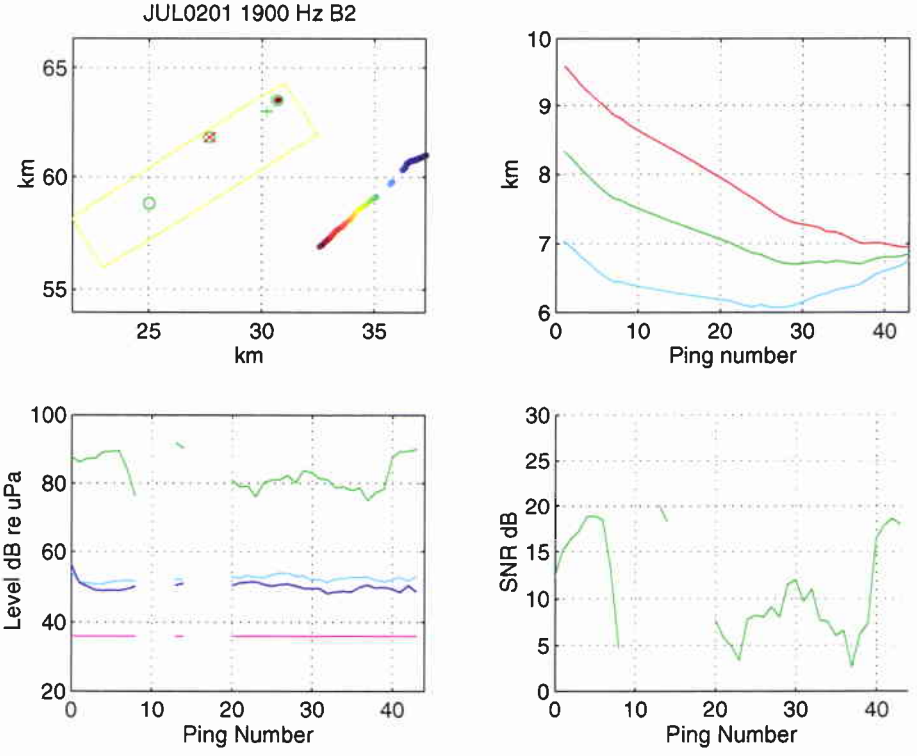

Figure B20

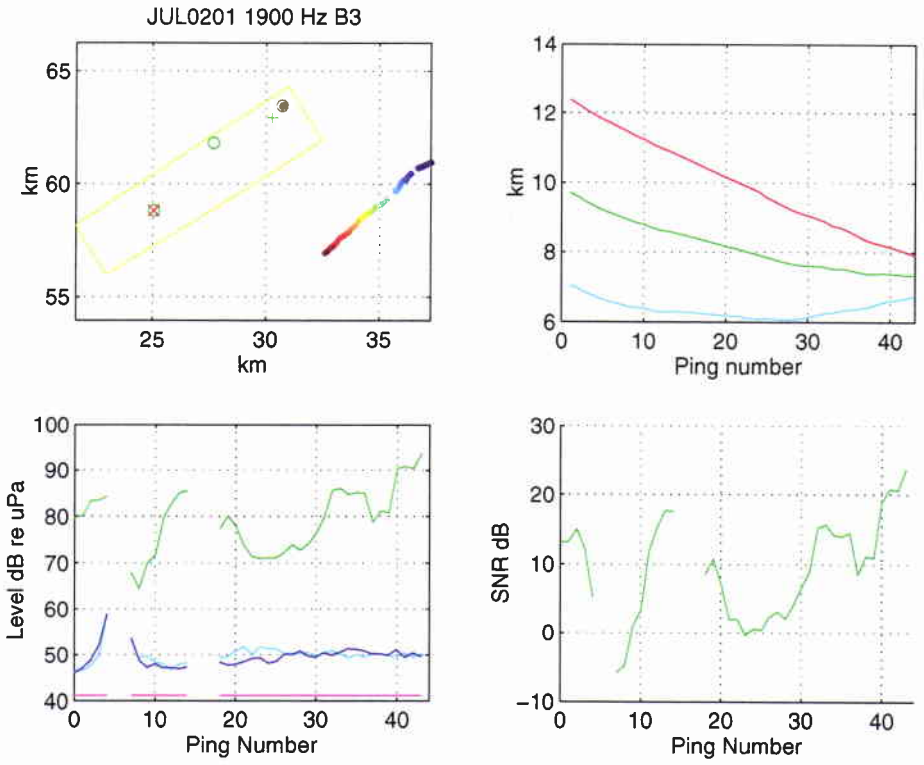

Figure B21

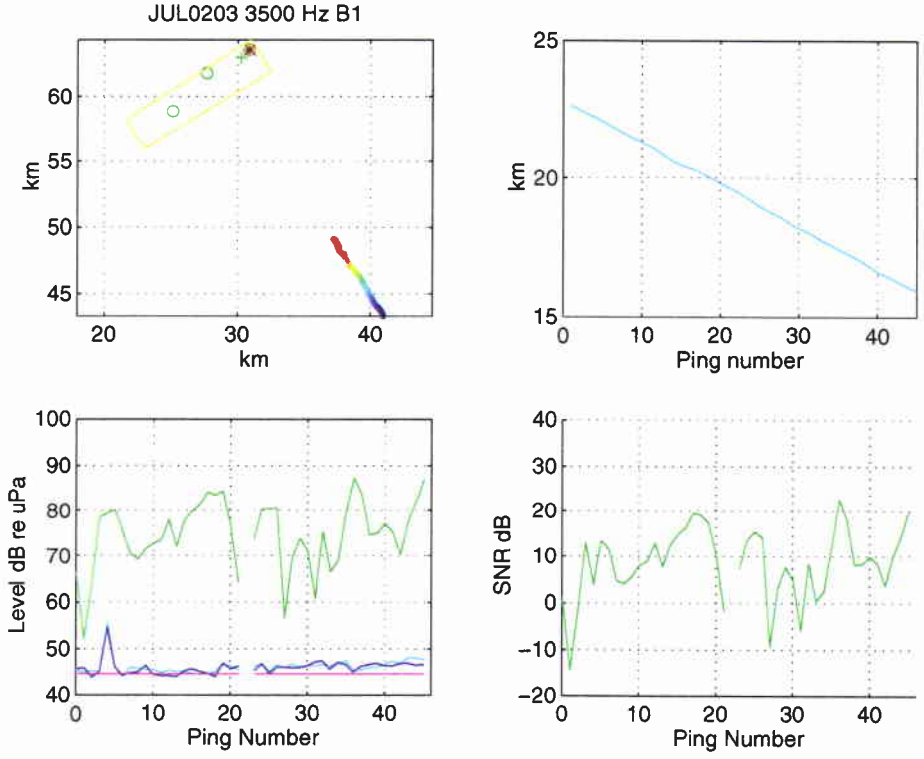

Figure B22

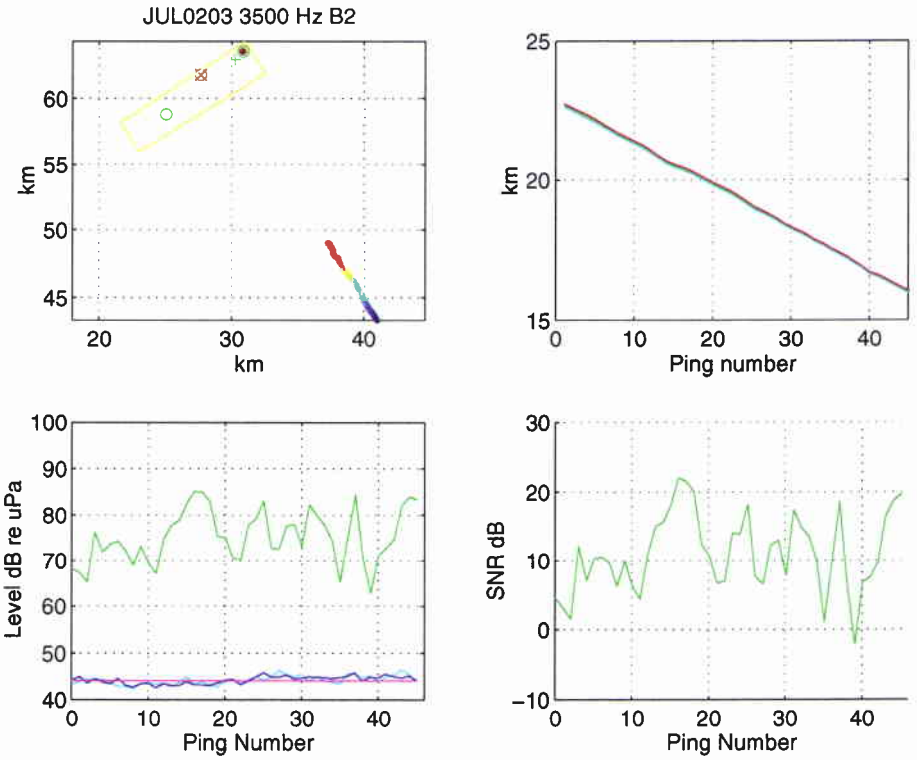

Figure B23

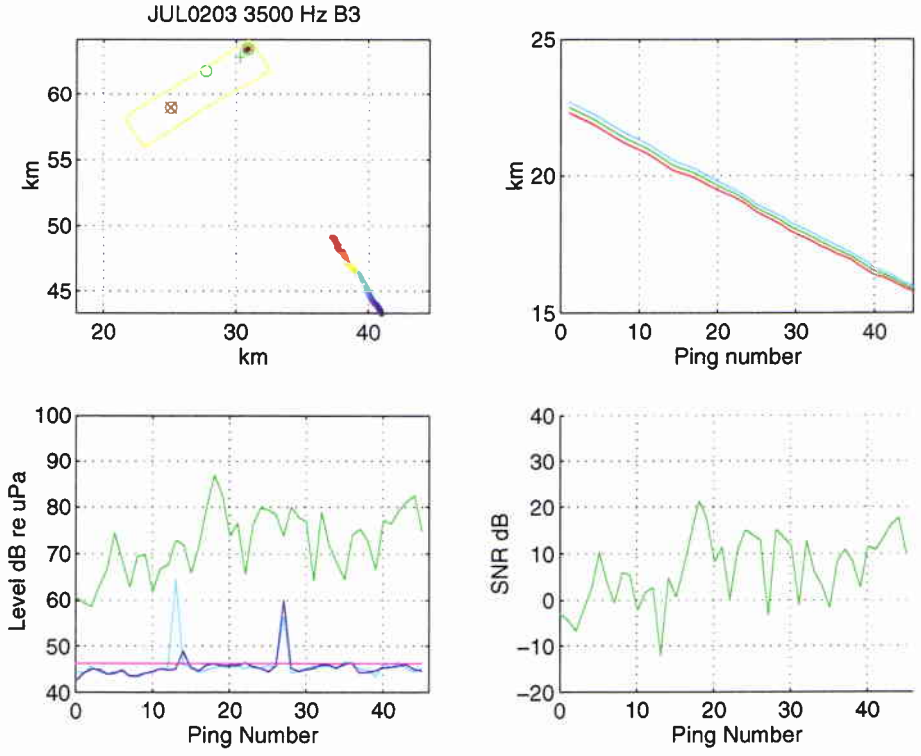

Figure B24

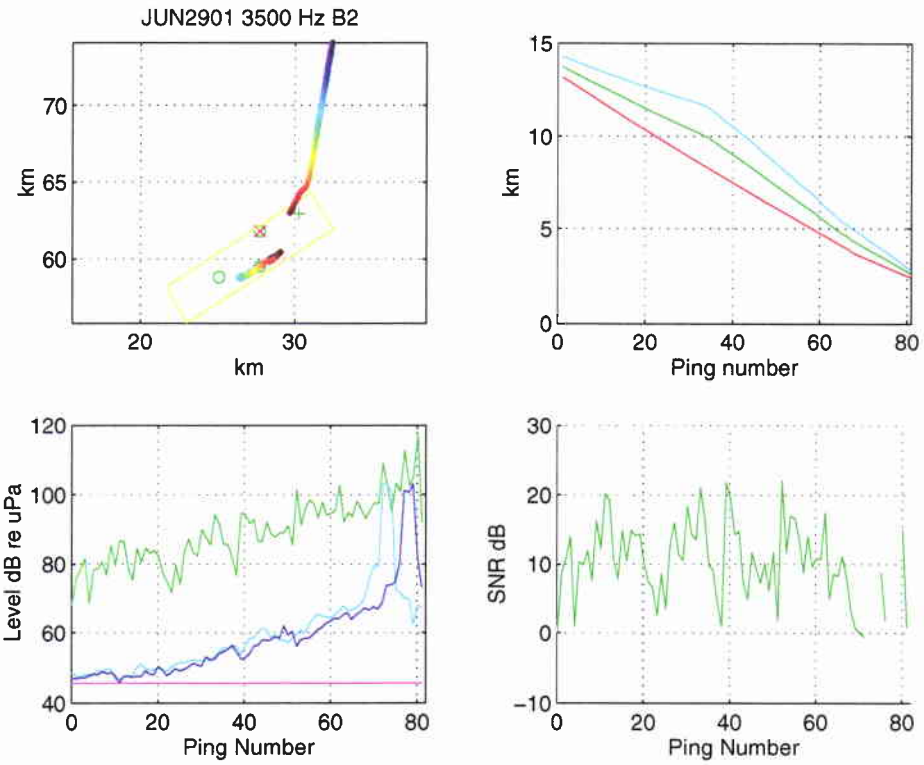

Figure B25

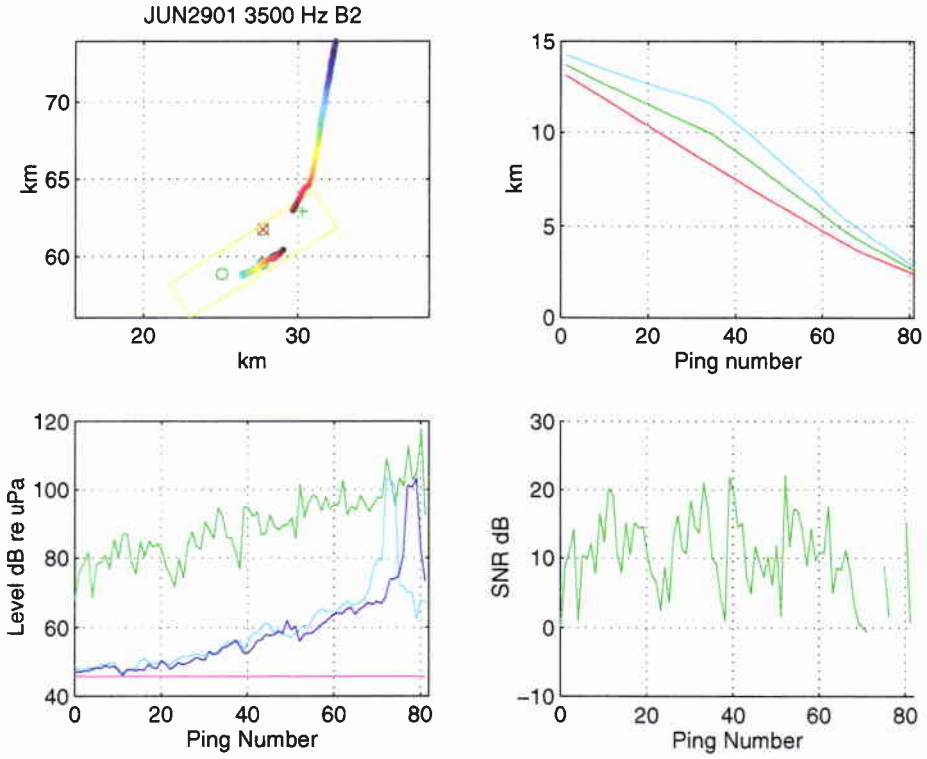

Figure B26

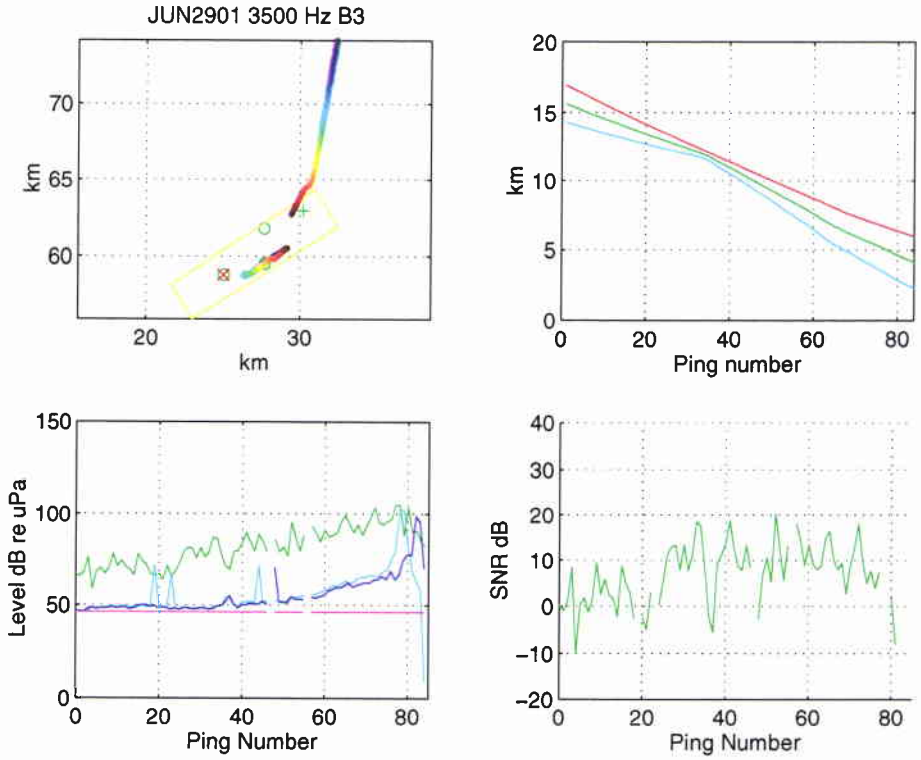

Figure B27

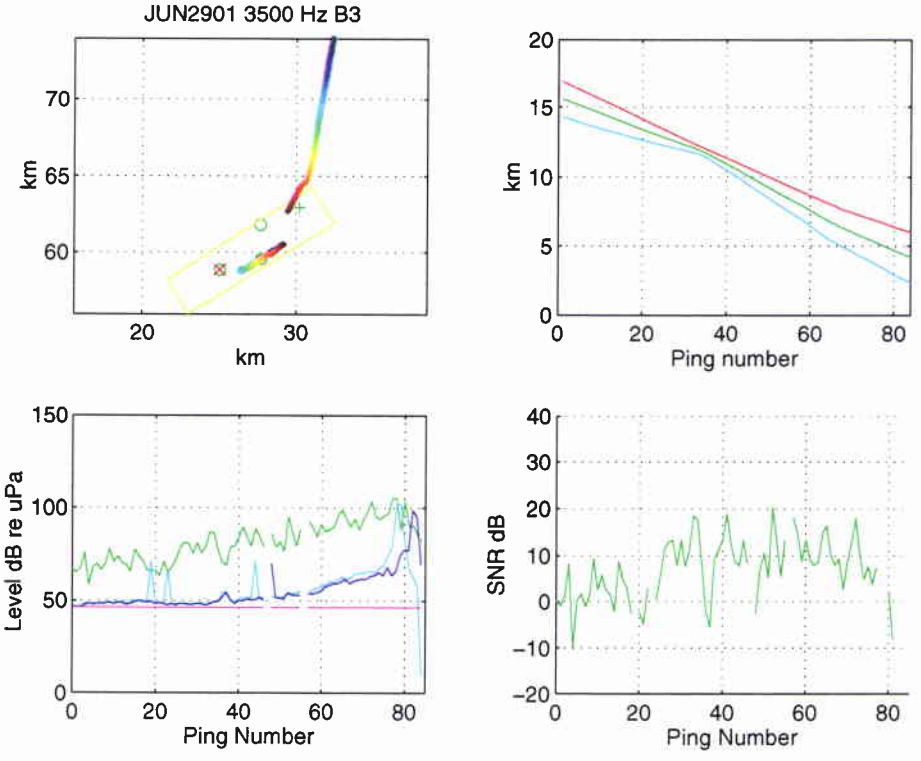

Figure B28

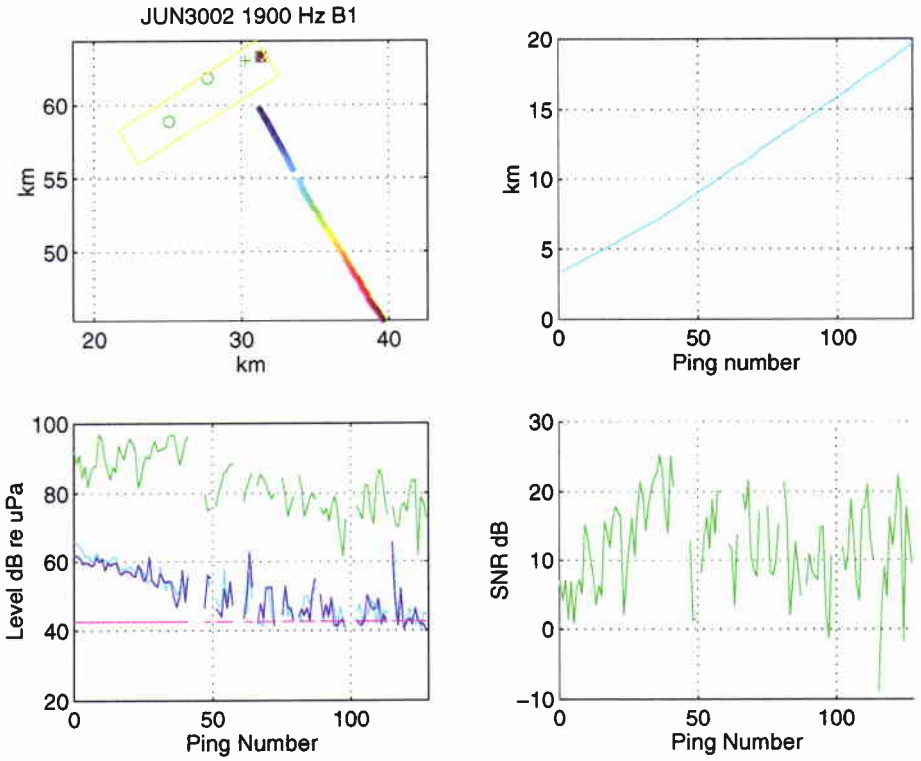

Figure B29

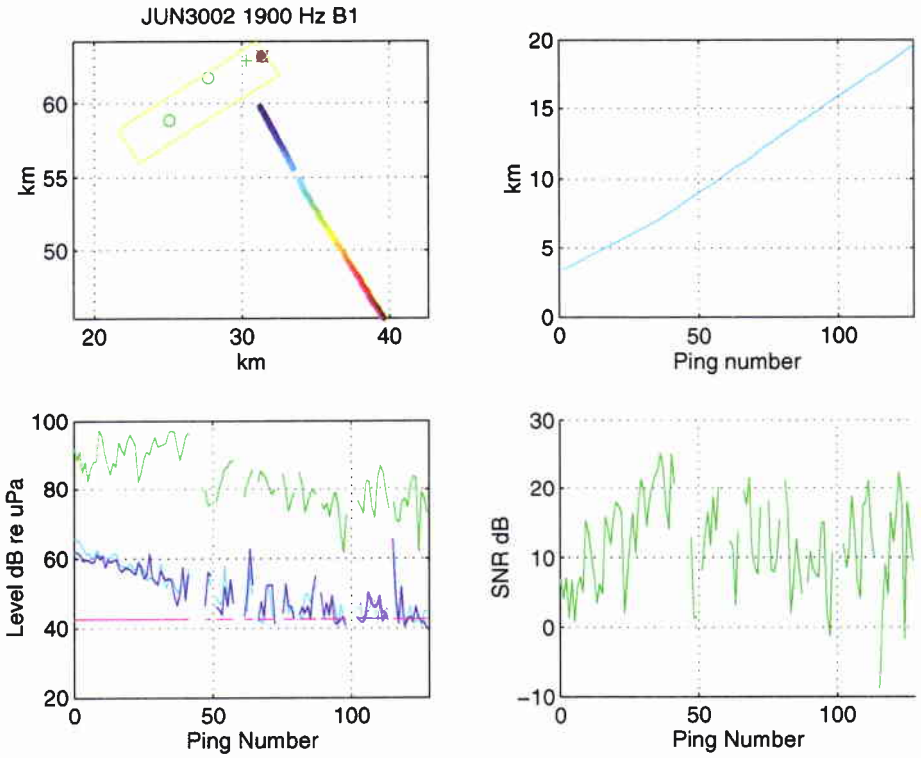

Figure B30

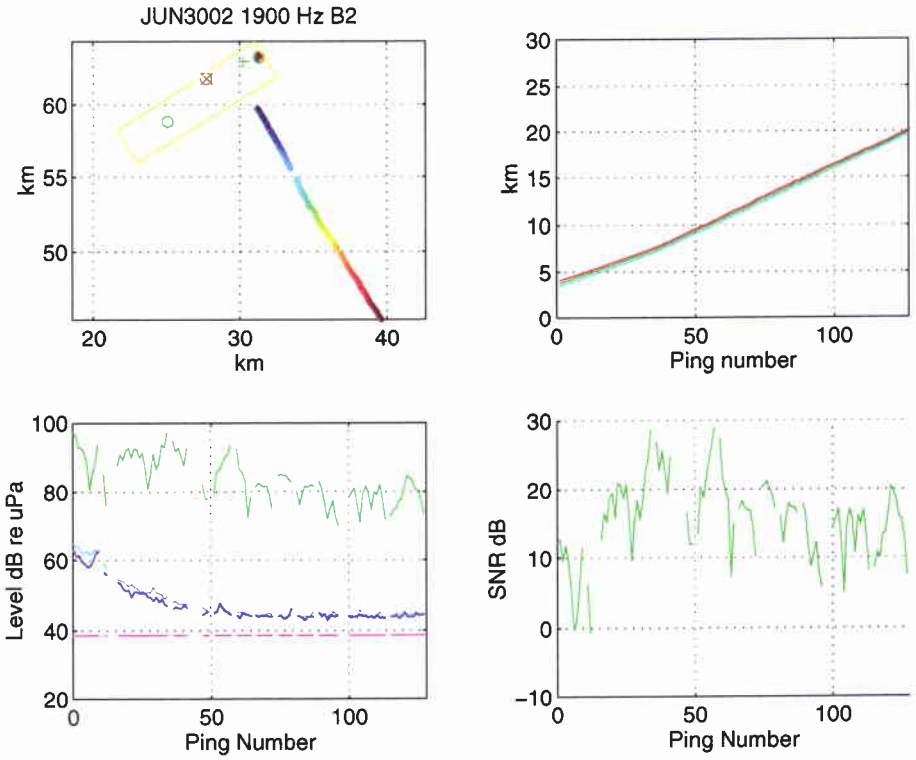

Figure B31

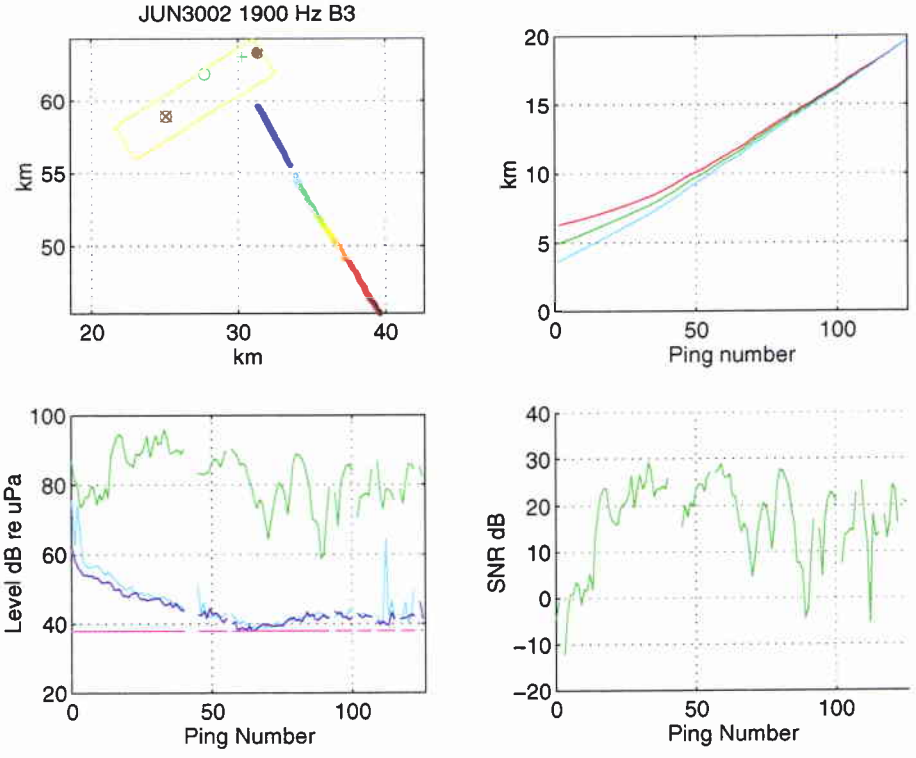

Figure B32

Report no. changed (Mar 2006): SR-288-UU

Document Data Sheet

NATO UNCLASSIFIED

Security Classification		Project No.
		021-1
Document Serial No.	**Date of Issue**	**Total Pages**
SR-288	April 1999	69 pp.

Author(s)

Mozzone, L., Bongi, S.

Title

Deployable Underwater Surveillance Systems.
Analysis of experimental results. Part III.

Abstract

Deployable Underwater Surveillance Systems (DUSS) are a new active sonar concept based on a distributed network of small multistatic transmitter / receiver nodes. This study analyzes data acquired during the period 29 June to 4 July, 1997, south of the island of Elba, with an experimental DUSS set moored to the sea bed and a towed, calibrated echo repeater target. Maximum detection ranges of 22 km were noise limited, while ranges of operational interest around 10 km were achieved with all target trajectories in reverberation. Sonar equation terms are measured and discussed. The two tested frequencies of 1.9 and 3.5 kHz showed equivalent performance. Multistatic receivers performed as well as monostatic receivers and extended system coverage. Multistatic receivers improved overall Signal to Noise / Reverberation and detection accuracy in an environment with significant signal fluctuations and contact fading.

The characteristics of the test system and experimental criteria are summarized.

Keywords

Active – Deployable – Multistatic – Sonar – Performance – Experiment – Analysis – Shallow Water– FM – Echo Repeater – Calibrated – Measurements

Issuing Organization

North Atlantic Treaty Organization
SACLANT Undersea Research Centre
Viale San Bartolomeo 400, 19138 La Spezia, Italy

[From N. America: SACLANTCEN (New York) APO AE 09613]

Tel: +39 0187 527 361
Fax:+39 0187 524 600

E-mail: library@saclantc.nato.int

NATO UNCLASSIFIED